University of Stavanger

Faculty of Science and Technology

MASTER'S THESIS

Study program/Specialization: Petroleum Geosciences Engineering	Spring semester, 2016 Open
Writer: Sindre Hadland	(Writer's signature)
Faculty supervisor: Chris Townsend External supervisor(s):	
Title of thesis: Geological Mapping and Investigation into a Proposed Syn-rift Alluvial Fan Deposit in the Kerpini Fault Block, Greece.	
Credits (ECTS): 30	
Keywords: Greece Gulf of Corinth Half-Graben Alluvial Fan Sedimentology Kerpini Fault Block	Pages: 123 +Front Page: 16 Stavanger, 14.06.2016

Geological Mapping and Investigation into a Proposed Syn-rift Alluvial Fan Deposit in the Kerpini Fault Block, Greece

By

Sindre Hadland

Master Thesis

Presented to the Faculty of Science and Technology

University of Stavanger

University of Stavanger

June 2016

Acknowledgment

I would like to thank my supervisor Chris Townsend for his support, guidance and many helpful discussions. His guidance and knowledge about the study area proved very helpful during the fieldtrips. I would also thank Alejandro Escalona for his feedback in the process of writing the theses, along with the discussions and ideas during the fieldwork. Thanks goes to my colleagues, Espen Sigmundstad and Stian Seglem Bjåland, which through discussion, feedback and motivation have contributed to greater knowledge and a better thesis.

I would also like to thank all my fellow master students at the University of Stavanger that made these two last year's fun and interesting.

Finally, I would like to thank my wonderful girlfriend, Bente, for her patience, support and motivation during these two last years.

Abstract

Geological Mapping and Investigation into a Proposed Syn-rift Alluvial Fan Deposit in the Kerpini Fault Block, Greece

Sindre Hadland

University of Stavanger

Supervisor: Chris Townsend

The Kerpini Fault Block is located in the southern part of the Gulf of Corinth rift system. The rift system consists of several east-west orientated half-grabens with associated syn-rift sediments. Kerpini Fault Block is one of the southernmost half-grabens within the rift systems, and is composed of several different stratigraphic units. The stratigraphic framework consists of a complex interaction of several stratigraphic units. One of these stratigraphic units situated in the southwestern part of the Kerpini Fault Block has been studied in detail in this project. This stratigraphic unit were suggested by Syahrul (2014) to be an internal alluvial fan within the Kerpini Fault Block. In order to achieve a full understanding of the proposed southwestern alluvial fan, and its part in the evolution of the Kerpini Fault Block, faults and other stratigraphic units within the Kerpini Fault Block and northern parts of Kalavryta Fault Block had to be mapped and described. Geological maps including both structural and stratigraphic features were created of the study area, along with detailed outcrop descriptions.

Three different alluvial fan facies has been identified, debris-flow, sheetflood and streamflow. These different facies help with concluding the presence of a sheetflood-dominated alluvial fan in the southwestern part of the Kerpini Fault Block. The facies gets more immature towards the southwestern corner, which suggests that the apex of the fan coincides with a step in the Kerpini Fault. The step is somewhat controlling the position of the fan and possibly also the deposition of the fan. The Kerpini Fault Block is composed of both pre and syn-fault strata. Pre-fault strata consists of alluvial conglomerates originating from the Kalavryta Fault, while the syn-fault strata consists of localized alluvial fan deposits limited to the Kerpini Fault Block.

Table of Contents

List of Figures

List of Tables

Chapter 1: Introduction

1.1 Background

The Gulf of Corinth is located in the northern parts of the Peloponnese Peninsula, Greece. The gulf has formed as a response to back-arc extension related to subduction at the Hellenic Trench (Taymaz et al., 2007), in which the exact initiation of the rifting is still debate (Armijo et al., 1996; Ford et al., 2013) but is believed to be of Pliocene age. Extension has resulted in a series of north dipping, ESE-WNW striking normal faults from the Kalavryta area in the south to the currently active gulf in the north. The north dipping faults form an asymmetric series of half-grabens, gradually stepping northwards. Classification for the overall stratigraphic configuration of the rift-system is terrestrial alluvial-fluvial sediments in the southern part transitioning to marine-brackish Gilbert-type deltaic and turbidite deposits in the north. Good exposure and well-preserved sedimentary deposits makes the northern Peloponnese Peninsula an excellent location for study the interaction between extensional half-grabens and sedimentary deposits. The study area is located in one of the southernmost half-grabens, the Kerpini Fault Block. Kerpini Fault Block is a tilted fault block with terrestrial syn-rift sediments sitting unconformable on Mesozoic basement. The Kerpini Fault Block is one of several fault blocks in the southern inactive rift-system with terrestrial syn-rift deposits, other fault blocks are the Kalavryta and Dhoumena Fault Blocks.

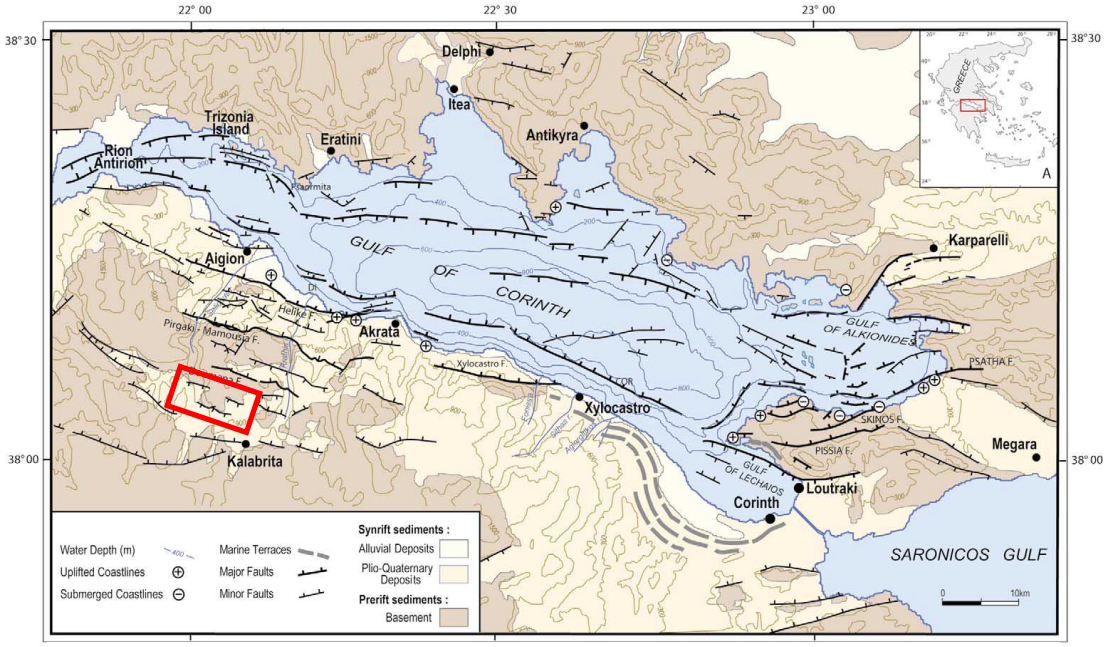

Figure 1: Structural map of the Gulf of Corinth rift system, the red box shows the study area (Kerpini Fault Block). (Modified from Moretti et al. (2003))

1.2 Geological Problem

Over the past 3-4 years, a number of master theses at the University of Stavanger have investigated the structural sedimentological development of the Kalavryta and Kerpini Fault Blocks. It started with Syahrul (2014) who tried to explain the lack of syn-fault characteristics in the sediments of the Kerpini Fault Block. As a part of his studies, he identified two separate fan deposits close to Kerpini village. One of these fan deposits, located southwest of Kerpini village will be mapped and described in detail during this study (referred to as Upper Conglomerates). The relative age of the Upper Conglomerates with regards to the Kerpini Fault and other stratigraphic units within the Kerpini Fault Block is not resolved. Subsequent studies have identified the complexity within the Kerpini Fault Block (Rognmo, 2015; Stuvland, 2015), with a number of different stratigraphic units and intra-block faults. Dahman (2015) identified the presence of a north-south striking fault at the eastern limit of the Kerpini Fault Block, which he characterized as a transfer fault. Along the strike of the Kerpini Fault, several steps have been identified (Stuvland, 2015; Wood, 2013). One of these steps coincides with the southwestern fan deposits identified by Syahrul (2014). The coincidence of the step in the Kerpini Fault and the fan deposits needed further work to try to determine if the two are related or if they are partly coincident at their location. Thus, aims of this study will be to:

1. Confirm the presence of the southwestern fan (Upper Conglomerates) identified by Syahrul (2014).
2. Determine the relationship between the Upper Conglomerates and the other stratigraphic units situated in the Kerpini Fault Block.
3. Determine the relative age of the Upper Conglomerates with regards to the Kerpini Fault.
4. Map facies changes in order to identify evidences for the Upper Conglomerates being an internal alluvial fan.
5. Determine if the Upper Conglomerates are likely to have been sourced from a step in the Kerpini Fault, and thus confirm their relationship.
6. Develop a tectono-sedimentary evolutionary model for the western portion of the Kerpini Fault Block.

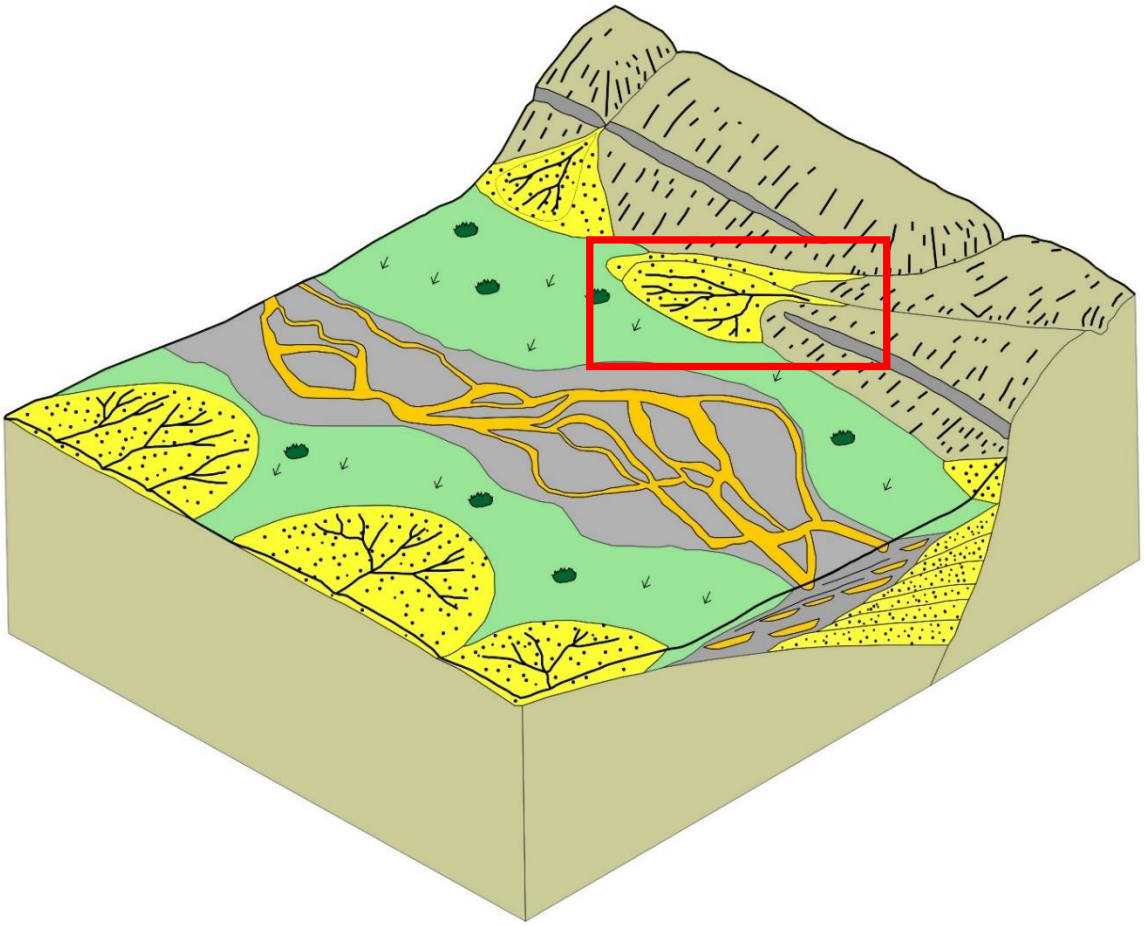

Figure 2: Conceptual figure of an active terrestrial half-graben with syn-fault deposits. Some of the geological problems related to this study can be shown by this figure. The red box shows an alluvial fan deposited syn-faulting sourced from a step in the fault, similar to what is believed to appear in the Kerpini Fault Block. Another geological problem that can be explain by this figure is to explain the relationship between the different stratigraphic units in the Kerpini Fault Block, illustrated in this figure by alluvial fans sourced from different directions and a fluvial system perpendicular to the alluvial fan deposits. (Modified from Leeder and Gawthorpe (1987)).

1.3 Objectives

The main objective of this study is to map and describe the Upper Conglomerates situated in the western part of the Kerpini Fault Block. A second objective is to use outcrop data to create evolutionary models, tying the deposition of the Upper Conglomerates with the other Kerpini Fault Block stratigraphic units and the movement of the Kalavryta, Kerpini and Dhoumena Faults. The results of mapping, descriptions and figures will be used to get a better understanding of the Kerpini Fault Block:

- Alluvial fan facies and facies distribution
- Interaction between faulting and sedimentation
- Its overall evolution

1.4 Data and Methodology

The methodology is divided into three stages:

1.4.1 Pre-field Work

During this stage, literature were studied in detail. There are a number of different theories and evolutionary models for the Gulf of Corinth rift system, so all papers were read with a critical state of mind. This was done in order to not be biased by different theories or models. In addition, sedimentological papers reviewing alluvial fan deposits were studied in detail. Especially, facies, facies distribution and sedimentological structures of alluvial fan deposits were studied. Maps, digital elevation models (DEM) and Google Earth were reviewed to pinpoint locations of interest and outcrops.

1.4.2 Fieldwork

The fieldwork was completed during two separate fieldtrips, with a total length of four weeks. Data such as fault strike, dip, dip direction and paleoflow directions were collected during the fieldwork. Most of the time was spend on outcrop studies, detailed description were made, facies logs were created and a number of photographs were taken. The outcrop data were mainly collected for studying alluvial facies and their distribution. Faults were mapped and measured, the best way of mapping faults proved to be mapping lithological contacts as fault planes were rarely exposed.

1.4.3 Post-field Work

At this stage, all the data were synthesized, studied and interpreted. Field data (strike, dip measurements etc.) were categorized and plotted in ArcGIS, the software proved a very helpful tool to finalize maps. Photographs were studied and figures created. All of these steps were performed in order to supply the findings, interpretation and analyses presented in this paper.

1.5 Previous Work

The northern part of the Peloponnese Peninsula has been studied for decades as the area offers excellent fault and outcrop exposure for structural and sedimentological studies. Many researchers have focused their studies in the northernmost part of the rift system, where the Gilbert-type deltas and youngest (recently active) faults are located. The southern areas of the rift system have not been as thoroughly studied. However, Ford et al. (2013) did a full study of the area from Kalavryta in the south to Helike in the north. The study focused on the tectono-sedimentary evolution of the rift system, where they classified three major stratigraphic groups

for the rift system (Figure 3 and 6). However, the coarse rift-system scale of the study implies that detailed intra-fault block scale features were overlooked.

In their studies of the Kerpini Fault Block, Ford et al. (2013) identified three stratigraphic units: Fluvial sandstones and conglomerates, Basal conglomerates and Coarse alluvial conglomerates (Figure 3 and 6). The Upper Conglomerates were classified as being Fluvial sandstones and conglomerates even though evidences for fluvial characteristics are sparse to none. There is a general theory among researchers (Collier and Jones, 2004; Ford et al., 2013; Sorel, 2000) that the Kerpini Fault Block sediments are a part of a bigger alluvial/fluvial system deposited syn-rifting (Gulf of Corinth rift). Their hypothesis is that sedimentation were widespread among several fault blocks (Kalavryta, Kerpini and Dhoumena Fault Blocks), sourced by large north-south orientated rivers.

Previous MSc Thesis from the University of Stavanger (Stuvland, 2015; Syahrul, 2014) have studied the Kerpini Fault Block sediments in more detail. In his studies of fault controlled sedimentation, Syahrul (2014) concluded that lack of increasing dip angle up-section (from older to younger sediments) could be explained by episodic movement of the Kerpini Fault. He also concluded that the present day Kerinitis and Vouraikos Rivers were the main source of sediments, with the main sediment supply coming from the south. Syahrul (2014) was the first author to suggest the presence of internal alluvial fans sourced from the uplifted footwall of the Kerpini and Dhoumena Faults. Stuvland (2015) concluded that the lack of increasing dip angle up-section (from older to younger sediments) is a result of the sediments being deposited pre-Kerpini Fault.

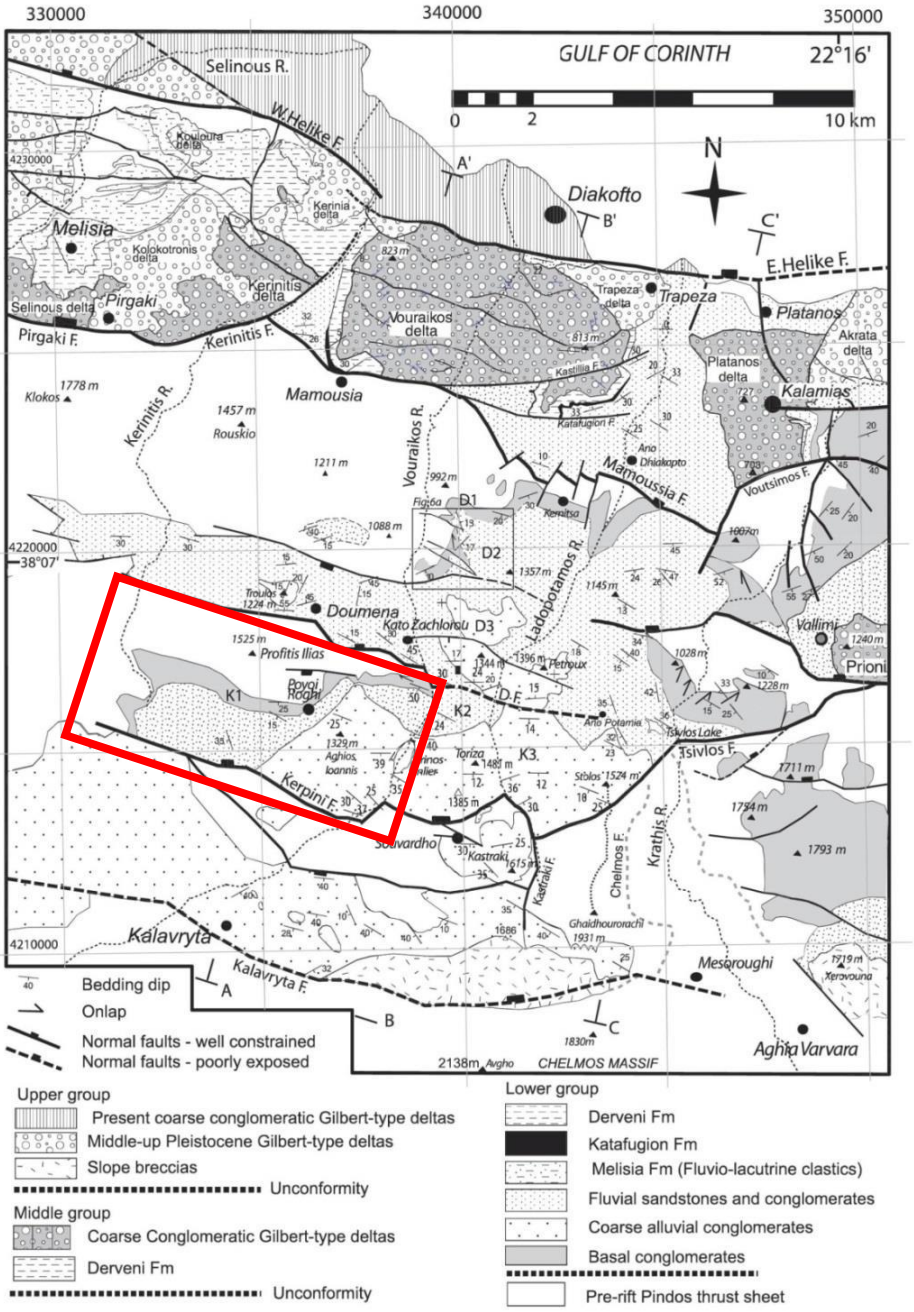

Figure 3: Structural and stratigraphic map from Ford et al. (2013) . The red box shows the extent of the Kerpini Fault Block, the main study area of this thesis. The figure shows that the stratigraphy of the Kerpini Fault Block is subdivided into three distinct stratigraphic units, Fluvial sandstones and conglomerates, Coarse alluvial conglomerates and Basal conglomerates. (Modified from Ford et al. (2013))

Chapter 2: Regional Geology

2.1 Plate Tectonics

In order to understand the structural and stratigraphic framework of the study area it is important to understand the plate tectonics of the Eastern Mediterranean Sea. The plate tectonics in the area is complex and affected by interaction of several tectonic plates, with the most contributory plates being the Nubian (African), Arabian, Eurasian and Anatolian Plates. The Anatolian Plate can furthermore be subdivided into two microplates, the Aegean and Anatolian Plates (Jackson, 1994). The Gulf of Corinth is located in the northwestern part of the Aegean Plate (Figure 4). To the south and west, the Aegean Plate is bounded by the Hellenic Trench, a trench formed as a response to the subduction of the Nubian Plate beneath the Aegean and Anatolian Plates. While the southern and western boundaries are well defined, the eastern boundary between the Anatolian and Aegean Plates is disputable. Scott (1981) defines the boundary to lie under the Mediterranean Sea, while (Papazachos, 1999) defines the boundary to lie in the western parts of Turkey. To the north, the right lateral North Anatolian Fault separates the Aegean and Anatolian Plates from the Eurasian Plate. The tectonic evolution of the area has been dominated by the subduction along the Hellenic Trench and the continental collision between the Arabian and Anatolian plates in Eastern Turkey (Taymaz et al., 2007). The subduction along the Hellenic Trench creates a "pull" force, while the continental collision creates a "push" force. The combination of these forces leads to a west-southwest propagation of the Aegean and Anatolian Plates along the North Anatolian Fault. Back-arc extension in the southern parts of Greece is a result of the slab pull from the subduction zone and the "rotational" movement of the Aegean and Anatolian Plates.

According to previous researchers (Gautier et al., 1999; Jolivet et al., 1994) the back-arc extension in the Aegean area initiated in the Oligocene, while the "rotational" movement of the Anatolian and Aegean Plates initiated at approximately 5 Ma (Armijo et al., 1996).

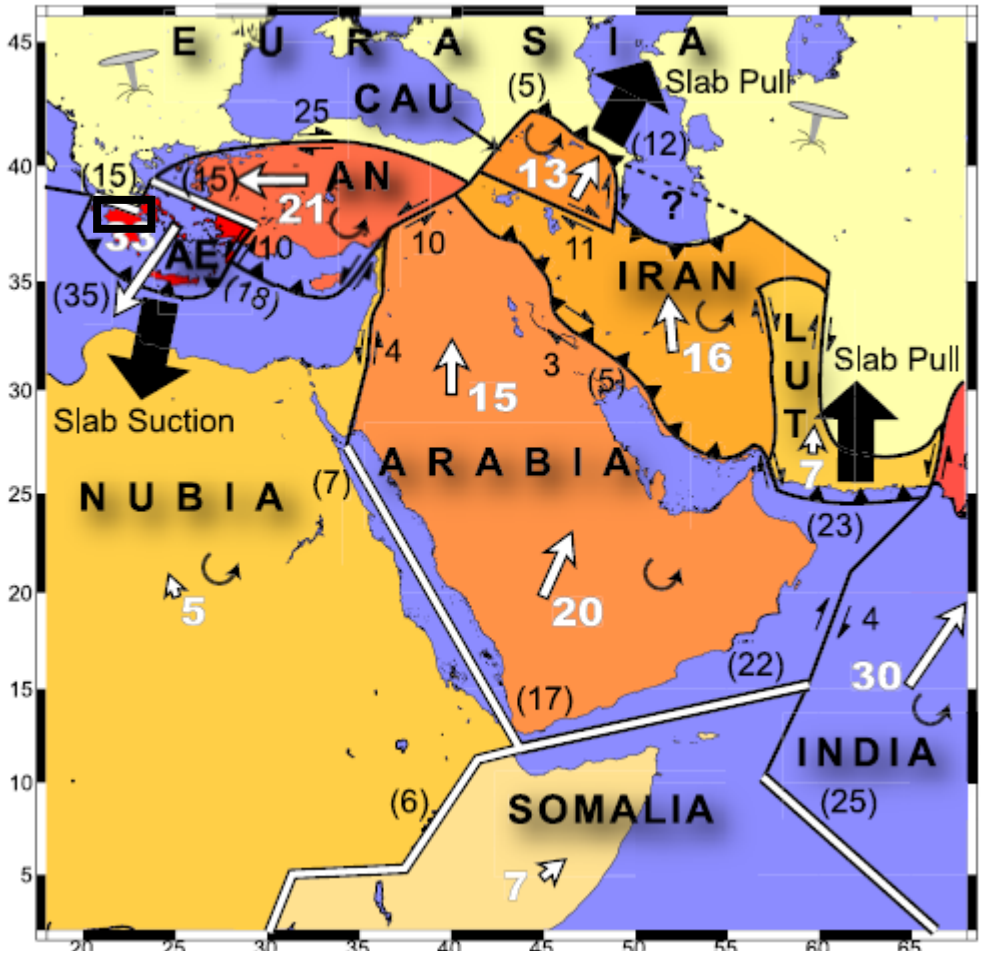

Figure 4: Plate tectonic map showing the interaction between African, Arabian, Anatolian and Aegean plates relative to the Eurasian Plate. It is the slab suction of the subduction of the Nubian Plate and the northwards movement of the Arabian Plate that contributes the most to the back-arc extension of the Aegean Plate. The Gulf of Corinth is located within the black box in the upper left corner of the figure. (Modified from (Reilinger et al., 2006))

2.2 Structural Framework

The Gulf of Corinth is a 115 km elongated graben, created as a result of back-arc extension, separating mainland Greece from the Peloponnese Peninsula. The gulf is bounded by north dipping faults on the southern margin and south dipping faults on the northern margin, and has evolved as a N100°E orientated symmetrical graben (Moretti et al., 2003) . In addition to the active rift system located within the gulf, there is a large portion of the inactive earlier rift preserved onshore, south of the gulf. The early rift offers good exposure of faults and outcrops due to rift related topographic elevation and river-incision. This makes the Corinth Rift an exceptional area for studying normal faulting and syn-rift deposits.

The onshore early rift area is characterized by a series of ESE-WNW orientated half-grabens located from the town of Kalavryta in the south to the active rift in the north. Sediments that sit unconformable on top of the basement mostly cover the half-grabens. All of the basin bounding faults dip north, with dip angles in the range of 40-60°. The oldest faults of the rift-system are located in the south, close to the town of Kalavryta. Sorel (2000) suggested a northward propagation of the north dipping faults, this implies that the faults and syn-rift sediments gets progressively younger as one moves closer to the active rift in the north. Collier and Jones (2004) suggested a model where the fault activity and displacement is spread along a series of north dipping faults (Kalavryta, Kerpini and Dhoumena Faults), and deposition occurs simultaneously in different half-grabens. The Corinth rift system is segmented, this is evident from the stepping of major north dipping normal faults along a north-south trend. Ghisetti and Vezzani (2005) claims that the segmentation of the Corinth rift system is a result of pre-existing structures in the pre-rift sequence (basement). In order to explain the earthquake activity in the Gulf of Corinth region, Sorel (2000) suggested a low-angle north dipping detachment fault (Khelmos Fault) along which all the steeper dipping normal faults detach (Figure 5). According to Sorel (2000), "Khelmos Detachment Fault" is the oldest and dominating fault of the rift system. Several researchers (Collier and Jones, 2004; Moretti et al., 2003), due to the lack of convincing evidences, have disputed the detachment model of Sorel (2000).

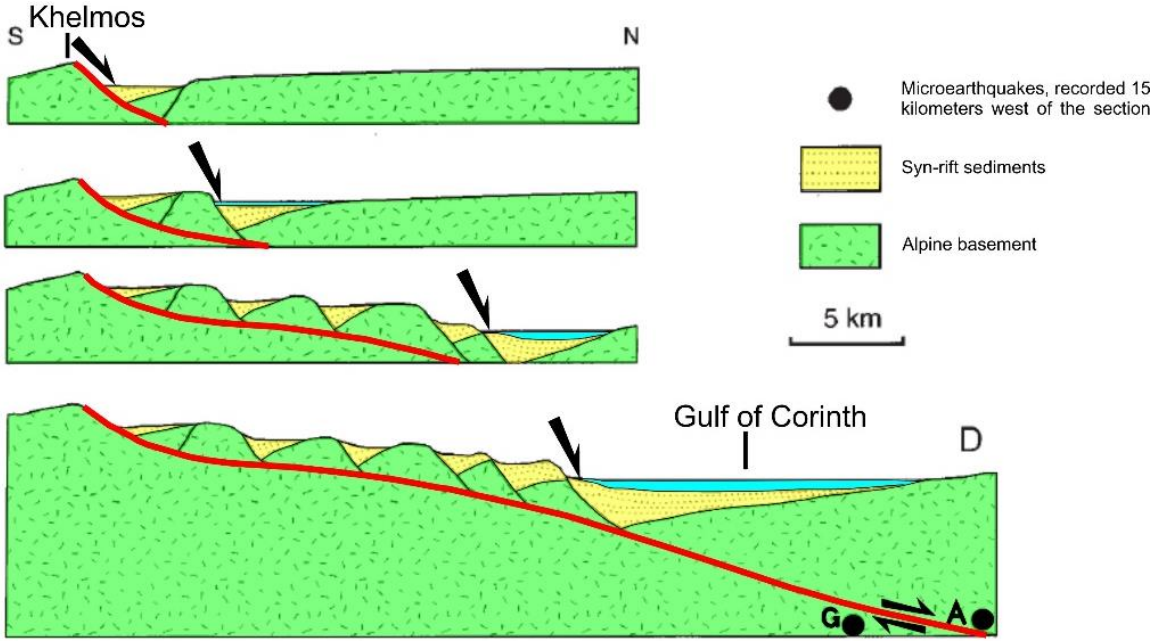

Figure 5: Structural evolution of the Khelmos Detachment Fault. All the younger north-dipping normal faults detach to the Khelmos Fault. The north-dipping faults gets progressively younger northwards. (Modified from Sorel (2000))

2.3 Stratigraphic Framework

2.3.1 Stratigraphic Framework - Gulf of Corinth Rift System

The Gulf of Corinth area has been subject of structural and sedimentological studies for decades. Many researchers has focused on the seismology and structural evolution of the rift system, while others have focused on the younger deposits, the Gilbert-type deltas and associated turbidite deposits. The stratigraphy of the southern part of the rift system, the early inactive rift, has not been studied as detailed as the younger marine/brackish deposits to the north. However, some researchers have looked at the rift system as a whole, also considering the southern deposits. Ford et al. (2013) published a paper with the objective to look at the tectono-sedimentary evolution of the Western Corinth Rift. The paper classifies three informal groups of syn-rift stratigraphy:

Lower group: The Lower group is widespread in southern parts of the region, stretching from the Kalavryta Fault Block in the south to the Pirgaki-Mamoussia Fault Block in the north. The characteristics of the group changes on a local scale, but on a regional scale it can be characterized by coarse-grained alluvial to fine-grained lacustrine successions (Ford et al., 2013). Even though there is local changes within the group, there is no evidences of marine influence within the youngest syn-rift stratigraphy (Ori, 1989).

Middle group: The Middle group is separated from the Lower group by an erosional unconformity where roughly 0,3 Ma of stratigraphy is missing (Ford et al., 2013). While terrestrial deposits characterize the Lower group, the Middle group character is marine/brackish ancient Gilbert-type deltas building northward. Laterally alongside the prograding Gilbert-type deltas, one can find distal turbidities and hemipelagic suspension deposits. The Middle group is mainly deposited in the Pirgaki-Mamoussia Fault Block with some portions of the turbidites and hemipelagic deposits stretching into the Helike Fault Block.

Upper group: The Upper group are mainly deposited offshore and consists of present day Gilbert-type delta conglomerates, distal turbidities and hemipelagic suspension deposits. Deposition of the upper group is still ongoing in the active parts of the Corinth rift system. Small portions of the upper group is found onshore in the Helike Fault Block, the onshore records of the Upper group shows progressive uplift (Ford et al., 2013).

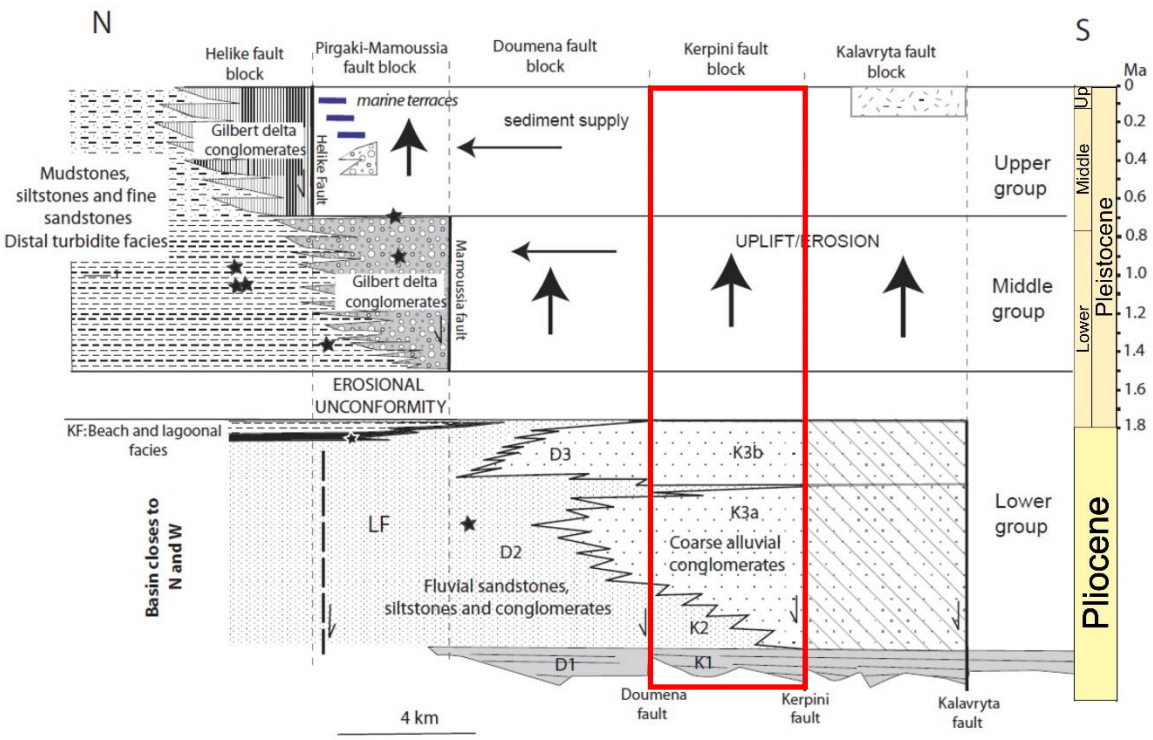

Figure 6: The syn-rift stratigraphy classification from Ford et al. (2013) resulted in the above wheeler diagram. Fault blocks are marked on the top of the figure, Basal conglomerates, Coarse alluvial conglomerates and Fluvial sandstones, siltstones and conglomerates are marked in the Kerpini Fault Block (red square).

2.3.2 Stratigraphic Framework - Kalavryta Region

Kalavryta Fault Block: The stratigraphy of the Kalavryta Fault Block is dominated by alluvial fan-conglomerates overlain by red shales (Rognmo, 2015). Sediments in the Kalavryta Fault Block are widespread and stretch for 5 km from the town of Kalavryta in the south to Skepasto Mountain in the north. Ford et al. (2013) interpreted the thickness of the Kalavryta Conglomerates to be a maximum of 1000 m, and Rognmo (2015) defined the maximum thickness of the red shales to be in the range of 50-70m.

Kerpini Fault Block: The stratigraphic framework of the Kerpini Fault Block is somewhat more complicated than for the Kalavryta Fault Block. The eastern extent of the fault block is marked by a thick sequence of conglomerates, referred to as the Roghi Conglomerates in this thesis. Roghi Conglomerates consists of thick to very thickly bedded cobble-boulder sized conglomerates, with occasional finer grained beds (sandy-pebbly). Ford et al. (2013) divides the rest of the sediments into Basal conglomerates and Fluvial sandstones and conglomerates. Syahrul (2014) defines the same sediments as Early Sandstone-Conglomerate. The basal sandstones and conglomerates of the Kerpini Fault Block are referred to as the Lower

Conglomerate unit in this thesis. Based on grain size anomalies Syahrul (2014) introduces the possibility of internal alluvial fans within the Kerpini Fault Block. These alluvial fan units are referred to as the Upper Conglomerates and Footwall Derived Fans in this thesis.

Dhoumena Fault Block: Ford et al. (2013) defined three stratigraphic units within the Dhoumena Fault Block based on grain size and facies. The basal unit is a coarse-grained conglomerate unit, which unconformably overlies the basement. The middle unit consist of orange-red siltstones, pebbly sandstones and thick conglomerate beds (Ford et al., 2013). These deposits are by Ford et al. (2013) interpreted to be a result of gravelly rivers and their floodplain deposits. The upper unit consist of massive, cobble and clast-supported conglomerates (Ford et al., 2013). Overall, the sediments in the Dhoumena Fault Block are finer than the sediments situated in the Kerpini Fault Block. There are a minimum of 1200 m of terrestrial sediments preserved in the Dhoumena Fault Block (Ford et al., 2013).

Chapter 3: Background Theory

3.1 Alluvial Fan Deposits

Alluvial fans are localized terrestrial deposits in which the sediments are deposited downstream from a point where water-driven flows expand. The point, from which the flows expand, normally tends to be a valley, gorge or any other feature that cuts through the topography (e.g. relay ramps). Alluvial fans are often deposited in mountainous areas or tectonically active areas where there is high topographic relief between the source point (apex) and the basin floor (Blair and McPherson, 1994b). The shape and size of alluvial fans are dependent on several factors, such as topographic relief, climate, source area lithology and catchment size (Reading, 1986). All of these factors play an important role for the distribution of alluvial fan sediments. Water is the main transport medium and large deposits are often coincident with flooding events or seasonal rain. Flooding and large volume of rain can lead to the development of channelization and/or incision of the fan surface. These channels and incision can erode into older deposits and control the distribution of sediments, the erosional effect will be highest close to apex where the discharge of the systems is highest. Fans can shift laterally to form depositional lobes, the point at which the fan starts to shift laterally is called the intersection point. The intersection point for small and medium sized fans can be located close to the apex. However, the lateral shifting is dependent on the depositional energy of the system and the slope angle. According to Blikra and Nemec (1998), the depositional slope for alluvial fans rarely exceed 10-15˚ at the apex and 1-5˚ at the toe, with higher depositional angle being classified as colluvial fan deposits. Immature gravelly deposits with a coarsening down-slope profile, dominated by avalanche or debris-flow processes typically characterize colluvial fans (Blikra and Nemec, 1998). Differentiating alluvial and colluvial fan deposits can be challenging, but alluvial fans can comprise a mixture between the two different types of deposits. Alluvial fan deposits are normally coarse-grained and poorly sorted, mainly due to short transport distance, mass wasting and flash flood processes triggered by high relief and rapid loss of flow capacity (Blair and McPherson, 1994a). Furthermore, Galloway and Hobday (1996) proposed a triangular classification scheme (Figure 7) for alluvial fan deposits based on dominating depositional processes (debris-flow fan, sheetflood fan and streamflow fan), the Galloway and Hobday (1996) classification will be further used in this study for classification of alluvial fan facies. As the classification scheme describes, it is normal to

have a mixture of depositional processes involved during the deposition of alluvial fans. Blair and McPherson (1994a) characterized alluvial fans based on sedimentary processes, but the geomorphic classification by Galloway and Hobday (1996) is more suited for the alluvial fans of the Gulf of Corinth rift system due to lack of clear bedding and sedimentary structures. The following sections will give a description of the three dominating alluvial fan processes.

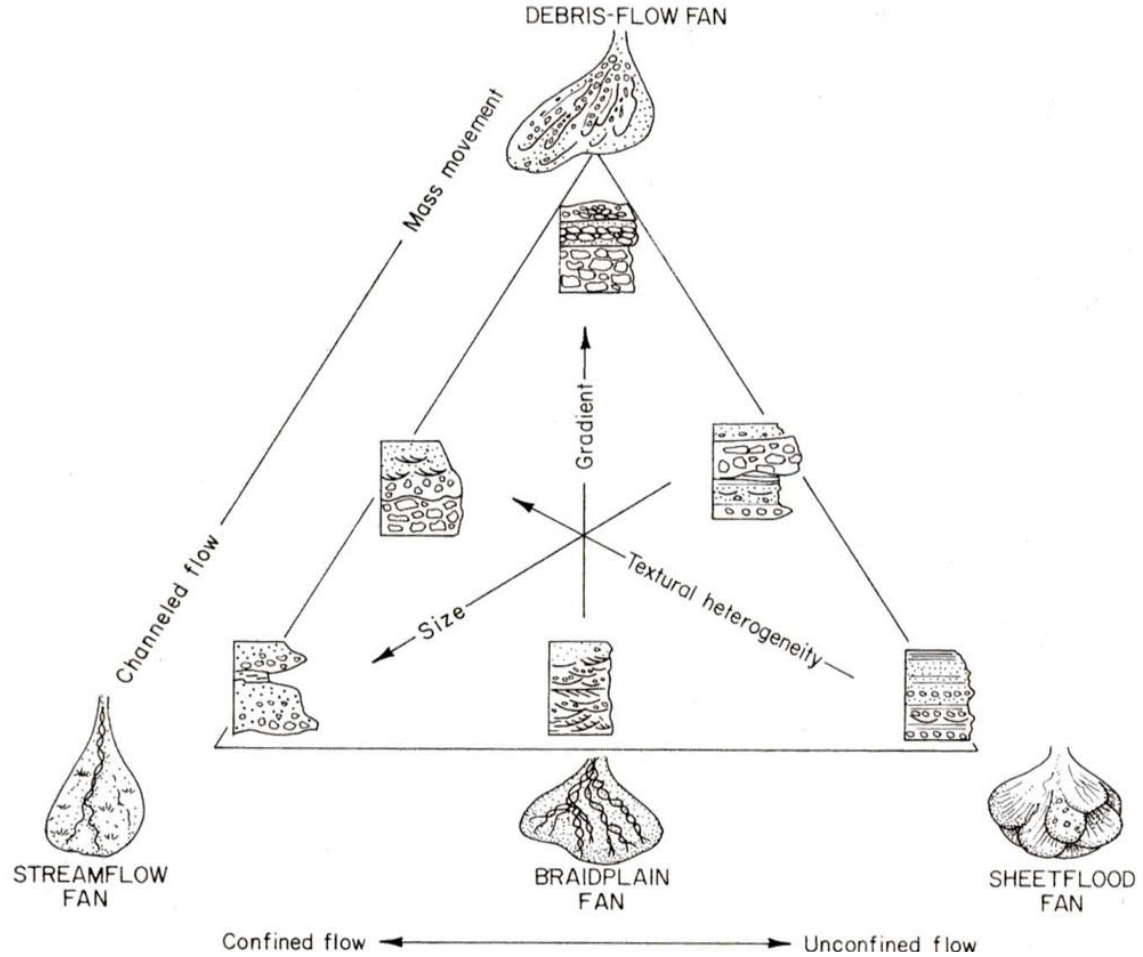

Figure 7: Galloway and Hobday (1996) classification of alluvial fan systems. The classification is based on the flow type, gradient, size and textural heterogeneity. Mass movement, high gradient, large size and large textural heterogeneity characterize debris-flow dominated fans. Sheetflood and Streamflow dominated fans have a more channeled flow, smaller gradient and are in general smaller. The type of flow, confined, perennial, unconfined or ephemeral flows are often used to separate between Sheetflood and Streamflow dominated fans. (Galloway and Hobday, 1996)

3.1.1 Debris-flow Dominated Fans

Debris-flow dominated fans are predominantly located in tectonically active areas where tectonic movement has created relief between the exit point and the basin floor, or in areas where flash/seasonal floods occur. Large amounts of unconsolidated sediments accumulate in the catchment (drainage basin) due to weathering and erosion, floods and/or tectonic activity can trigger the sediments to be deposited downslope. Independent of the trigger mechanism, the presence of fluids, in most cases water, is essential for debris-flows to initiate. The flows might initiate as a colluvial gravity flow, but will transform to debris-flows as water and air is trapped in the flow (Galloway and Hobday, 1996). Debris-flows show a large variety of flow types, such as turbulent flow, fluidized flow, viscous flow and non-viscous flows(Blair and McPherson, 1994b). The competence (ability to transport large clasts) for individual debris-flows are mainly determined by the matrix strength and density, which is a function of matrix clay content (Hampton, 1975). Due to the high depositional energy of the flows, the basal contact will be sharp or in some cases erosive. Debris-flow dominated fans have the highest depositional energy and are the only fan type characterized by mass movement rather than channeled flow, based on Galloway and Hobday (1996) classification scheme. Alluvial fans dominated by debris-flows tend to be coarse grained, poorly sorted, clast supported conglomerates. The thickness of individual flows can vary from one to 10 m in the catchment channels/apex and decrease downfan (Blair, 1987). Individual flows will lose moist downfan, which in most cases will lead to strengthening of the matrix (Rust, 1978), and more pronounced stratification and organization of grains in the proximal parts of the flow. An idealized debris-flow dominated alluvial fan will show a fining upward and downfan clast size reduction, graded to reverse graded units, which thickens upward (Galloway and Hobday, 1996). Paleoflow indicators within high energy/velocity debris-flows are sparse, but occasionally flows display imbrications in the upper parts of the units. Imbrication is a type of bedding where disk-shaped, flatten pebbles/cobbles are deposited at an inclined angle forming an overlap with adjacent clast (Figure 8).

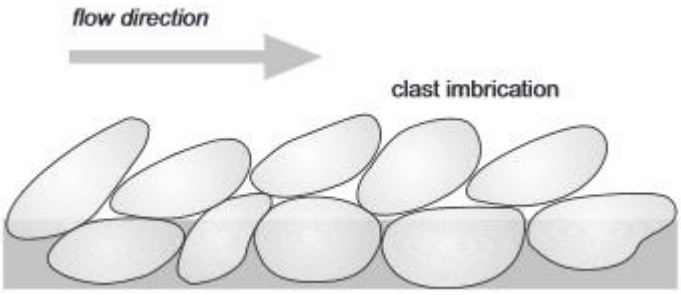

Figure 8: Example of imbrication where the long axes of the disk-shaped clasts are orientated in the same direction as the flow. (Nichols, 2009)

3.1.2Sheetflood-Dominated Fans

Sheetflooding and streamflooding are terms used to describe sheetflood-dominated alluvial fans, for simplicity, sheetflood will be used as a unifying term for the following subsection. Sheetflooding is characterized as an unchannelized flow often related to heavy rainfall, whereas streamflooding is characterized as broad, poorly defined channelized flows within ephemeral channels (Galloway and Hobday, 1996), much like a streamflow downslope of the intersection point (Hooke, 1967). Sheetfloods are short-lived and episodic with shallow water depth, but can cover large areas of a fan surface. Grainsize normally ranges from medium to coarse sand with occasional gravel and boulders. Blair (1987) observed conglomeratic sheetfloods deposited by supercritical turbulent flows in combination with debris-flows deposits in the 1982 Roaring River flood, Rocky Mountain National Park, Colorado. The observations by Blair (1987) prove the complexity of sheetfloods, where the character of the flow itself is more important than the resulting deposits. Supercritical flows are dependent on the Froude number, which is the ratio between fluid inertial forces and fluid gravitational forces (Prothero and Schwab, 2013). A Froude number less than 1 indicates that velocity of the surfaces waves in the flow is higher than the flow itself, allowing the waves to travel upward. In supercritical flows, the Froude number exceeds one and the surface waves does not migrate upward but rather in the direction of the main flow, resulting in higher flow-velocity. Supercritical flows are also called rapid flow or shooting flows. Sheetfloods and supercritical flows in alluvial fan deposits often combines with low clay content in the sediments. Sheetfloods are often deposited in the latest stages of fan progradation or as the fan is retrograding due to lack of sediment input or loss of channel/stream activity (Blair and McPherson, 1994b). Normal thickness of sheetflood units ranges from 5-20 cm, but often occurs as amalgamated units. Sandy sheetflood deposits often display planar,

parallel and ripple lamination while the coarse sheetflood deposits often display imbrication and cross-stratification (Blair and McPherson, 1994b; Galloway and Hobday, 1996).

3.1.3 Streamflow-Dominated Fans

While episodic deposits characterize debris-flow and sheetflood dominated fans, streamflow-dominated fans have a more stable sediment supply through perennial streams. Some fans can have single concentrated distributary channels, while others have numerous channels migrating laterally over the fan, constantly reworking the fan surface. The lack of high-energy currents and streams means vegetation can settle on the surface and stabilize sandy/gravelly deposits, creating meandering channel belts. Streams lose energy rapidly downslope, resulting in coarser poorly sorted conglomeratic deposits in the proximal parts close to the apex. Average grain size decreases downslope, and suspension processes are more prominent in the distalmost parts of the fans. Longitudinal gravel and sandbars are common in the mid to distal parts of streamflow-dominated alluvial fans. Sedimentary structures of streamflow-dominated alluvial fans change downfan. Boulder sized grains tend to show signs of imbrication in the upper parts of the fan. Gravel and sandbars can display a variety of sedimentary structures such as horizontal stratification, trough cross-bedding, planar cross-bedding and ripples (Galloway and Hobday, 1996). Distal sandy facies and bars display most of the sedimentary structures, due to the loss of stream velocity downfan. According to Hooke (1967) streamflow-dominated fans can lose their identity at the intersection point, downslope from the intersection point channels becomes broad and poorly defined. On smaller fans, coarser channelized facies are dominating and the distal suspension-dominated sandy facies are often absent (Galloway and Hobday, 1996).

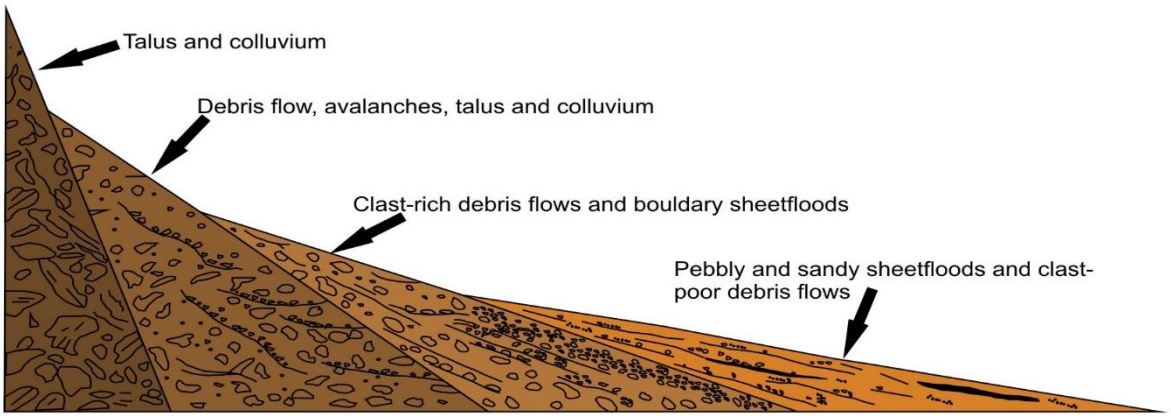

Figure 9: Cross-section of facies distribution in a debris-flow dominated alluvial fan, debris-flows dominate the proximal facies while sheetfloods are more pronounced in the distal facies. Notice decreasing grain size, better grain organization and loss of depositional energy (capacity) downfan. (Modified from Blair and McPherson (1994a))

3.2 Rift Basins and Half-Graben Formation

3.2.1 Half-Graben Geometry

Rift basins are generally formed as a response to divergent movement of tectonic plates, the divergent movement leads to a collapse of the crust and formation of normal faults as the crust accommodate stress. The upper parts of the crust normally deforms by brittle failure (faulting) while the lower parts of the crust deforms by ductile failure (Twiss and Moores, 2007). Rift basins and their infill are heavily influenced by the displacement geometry of the basin bounding normal faults. The most typical rift basin is a fault-bounded feature known as a half-graben. A half-graben has a triangular geometry, where the boundaries of the feature are the bounding fault, the rift onset unconformity (unconformity between pre-rift and syn-rift deposits) and the post-rift unconformity (unconformity between syn-rift and post-rift deposits) (Schlische, 1991). For active or present day half-grabens, the post-rift unconformity is equivalent to the topography also known as the present –day depositional surface (Schlische, 1991). Whereas the hanging wall is downthrown, the footwall is often uplifted. Sediments deposited on the uplifted footwall block are commonly eroded and could potentially be redeposited in the hanging wall accommodation space. The geometry and size of a half-graben is dependent on the displacement profile of the bounding fault(s), (Contreras et al., 1997; Gibson, 1989; Schlische, 1991; Schlische and Anders, 1996); the displacement is highest at the fault center and decreasing along the strike of the fault, towards the tip line. Parallel to the fault-strike, the displacement of an initial horizontal surface decreases with greater distance to the fault. Individual faults grow with time allowing for increased displacement of the bounding fault, the width of the half-graben is also increasing with time. The width of the basin is increasing as a result of (1) the width of the hanging wall deflection is increasing (Barnett et al., 1987) and (2) the length of the basin bounding fault is increasing (Cowie, 1998).

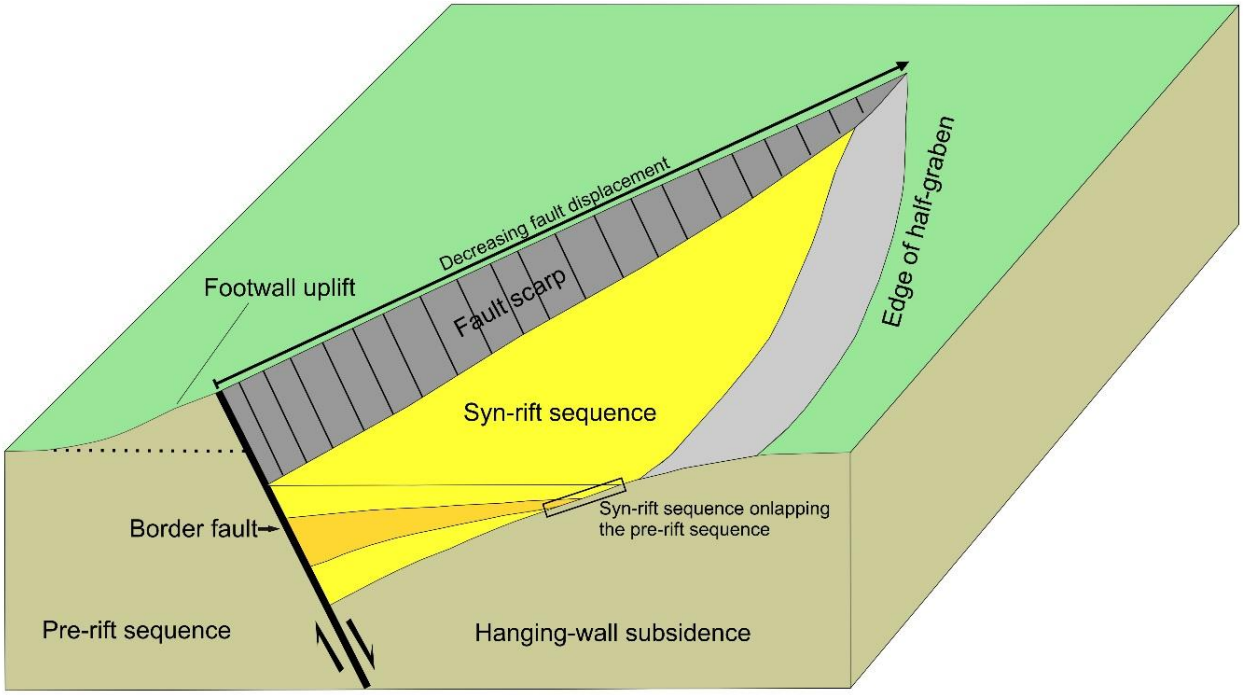

Figure 10: Conceptual figure of a half-graben showing the main processes and features. The relationship between the syn and pre rift sequences are nicely exposed along with the subsidence and uplift related to the fault movement. (Modified from (Schlische, 1994))

3.2.2 Sedimentation within Half-Grabens

Gawthorpe and Leeder (2000) suggested a tectono-sedimentary evolutionary model for continental extensional basins, from rift initiation to "fault death" stage. Their evolutionary model is suitable as an analogue for the early stages of the Corinth rift system. At the initiation stages of the Corinth rifting, the sedimentary deposits were only terrestrial with no marine influence. Figure 11, 12 and 13 displays the conceptual model of sedimentary input into an evolving rift system. The following section and figures will in simple manners explain some of the stages in the tectono-sedimentary evolutionary model for extensional continental basins from (Gawthorpe and Leeder, 2000).

Stage 1: Initiation Stage

Figure 11 displays the initiation stage of tectono-sedimentary model from Gawthorpe and Leeder (2000). During the early rift stage, several sub-basins are formed in the hanging wall of propagating normal fault segments. The sediment supply is mainly dominated by large antecedent fluvial systems, the fluvial systems can either incise/erode the footwall (1) or migrate around the fault tip (2). More importantly, the model displays different types of alluvial fans, alluvial fans where the sediments are mainly derived from the fluvial systems (these fans tend to be larger) and alluvial fans where the sediments are derived from local erosion of the footwall (drainage catchments).

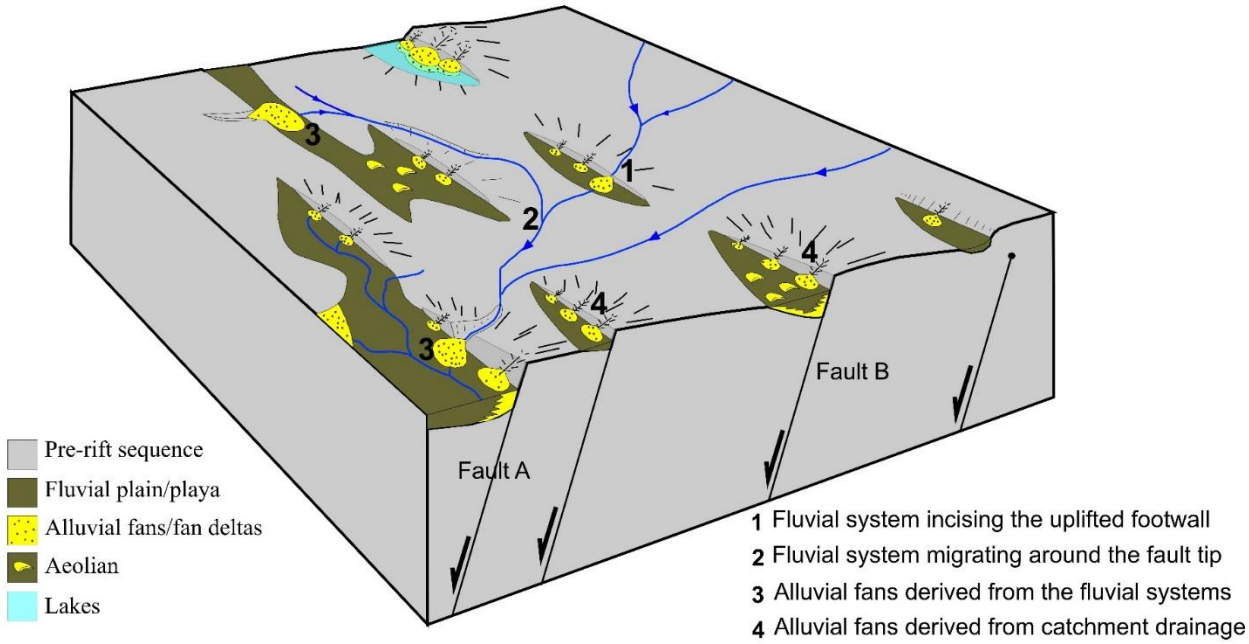

Figure 11: Fault initiation stage. (Modified from Gawthorpe and Leeder (2000))

Stage 2: Interaction and Linkage Stage

Figure 12 displays the second stage of the evolutionary model, at this stage the normal fault segments seen in Figure 11 has linked to form two continuous normal faults. The fluvial systems are changing pathways as a response to the uplifted footwalls, and have to incise and erode the uplifted footwall in order to keep its path. Alternatively, they use the fault segment boundary (shown in Figure 11 & 12) as a pathway. Alluvial fans are deposited from both margins of the half-graben, sourced from drainage catchments in the footwall and from fluvial systems. The size of the alluvial fans and catchment drainages decreases towards the tip of the faults. Fault A and B display different displacement and sediment supply. Fault A has high displacement and high sediment supply while Fault B has low displacement and low sediment supply.

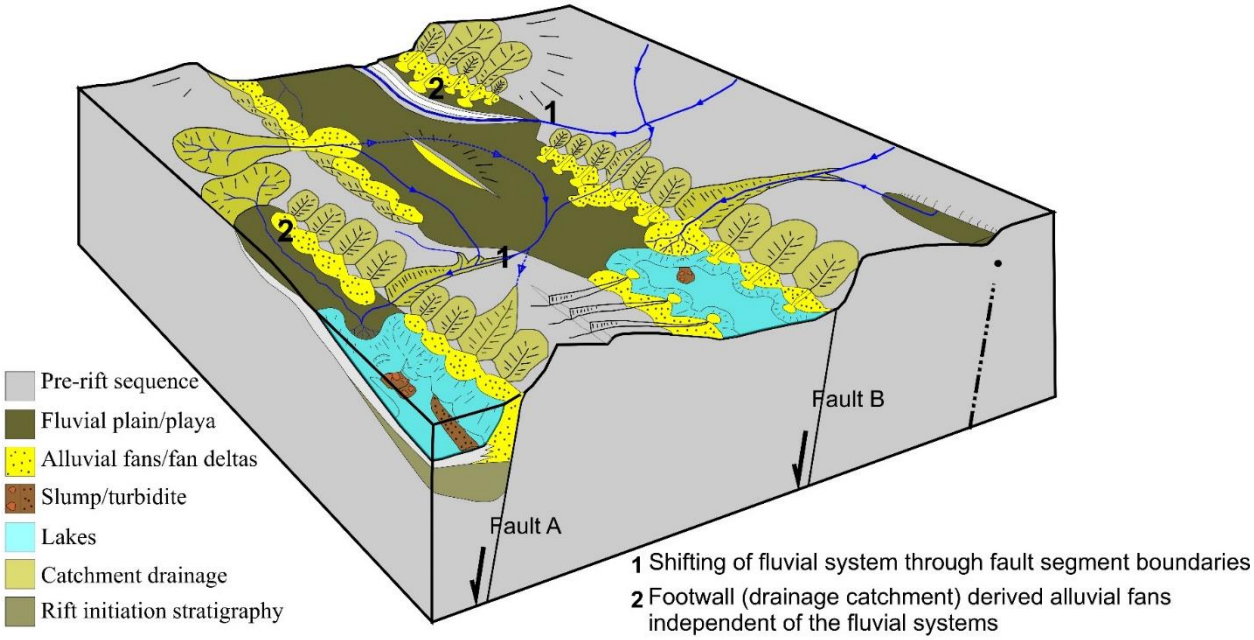

Figure 12: Interaction and linkage stage. (Modified from Gawthorpe and Leeder (2000))

Stage 3: Fault Death Stage

The final stage of the tectono-sedimentary evolutionary model for continental environments is the "fault death" stage. At this stage displacement of the main faults, Fault A and B, has ceased and the main displacement has shifted to the hanging wall of Fault B (Fault C). This implies uplift, incision and reworking of older catchment derived alluvial fans. Due to the extensive footwall uplift, the fluvial systems have shifted, and now run parallel to the normal faults.

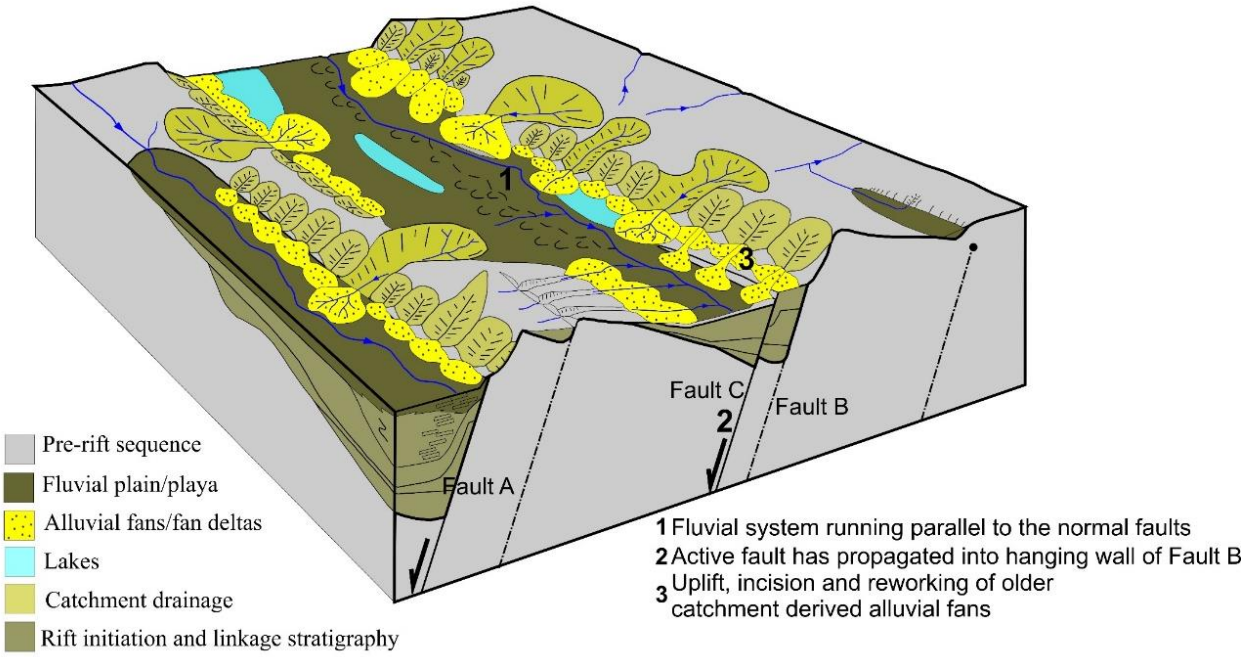

Figure 13: "Fault death" stage. (Modified from Gawthorpe and Leeder (2000))

Chapter 4: Methodology

The methodology chapter will provide an insight into the methods and approaches used to collect and interpret the data used in the study. The majority of the data were collected in the field, while the processing and interpretation of the data were completed by the use of different software in the post-field stage of the study.

4.1.1 Pre-field Work - Planning

In order to fulfill the objectives set for this study a large area within the Kerpini Fault Block and northern parts of the Kalavryta Fault Block was mapped. The size of the study area means that the pre-field work was important in order to cover the required area. In order to do so, maps were studied to find the best suitable roads and tracks. Hardcover maps and digital elevation maps (DEM) proved too "rough" with resolution around 30 m. Where maps proved to be inadequate, Google Earth was a useful tool in filling the details. The ability to view the study area in three dimensions proved very valuable when planning the locations and outcrops to study. In addition to plan different study locations, literature was thoroughly studied.

4.1.2 Fieldwork – Data Gathering

The data gathering can roughly be subdivided into two parts, stratigraphic data and structural data. The stratigraphic data includes outcrop descriptions, facies studies, bedding dips and paleoflow directions. Structural data includes fault strike/dip, and mapping contacts (unconformity/faults). Six simple steps from Tucker (2011) were used to describe outcrops, the steps are as followed: 1. Lithology 2. Texture 3. Sedimentary structures 4. Color 5. Geometry and relationships 6. Fossils. Grain size, sorting, matrix content and roundness of clasts were important contributors when describing facies. In order to find an average clast size for different facies and outcrops, the 10 largest conglomerate clasts within an area of 1x1m were measured and averaged (Figure 15). Throughout this thesis, grain and clast size will be discussed, Figure 14 shows a table used to classify the different grain/clast sizes. Paleoflow indication data were collected by searching for imbricated disc and tabular shaped clasts (Figure 16). By using this method, it is hard to determine/measure an accurate flow direction, but general flow directions/trends were obtained. The majority of strike and dip angles date were measured by using a Krantz geological compass, this is a well know geological compass to measure exposed bedding. Some fault strike measurements were obtained using a SILVA Sighting Compass with Mirror, this is a compass which makes it possible to measure strike angles from a distances by

sighting. The accuracy of strike/dip measurements on exposed bedding are not especially accurate due to the rough surface, but are considered good enough to give a representative measurement. The measurement done with the SILVA sighting compass is considered to be fairly accurate. All outcrops, locations and measurements were recorded by a GPS waypoint.

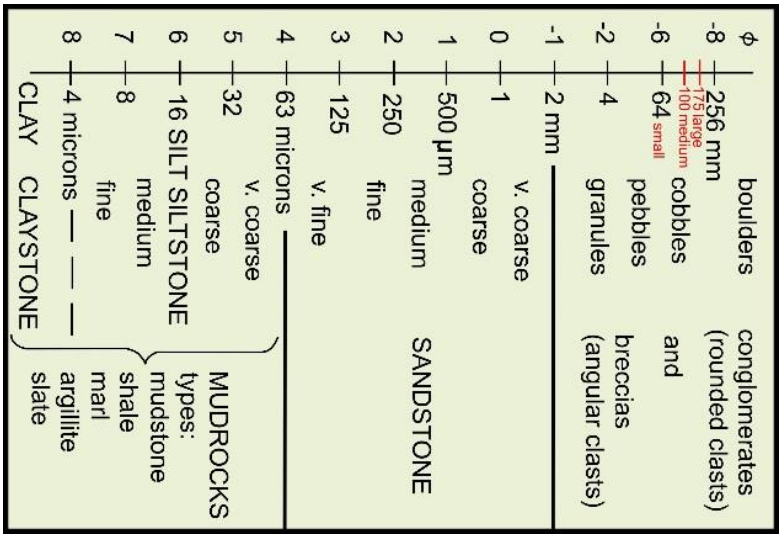

Figure 14: Definition of the grain/clast size used in this study. Additional classification of cobble sized clasts (marked with red) has been added for further detail in the outcrop description. Modified from (Tucker, 2011)

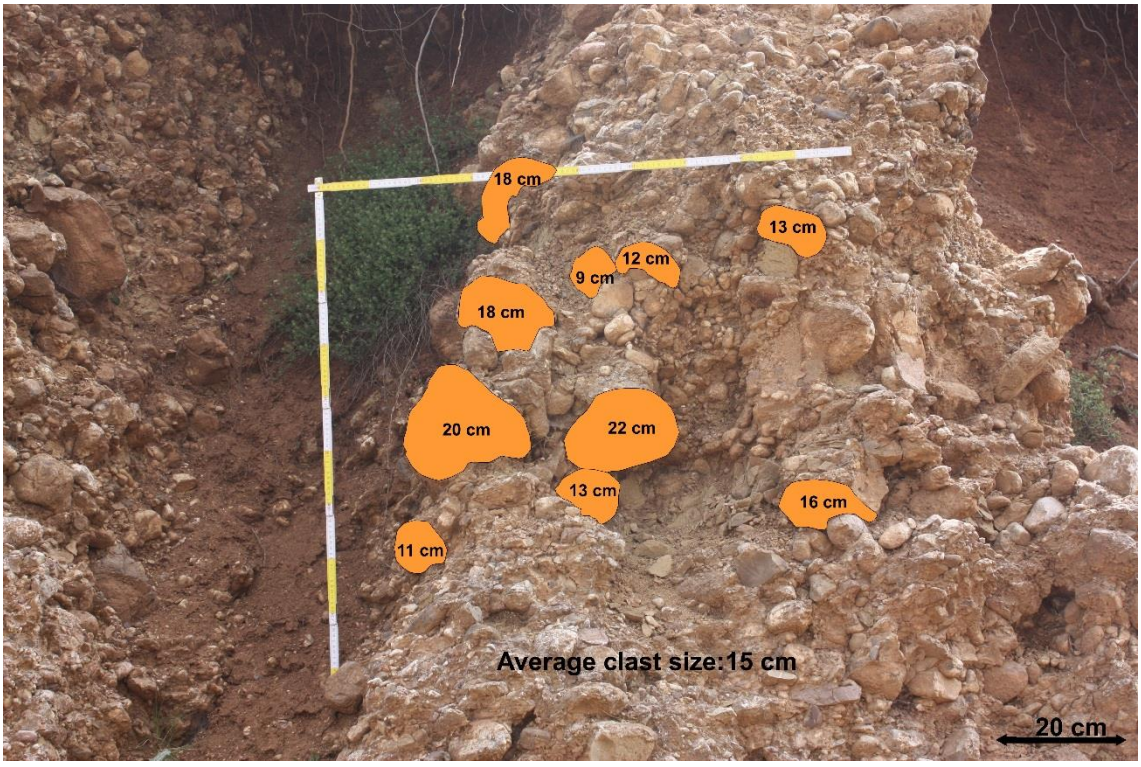

Figure 15: Example of how the average grain size of an outcrop is measured. The ten largest conglomerate clasts within an area of 1x1 m is measured and averaged following the method of Tucker (2011)

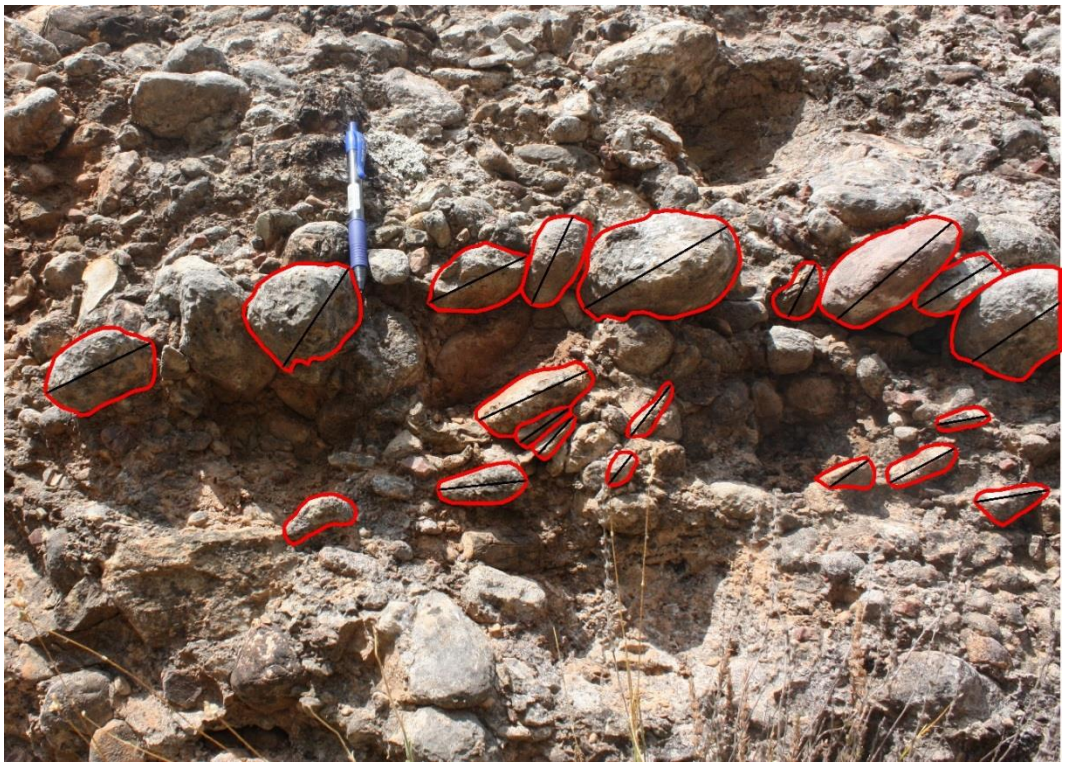

Figure 16: Example of imbrication in the Upper Conglomerates, clasts are dipping down to the left indicating transport to the right. This figure displays what might be the best example of imbrication found within the different conglomeratic units in the study area.

4.4.3 Post-field Work – Processing and Interpretation of Data

Upon returning from the field, all the data were synthesized and categorized according to their relevance. Geo-referenced geological maps including dip angles, dip directions and paleoflow directions were created by using ArcGIS. Cross-sections created in the field were digitized without vertical exaggeration in CorelDRAW by using an elevation profile from a DEM. In addition to creating the cross-sections, CorelDraw were used to modify figures from previous publications and modifying pictures taken in the field.

Chapter 5: Field Observations – Stratigraphic Units

5.1.1 Introduction

There are a number of different stratigraphic units within the Kerpini and Kalavryta Fault Block, each unit will be described separately in the following chapter. The description will include lithology, rock texture, geometry of unit and the extent of individual units. Being the main focus of this study, the Upper Conglomerates will be described in further details than the other stratigraphic units. The other units must also be considered, as their development is interlinked with the Upper Conglomerates and the general development of the Kerpini Fault Block.

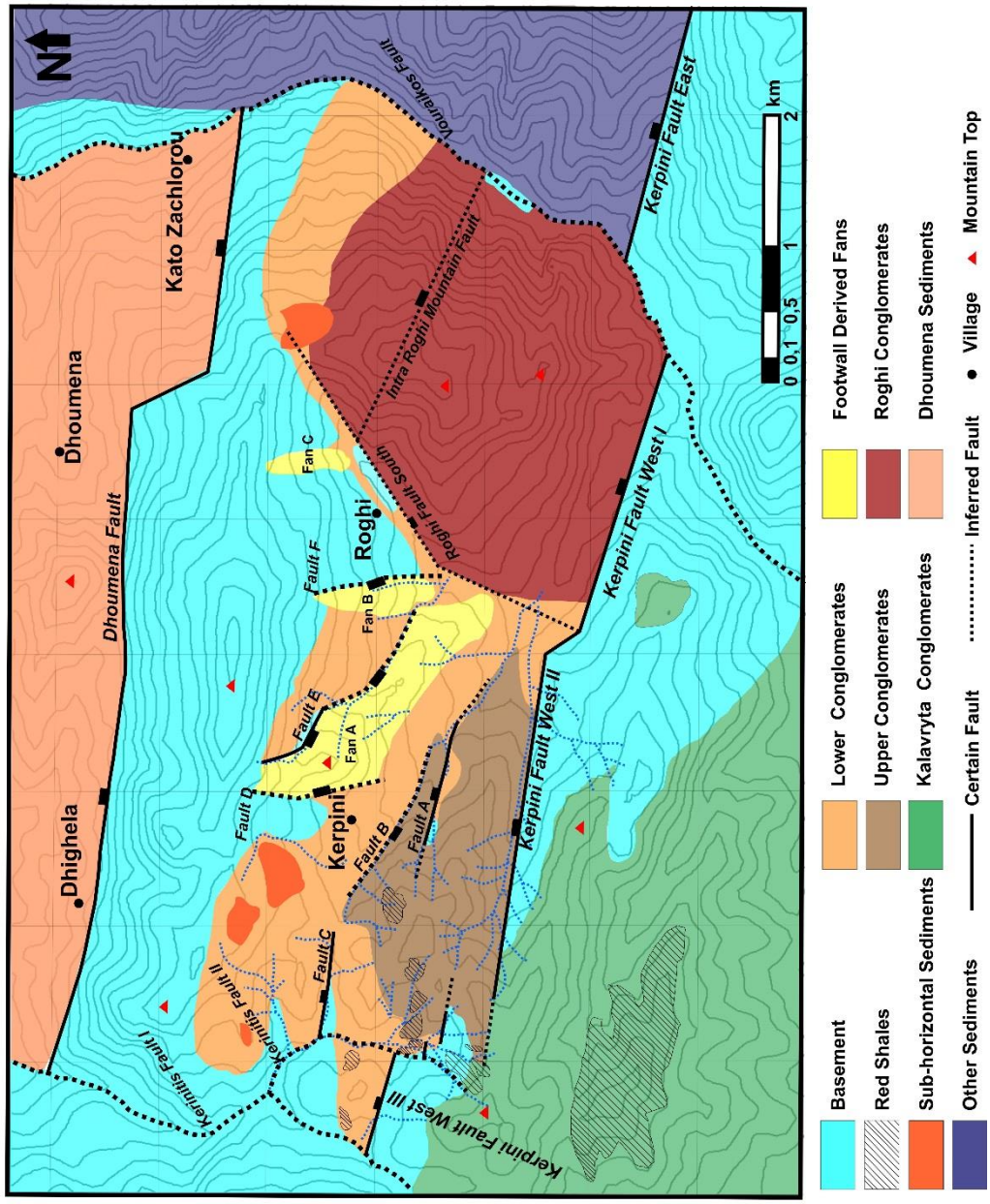

Figure 17: Geological map of the study area with all the faults and stratigraphic units marked. The legend below the map shows the color-coding of the different stratigraphic units and the certainty in the faults. The Upper Conglomerates are marked with a light brown color and are situated in the southwest corner of the fault block.

Stratigraphic unit	Color code	Location(s)	Lithology	Max preserved thickness (m)	Grain size	Dip/Dip direction (°)	Contacts
Basement		Kalavryta Fault Block	Deformed and metamorphosed limestone and chert	Unknown	N/A	N/A	Kalavryta Conglomerates and Lower Conglomerates sits unconformably on top of the basement
		Immediate footwall of the Kerpini Fault					
		Northern part of the Kerpini Fault Block					
		Footwall of faults A,C,D and E					
Kalavryta Conglomerates		Kalavryta Fault Block	Conglomerate and sandstone	500	Conglomerate: Large cobbles-boulders Sandstone: Coarse to very coarse	24/163	Sits unconformable on the basement in the Kalavryta Fault Block
		Immediate footwall of the Kerpini Fault					
Lower Conglomerates		Immediate hanging wall of the Kerpini Fault in the west	Conglomerate and sandstone	600	Conglomerate: Pebbles-large cobbles Sandstone: Coarse to very coarse	25/195	Sits unconformable on the basement in the Kerpini Fault Block
		Middle of the Kerpini Fault Block					Underlies the Upper Conglomerates and sits unconformably on top of the basement
		West of Roghi Mountain					Underlies the Dhoumena footwall-derived fans and sits unconformably on top of the basement
Roghi Conglomerates		Roghi Mountain	Conglomerate and sandstone	900	Cobbles-Boulders	25/185	Sits unconformable on the basement in the Kerpini Fault Block
Red shales		Kalavryta Fault Block	Red shale/soil	Kalavryta Fault Block: 70	Clay-Silt	N/A	Kalavryta Fault Block: Sits on top of the Kalavryta Conglomerates
		Southwestern Kerpini Fault Block		Kerpini Fault Block: 15			Kerpini Fault Block: Sits on top of the basement, Upper and Lower Conglomerates. Interpreted to be a soil profile
Dhoumena footwall-derived fans		Northeast of Kerpini Village	Conglomerates, sandstone and marl	250	Silt-Cobbles	25/187	Sits unconformable on top of the basement, and on top of the Lower Conglomerates
		Northwest of Roghi Village					Sits unconformable on top of the basement, and on top of the Lower Conglomerates
		Northwest of Roghi Mountain					Sits unconformably on top of the basement
Sub-horizontal Sediments		Northwest of Kerpini Village	Conglomerates	100	Pebbles-Cobbles	N/A	Sits on top of the Lower Conglomerates
		Northwestern part of Roghi Mountain	Conglomerates	150	Pebbles-Cobbles		Sits on top of the Lower Conglomerates
Upper Conglomerates-Southern Lobe		Immediate hanging wall of the Kerpini Fault	Conglomerates, sandstone and marl	300	Silt-Boulders	25/176	Sits on top of the Lower Conglomerates
Upper Conglomerates-Northern Lobe		Immediate hanging wall of the Fault A	Conglomerates, sandstone and marl		Silt-Boulders	20/147 (South dipping beds) 24/61 (North dipping beds)	Sits on top of the Lower Conglomerates
Upper Conglomerates-Western Conglomerates		Immediate hanging wall of Kerpini Fault Step 3	Conglomerates		Cobbles-Boulders	22/190	Sits on top of the Lower Conglomerates

Table 1: Summary of the different stratigraphic units within Kerpini and Kalavryta Fault Blocks. The data shown in the table originate from field observations and cross-sections.

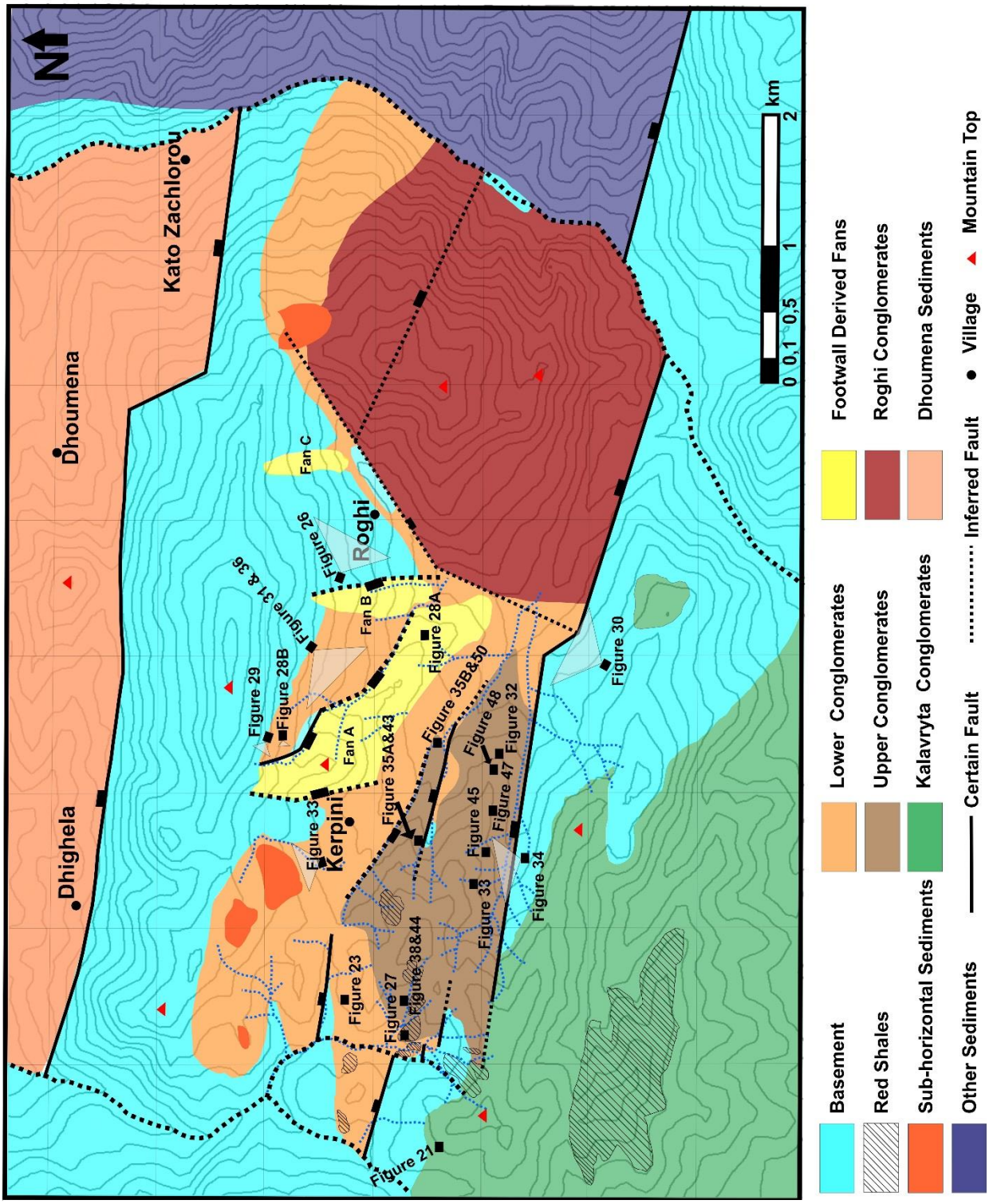

Figure 18: Geological map of the study area showing the locations of the figures in the following subsections. Overview figures are shown by a triangle that more or less represents the view of the photo in the figure.

5.1.2 Basement – Kerpini and Kalavryta Fault Blocks

The basement of the Corinth Rift system is composed of Upper Triassic-Jurassic carbonates and Upper Cretaceous-Tertiary sandy turbidities (Degnan and Robertson, 1998; Skourlis and Doutsos, 2003) and is considered as the pre-rift sequence. This stratigraphic unit is heavily deformed and metamorphosed as a result of thrusting from Cretaceous to Miocene times (Ford et al., 2013). At the locations where it is exposed the deformation is visible as numerous fractures and folds. In addition to being deformed, the carbonates are heavily weathered and eroded. The deformation and weathering makes it hard to do any type of measurements on the basement unit. Within the Kerpini Fault Block two types of basement lithology has been distinguished, grey to brownish limestone (Figure 19) and red chert (Figure 20). The relation between the two different basement lithologies has not been studied in this thesis and will not be of any importance. Red cherts have only been distinguished at certain locations, which means that the main portion of exposed basement is grey to brownish limestones. Folding is more pronounced in the grey/brownish limestone, while fractures are distinguishable in both lithologies.

Figure 19: Grey to brownish carbonate basement outcrop in the easternmost parts of the Kalavryta Fault Block, in the immediate footwall to the Kerpini Fault. The outcrop clearly displays the chaotic nature of the basement carbonates with folding and fractures.

Figure 20: Red chert-basement outcrop located between the Northern and Southern Lobes in the central parts of the Kerpini Fault Block. Fractures and cleavages are clearly visible within the chert. Nodules within the red chert are common.

The basement is exposed at several locations within the Kerpini and Kalavryta Fault Blocks, Figure 22 display a map of all the basement outcrops located within the study area. Basement outcrops described below are marked on the map with a number to show their location. Basement is exposed north of the Kerpini and Roghi villages, in the slope towards the Dhoumena footwall (1). Along this slope, there is a low angled unconformable contact between the basement and overlying sediments. The elevation of the contact varies from east to west, with a basement high located north-west of Kerpini village (2). At this location, the basement-sediment contact drops down towards Kerpini village before it rises again towards the Dhoumena footwall. This basement high is one of the locations where red cherts are observed. In the westernmost part of the Kerpini Fault Block, close to Skepasto Mountain, the basement is located close to the Kerpini Fault, as the basement-sediment contact has dropped down (3). The Kerinitis River and a large mountain composed of basement, Skepasto Mountain, marks the westernmost extent of the Kerpini Fault Block (4). Skepasto Mountain is an elevation standing out with approximately 300m of relief compared to nearby topography.

Beside the clearly exposed basement in the northern parts of the fault block, smaller basement outcrops are observed in the southern and eastern parts of the Kerpini Fault Block. Basement

(red chert) is observed between the two lobes of the Upper Conglomerates (5), in a river valley, in the proximity of the Kerpini Fault (Figure 21). This basement outcrop occurs at an unexpected structural position and therefore needs further explanation. This small basement outcrop is roughly 80m long (east-west direction) and 50m wide (north-south direction), and consists of a combination between loose-weathered and solid chert. Due to dense vegetation and recent soil at the outcrop location, an exact contact between the basement and sediments could not be established.

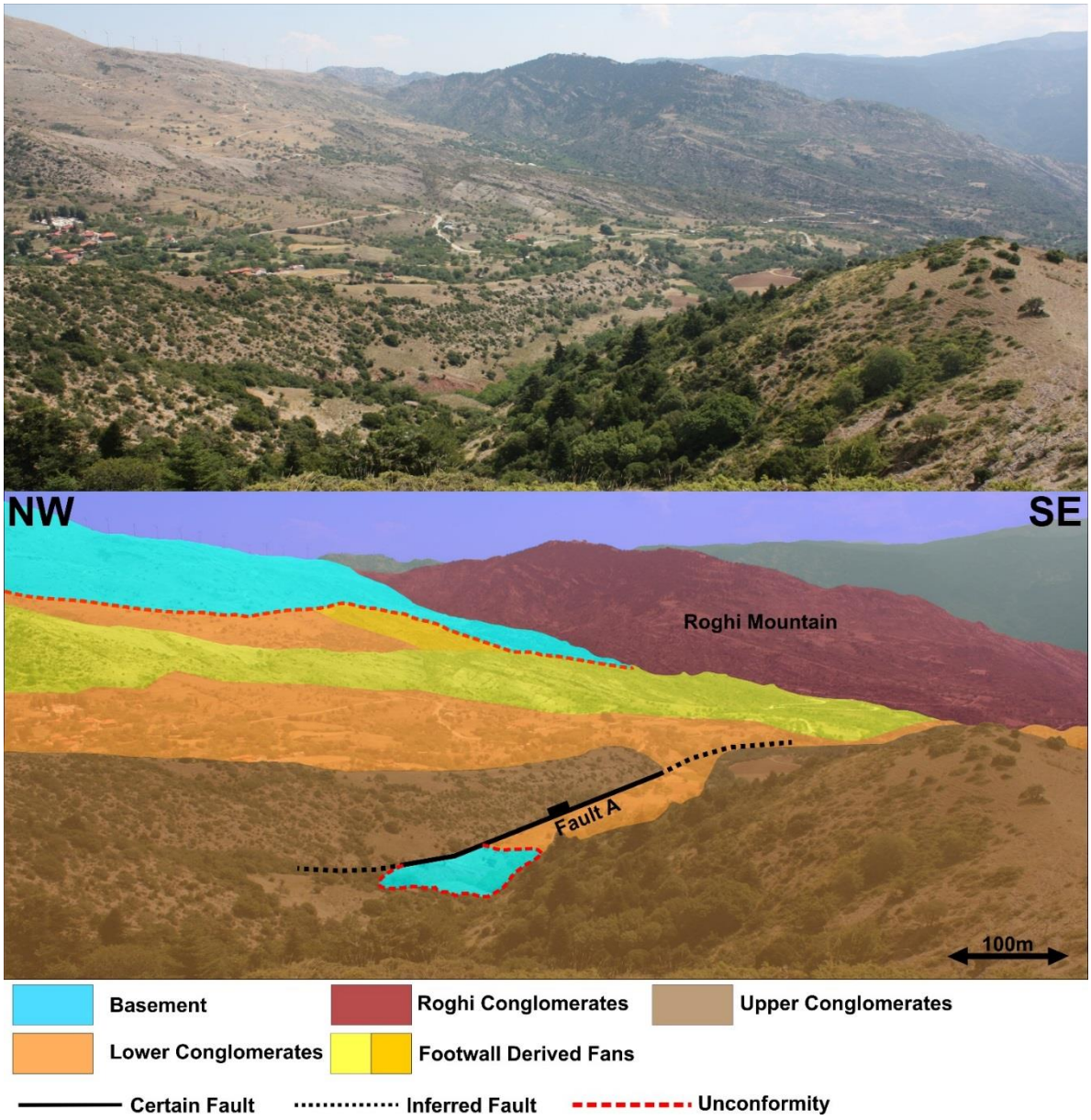

Figure 21: Basement outcrop between the Southern and Northern Lobe of the Upper Conglomerates. The topographic position of the basement outcrop indicates a fault immediately north of the outcrop, meaning the basement is a part of the uplifted footwall of the fault. Scale is relative to the small basement outcrop

At the eastern limit of the outcrop, the basement disappears beneath recent soil and the Lower Conglomerates. At the western limit, the basement disappears beneath the Upper Conglomerates. As Figure 21 shows, the basement is uplifted as a response to Fault A.

Moving towards the eastern boundary of the fault block, south of Roghi Mountain, basement is exposed in what used to be a quarry (Figure 19). This basement outcrop is located in the Kalavryta Fault Block in the immediate footwall to the Kerpini Fault, at the lowest elevation point of the fault block, in an area believed to be the depocenter of the Kerpini Fault Block (6). There are no syn-rift sediments in this immediate area. Moreover, the basement can be followed westwards in the footwall to the Kerpini Fault, where eventually it is overlain by syn-rift sediments and a clear unconformity can be mapped (7).

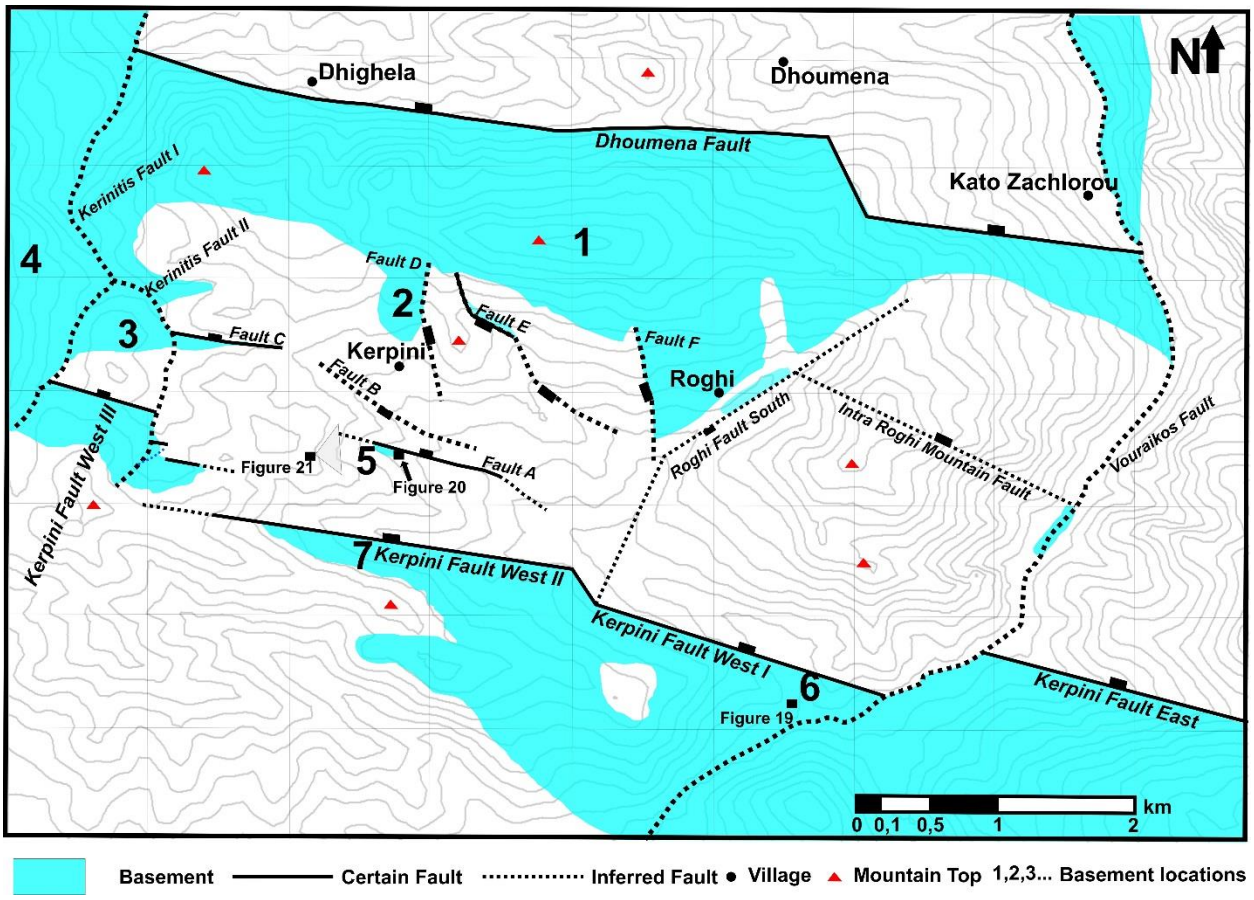

Figure 22: Map of the basement in the Kerpini and Kalavryta Fault Blocks. The position of figure 19.20 and 21 is marked on the map. In addition, the locations of the different basement outcrops/locations described in subsection 5.1.2 are marked on the map. 1. Basement north of Kerpini and Roghi villages towards the Dhoumena footwall. 2. Basement high northwest of Kerpini village. 3. Lower basement-sediment contact in the western part of the Kerpini Fault Block. 4. Skepasto Mountain. 5. Chert-inlier 6. Basement in the Kalavryta Fault Block. 7. Basement in the Kalavryta Fault Block overlain by Kalavryta Conglomerates.

5.1.3 Kalavryta Conglomerates – Kalavryta Fault Block

The Kalavryta Conglomerates lie unconformably above the basement in the Kalavryta Fault Block (green unit in Figure 18). Outcrops in the proximity to the Kerpini Fault have been studied, in order to understand if there is any relationship between the Kalavryta Conglomerates and the Lower Conglomerates. This unit is important for the evolution of the Kerpini Fault Block. This is because it is cut by the Kerpini Fault and must therefore be present in the Kerpini Fault Block, unless it was eroded subsequent to faulting. The unit mostly consists of cobble-boulder sized conglomerates with occasional thin sandstone/ pebble-conglomerate lenses. Some of the sandstone/fine conglomerate beds have channel like characteristics, such as the geometry and texture. The channels display a grain size varying from coarse sandstone to pebbly conglomerates. Conglomerates, the main lithology, generally show cobble-boulder clast size with a northwards fining trend. The clast size is on average between medium cobbles and boulders (100-256mm) in the southern part of the studied area. The Kalavryta conglomerates continue further southwards, but only the deposits in the proximity to the Kerpini Fault Block have been studied in this thesis. Further towards the north and the Kerpini Fault, the grain size decreases and is in the range of small cobbles to medium cobbles (64-100mm).

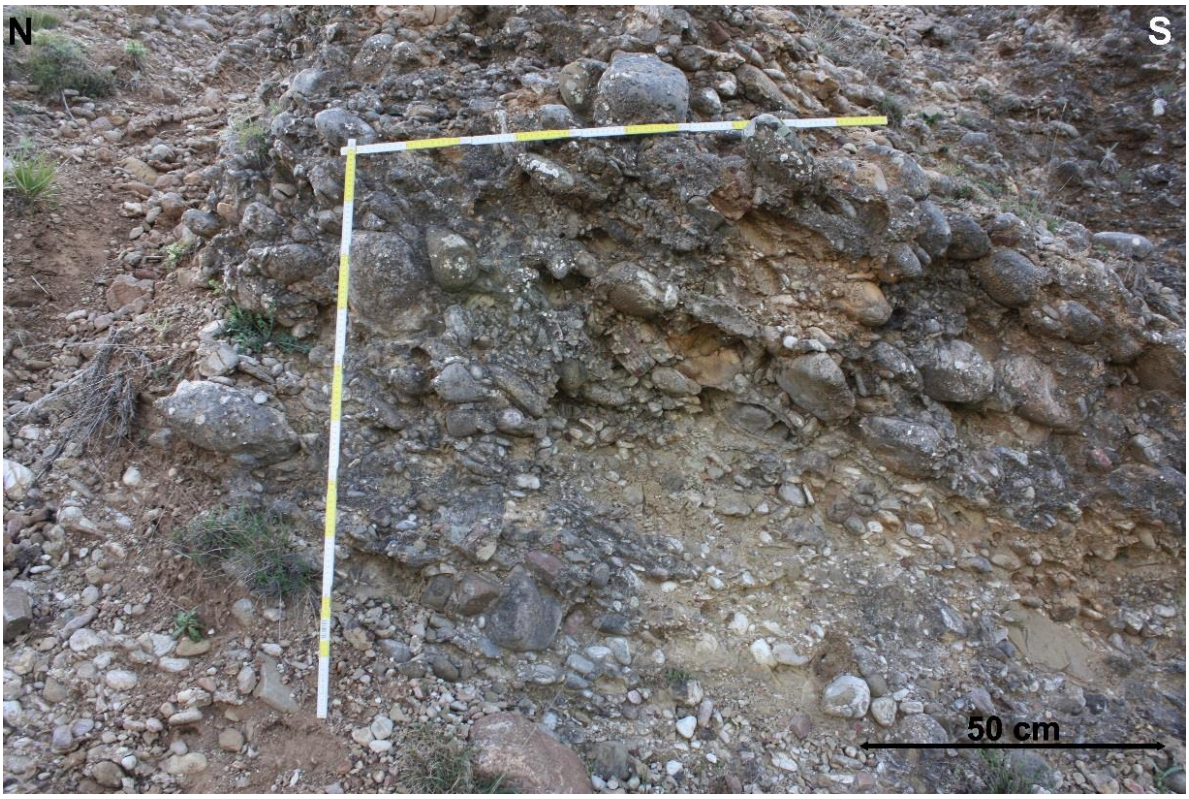

Figure 23: Chaotic and unorganized Kalavryta Conglomerates. This figure displays an outcrop where large clasts are deposited within the same bed with no clear bed boundary (upper nor lower).

Beds and bedding contacts are poorly defined, but in some outcrops there seems to be a trend where the larger clasts (boulders and large cobbles) are within the same bed but without a clear bed boundary (Figure 23). Apart from the possible beds with larger clasts, the conglomerates are poorly sorted and unorganized. The sorting and organization does not change, even though the clast size decreases northwards. The cobble-boulder sized conglomerates in the south are more clast supported than the conglomerates towards the Kerpini Fault, meaning that the northern conglomerates are more matrix supported.

Most of the clasts are limestone clasts, with some chert and sandstone clasts. The amount of sandstone clasts is higher in this unit than any of the other conglomeratic units. Sandstone clasts are often rounded with high sphereicity and the clast size varies from pebbles to boulders. Limestone clasts are subrounded to sub-angular and vary between high and low sphereicity. Chert clasts are smaller than the other two lithologies and rarely exceed pebble size (64mm).

Due to the Kalavryta Conglomerates not being the focus of this project, only a few dip and dip direction measurements were taken. The dip and dip direction data collected display a uniform trend, with a southeast dip direction and a dip angle in the range of 21˚ to 27 ˚. Any decrease of dip angle up the section is not observed, neither is there any differences in dip angle between the finer conglomerates in the north and the coarser conglomerates in the south.

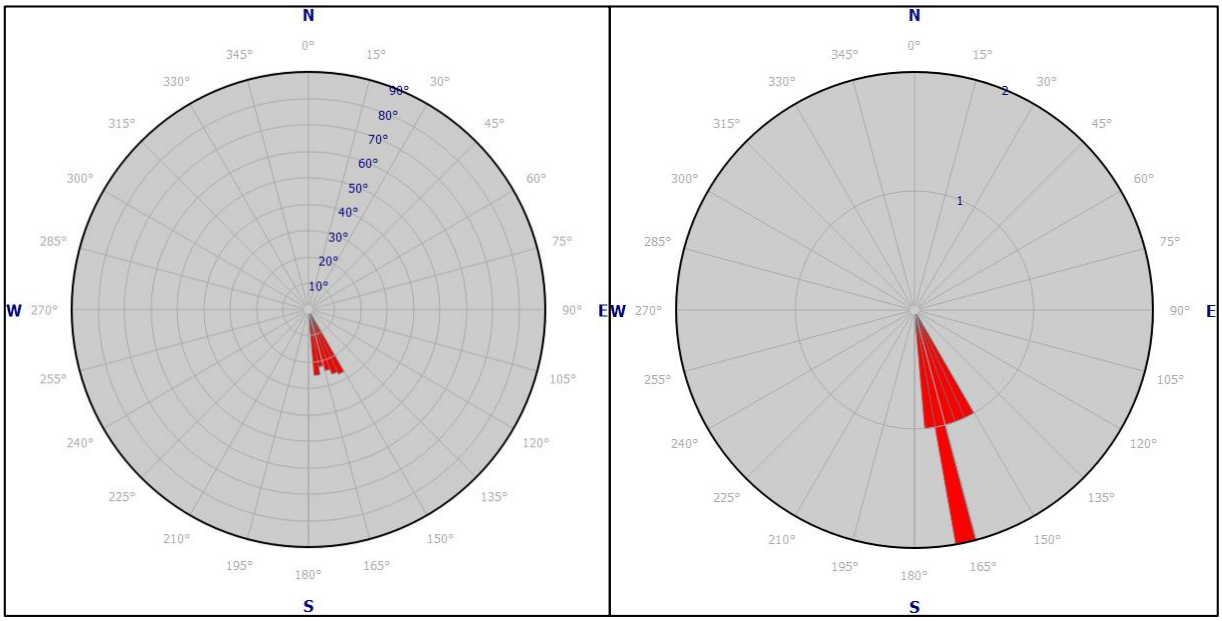

Figure 24: Rose diagram showing the dip angle and dip direction for the Kalavryta Conglomerates. The left diagram shows the dip angle increasing from the center of the diagram and the dip direction is shown in the outermost sector. The right diagram shows the dip direction along with the number of measurements, the sectors shows the number of measurements.

5.1.4 Lower Conglomerates – Kerpini Fault Block

The Lower Conglomerates unit sits unconformable on top of the basement in the Kerpini Fault Block. The unit is widespread in the Kerpini Fault Block, stretching from the Roghi Mountain in the east to the Kerinitis River in the west (orange unit in Figure 18). Sandstone and fine-grained conglomerate facies is recognized as channel shaped normal graded sandstone/conglomerate bodies within the coarser-grained conglomerates (Figure 25). Observations suggest a finer-grained channel deposits within larger-clast alluvial conglomerates. From this stage, the finer sandstone/conglomerates will be referred to as fluvial facies while the coarser conglomerates will be referred to as alluvial facies. An average grain size for the whole unit is hard to obtain due to the mixture of sandstone and conglomeratic facies. The grain size for the fluvial facies range from coarse sandstone to pebbly conglomerates, with an average of very coarse-grained sandstone (2-3mm). Alluvial facies display grain sizes ranging from pebbles to large cobbles, with some occasional boulders. The alluvial conglomerates appear massive, chaotic and ungraded, with poorly exposed bedding. Conglomerate clasts are predominantly grey to brownish limestones with some occasional red chert clasts, the ratio between limestone and chert clast is roughly 1:30. Limestone clasts are sub-angular to angular with high sphereicity, while chert clasts are subrounded to rounded with high sphereicity.

Figure 25: Lower Conglomerate Unit. The Lower Conglomerate Unit can be subdivided into fluvial and alluvial facies, the fluvial facies has been outlined in the figure. The alluvial facies consists of conglomerates with large clast size, while the fluvial facies consist of a mixture of pebbly conglomerates and coarse/very coarse sandstone. The fluvial facies appear as lenses within the alluvial conglomerates.

Poor exposure of beds within the Lower Conglomerates unit makes dip and dip direction measurements challenging. However, the exposed bedding displays a SSW dip direction. Dip directions in the middle and eastern part of the fault block tend to have a more SSW trend, while the western parts display a more pronounced south dipping trend. Average dip angle for the Lower Conglomerates unit is 26 °. There is no dip angle trend observed from east to west, as there is with the dip direction measurements. Any significant changes of dip angles up section are not observed. Paleoflow indicators such as imbrication are rare due to the chaotic and ungraded nature of the alluvial conglomerates. Due to weathering, it is difficult to predict any paleoflow directions from the fluvial facies. The few paleoflow indicators observed suggest a flow from the south.

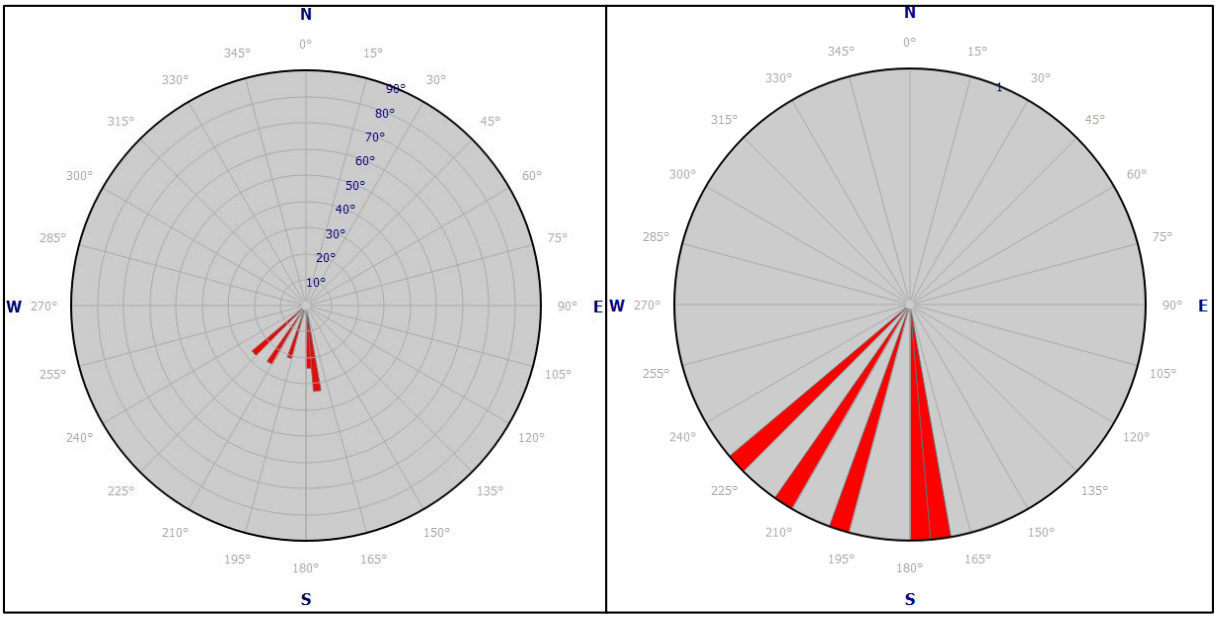

Figure 26: Rose diagram showing the dip angle and dip direction for the Lower Conglomerates.

The Lower Conglomerates unit gets thicker towards the depocentre in the eastern part of the fault block. This observation is based on the projection of the unconformity plane from the northern contact between the lower unit and the basement into the Kerpini Fault in the south (subsection 6.9). In the westernmost parts of the fault block, the Lower Conglomerates is in direct contact with the Kerpini Fault (Figure 18). Moving eastward, the Lower Conglomerates unit underlies the Upper Conglomerates (described in subsection 5.2) and the Footwall Derived Fans. The eastern extent of the unit is towards the Roghi Mountain where it is possibly displaced by the Roghi Fault South.

5.1.5 Roghi Conglomerates – Kerpini Fault Block

The Roghi Mountain is a feature that stands out in the Kerpini Fault Block. It is a 1 km (minimum) thick pile of cobble-boulder sized conglomerates. Due to steep topography and large amounts of vegetation, the middle and upper parts of the unit has limited accessibility. Roghi Mountain is displayed as the ruby red unit in Figure 18, bounded by the Kerpini Fault to the south, the Vouraikos Valley to the east, Roghi Fault South to the west and the unconformity to the north. Dahman (2015) concluded that a high angled transfer fault is located in the Vouraikos Valley. This transfer fault acts an eastern boundary to the Kerpini Fault West, the fault block itself and the western extent of the Roghi Conglomerates.

Its massive beds only visible from a distance characterize the Roghi Conglomerate unit. The bed thickness varies from 1 m to 10 m, with the thickest beds lying in the lower parts of the mountain. Clast size, organization and grading seem to be independent of the bed thickness. Clast size is in general large cobbles and boulders with an average of approximately 15-20 cm, there are finer grained sandstone beds in between the thicker and larger clast sized conglomerate beds. The majority of the beds appear chaotic and ungraded, which could indicate high depositional energy with low fluvial/water contribution. The Roghi Conglomerates are polymictic, with limestone, chert and sandstone clasts. Limestone clasts are sub-rounded to angular, chert clasts and rounded to sub-angular while the sandstone clasts are sub-rounded to sub-angular. Limestone clasts are more abundant than the other two types of clast lithologies. The conglomerates are clast supported with medium to coarse sandy matrix, matrix-sand is poorly sorted and ungraded. A slight northwards fining of the clast size is observed. From south to north the clast size only decreases a few cm, this implies that the whole unit is characterized by coarse-grained (boulder and cobble) conglomerates.

Correlate of beds between the west and east section of the mountain proves challenging. The reason being that the thickness of the beds varies from the east to the west, and the dip angle and dip direction of the beds changes from east to west. Possible explanations for these phenomena are internal faulting (within the mountain) and/or facies changes across the unit. Two simultaneous master projects are investigating either if the changes from west to east can be explained by facies changes or if the changes are structurally controlled. Figure 28 display a picture of the western section of Roghi Mountain. Beds in the western section (Figure 28) of the

mountain are in general thinner than in the eastern section. In the middle of Figure 28, dip angle of the beds decrease, from 25° in the northern parts to 20° in the southern part. Thus, it is evident that there are changing dip angles in both east west and north-south direction.

Limited dip angle and direction measurements were made, as Roghi Conglomerates is not the focus of this study. As the accessibility of the unit is limited, some of the measurements were done from a distance and hence the uncertainty of these measurements is higher. A general southward dip direction towards the basin bounding Kerpini Fault is observed. The dip angles vary from 22°-27°, with no distinct decrease of dip angle observed within the younger strata.

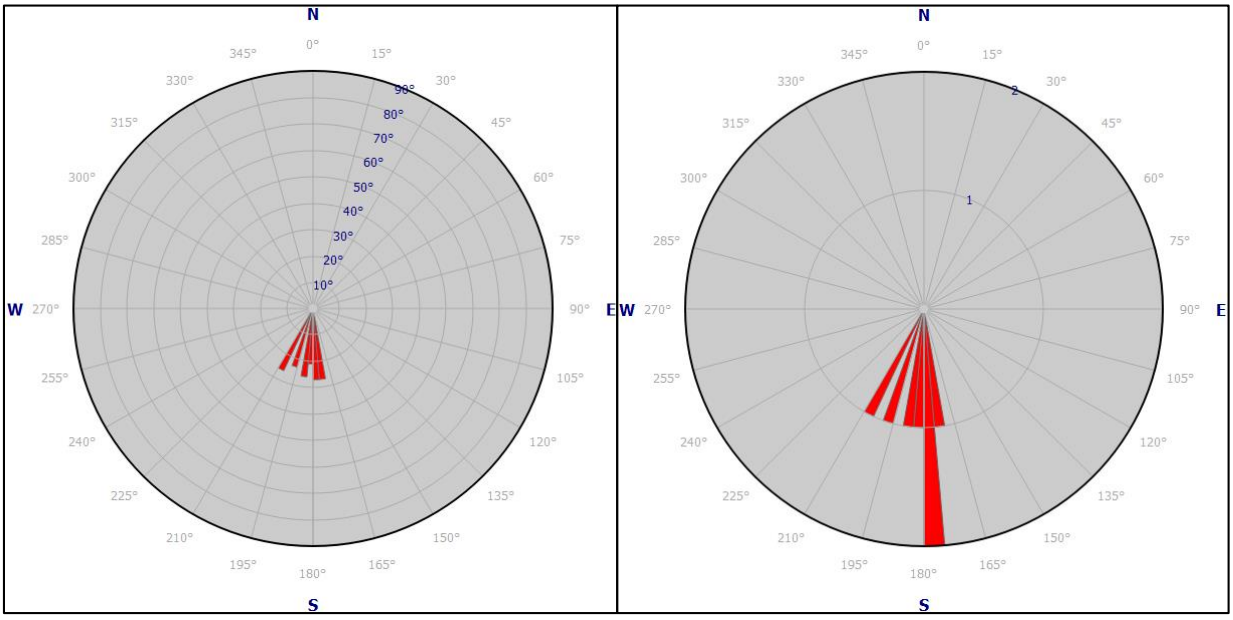

Figure 27: Rose diagram showing the dip angle and dip direction for the Roghi Conglomerates (Roghi Mountain).

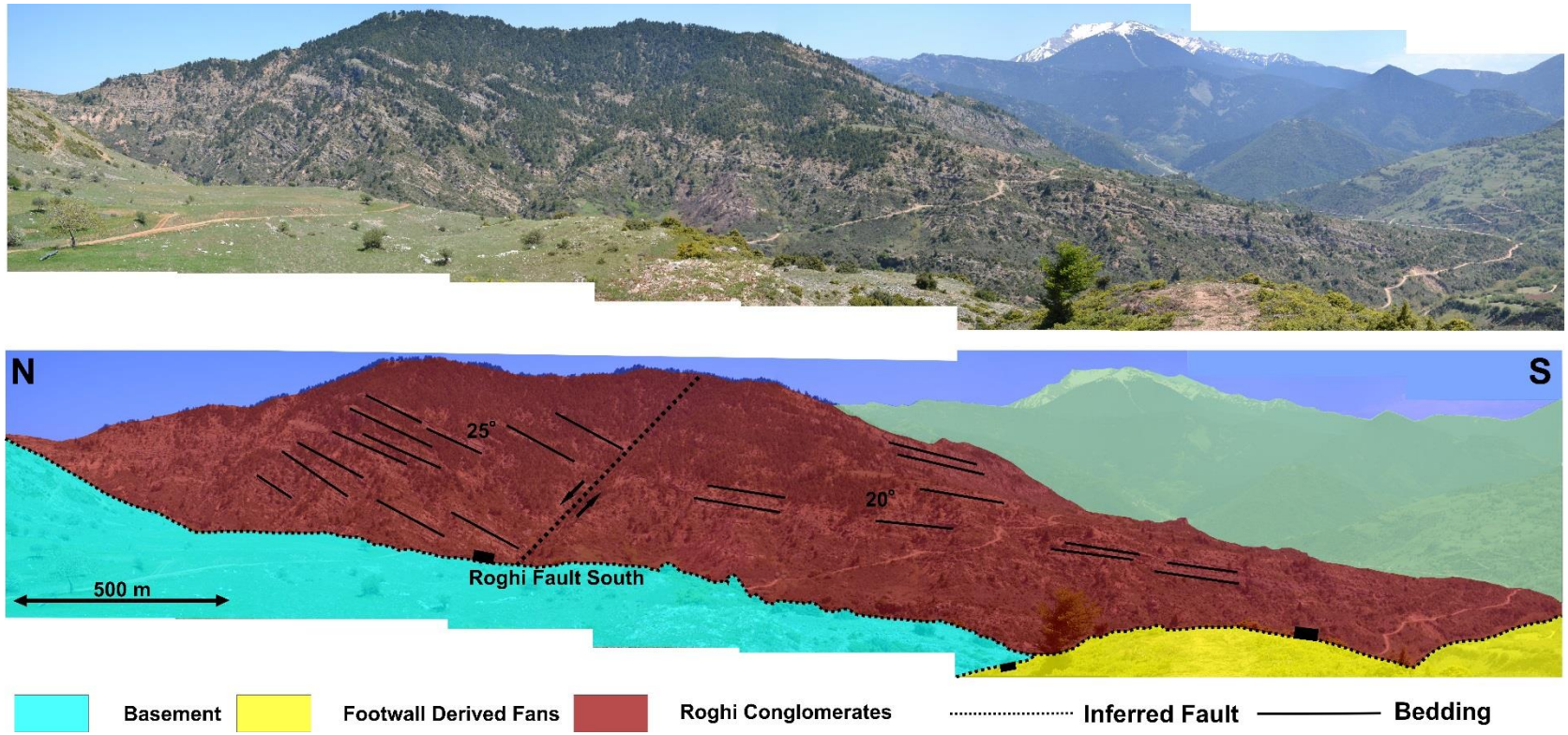

Figure 28: Western section of Roghi Mountain. Notice the change of bedding dip in the middle of the mountain, which has been interpreted to be a result of a normal fault within the mountain. The massive bedding of the conglomerates is also noticeable in the figure. Scale is relevant to Roghi Conglomerates Photograph kindly provided by the University of Stavanger, Chris Townsend.

5.1.6 Red Shales – Kalavryta and Kerpini Fault Blocks

The Red Shales located within the Kalavryta and Kerpini Fault Blocks have been studied in detail by Rognmo (2015), without reaching a satisfactory explanation of their presence and their locations. The Red Shales are found at several different locations within the two fault blocks, at the uplifted footwall of the Kalavryta Fault, in the immediate footwall of the Western Kerpini Fault III, at the top of the Upper Conglomerates and within the Lower Conglomerates. The unit is marked by black stripes in Figure 18. As the name of the unit states, these sediments are very fine-grained (shale-silt) but are often found in combination with conglomerates (Figure 29). The conglomerates stand out, almost like pillars within the Red Shales. Several authors (Rognmo, 2015; Stuvland, 2015), have mapped fine-grained sediments, interpreted to be of lacustrine origin, in the southern part of the Kerpini Fault Block. These sediments are clearly in-situ in the Kalavryta Fault Block where they overly the Kalavryta Conglomerates. Lacustrine sediments in the southern part of the Kalavryta Fault Block appear loose and weathered, but by digging into it, it is consolidated Red Shales. The Red Shales found in the Kerpini Fault Block and in the northernmost Kalavryta Fault Block are unconsolidated, loose and weathered. It is unclear if the unconsolidated and loose sediments are in-situ. Some occurrences are more convincing than others. Therefore, it is possible that they are red soil deposits originating from the Kalavryta Fault Block as a late/recent soil deposit.

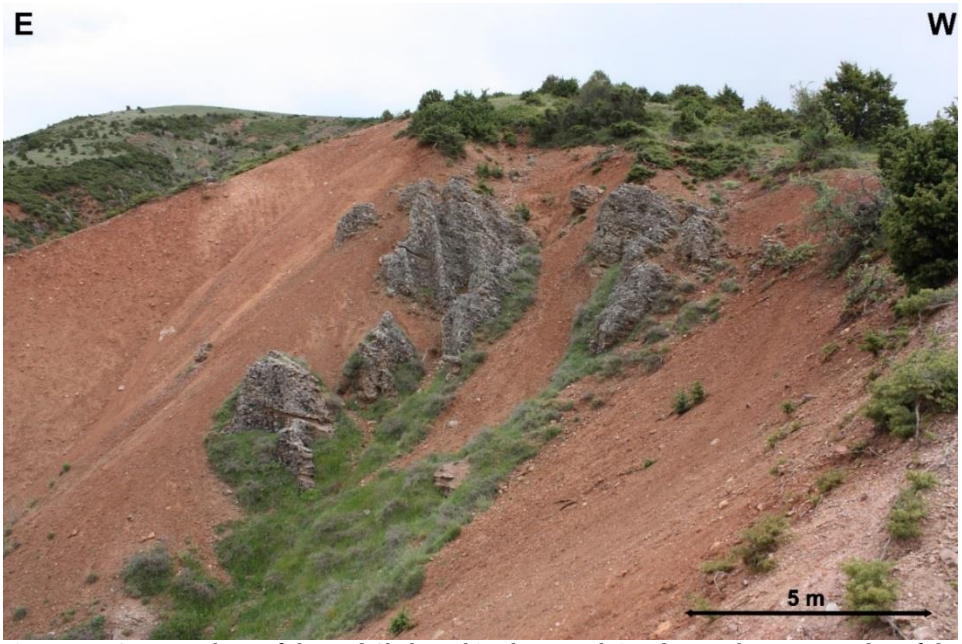

Figure 29: Outcrop photo of the Red Shales. This photograph is taken at the western edge of the Upper Conglomerates, where conglomerates are observed within the Red Shales. The shales found in the Kerpini Fault Block are mostly unconsolidated and weathered, as they appear in the figure.

5.1.7 Footwall Derived Fans – Kerpini Fault Block

The Footwall Derived Fans sits in the middle of the slope towards the Dhoumena footwall (Figure 32). Three different and independent fans have been recognized during this study (Fan A, B and C). Fan A and B have been outlined in Figure 32 while the Fan C sits further to the east, close to Roghi Mountain. The geometry and topographic expression of these deposits gives a good indication of being alluvial fans sourced from the north. Syahrul (2014) identified Fan A as being an individual fan during his study, based on the topographic expression of the deposits. The size of the fans decrease eastward with the biggest fan, Fan A, located just east of Kerpini village. This fan measures almost two kilometers in northwest-southeast direction. The two fans located further to the east, Fan B and C, measures 700-900 m in north-south direction and approximately 300 m in east-west direction. For Fan B and C, the apex is not easily identified. Erosion and recent road construction have altered the northernmost parts of Fan B and C. The apex of Fan A is located northeast of Kerpini village; Figure 30 shows the apex of Fan A and the unconformity contact between the fan and the basement.

Detailed investigation of the Footwall Derived Fans reveal that the average clast size of the conglomerates are smaller than for the other conglomerate deposits found within the Kerpini Fault Block. Fan B (Figure 32) has a larger clast size than the two other fans. Average clast size for Fan B is in the range of 10-15 cm, whiles the westernmost (Fan A) and easternmost (Fan C) fans have an average clast size of 7-10cm. All the deposits show a southward fining trend, where the coarsest conglomerates are found near the apex, and the distal parts of the fans show a significant amount of sandstone and marl.

Bedding and bed contacts are partly well exposed, the bedding gets more pronounced southwards, towards the distal part of the fans. The depositional energy is clearly higher close to the apex, which might account for the bedding being less pronounced in the proximal areas. Some beds in the distal areas have normal grading (fining upwards) and moderate to well sorted clasts. The conglomerates are clast-supported with medium to coarse poorly sorted sandy matrix. Figure 31 compares the distal and proximal parts of Fan A. In this figure one can observe that bedding is better developed and there is more sand in the distal parts (Figure 31A), but thickly bedded conglomerates are present in the proximal areas (Figure 31B).

Smaller clast size and better clast organization in combination with more pronounced bedding and bed contact might suggest a stabile sediment supply rather than episodic deposition. Isolated sandstone beds with normal grading could represent channels, which indicate a more channelized mass movement across the fan surface. There are some specific elements needed to initialize an alluvial fan, there have to be a slope present and there needs to be fluids available for sediment transportation. Detailed study of these fans (Fan A, B and C) are outside the scope of this project, but it is important to consider how they developed in relation to the Upper Conglomerates and the rest of the Kerpini Fault Block. Therefore, the Footwall Derived Fans will be further discussed in the discussion chapter (Chapter 7).

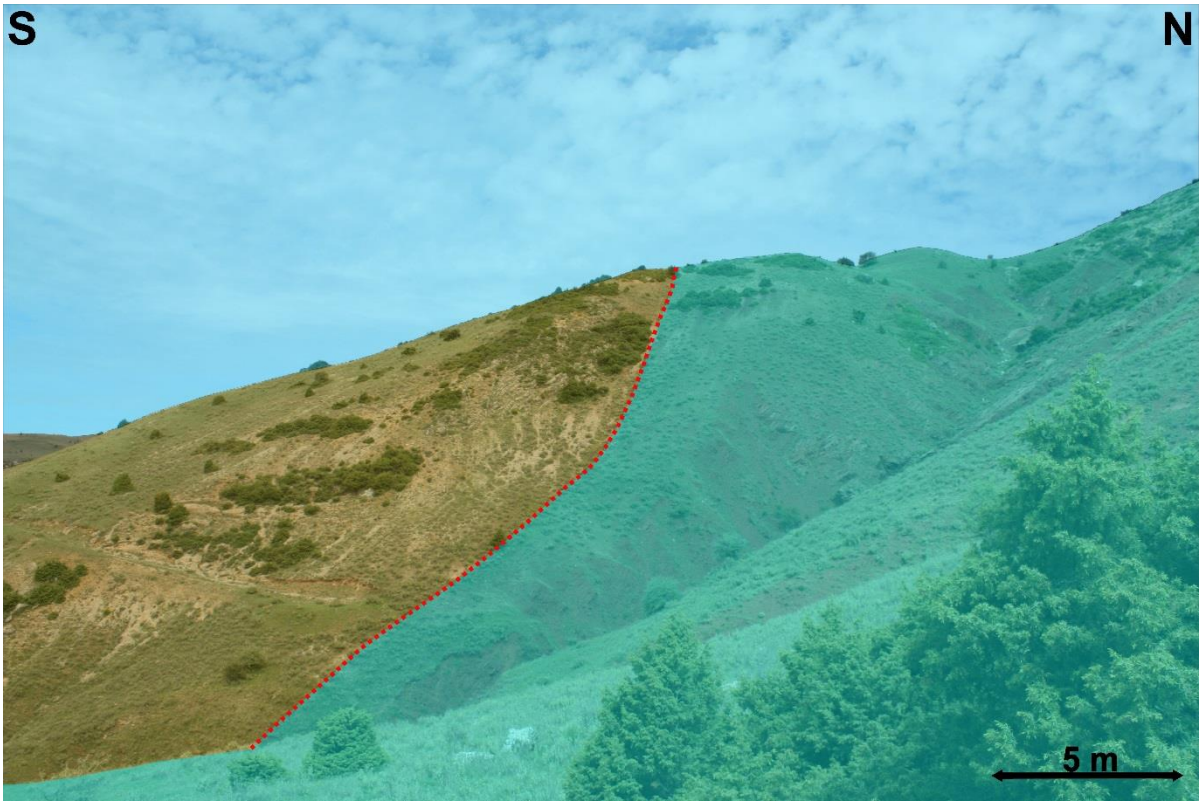

Figure 30: Photo taken looking west at Fan A. The dashed red line represents the unconformity between Fan A and the basement, the unconformity surface appears as a relative planar surface. Apex of Fan A sits on the unconformity surface. Scale is relevant to back of figure.

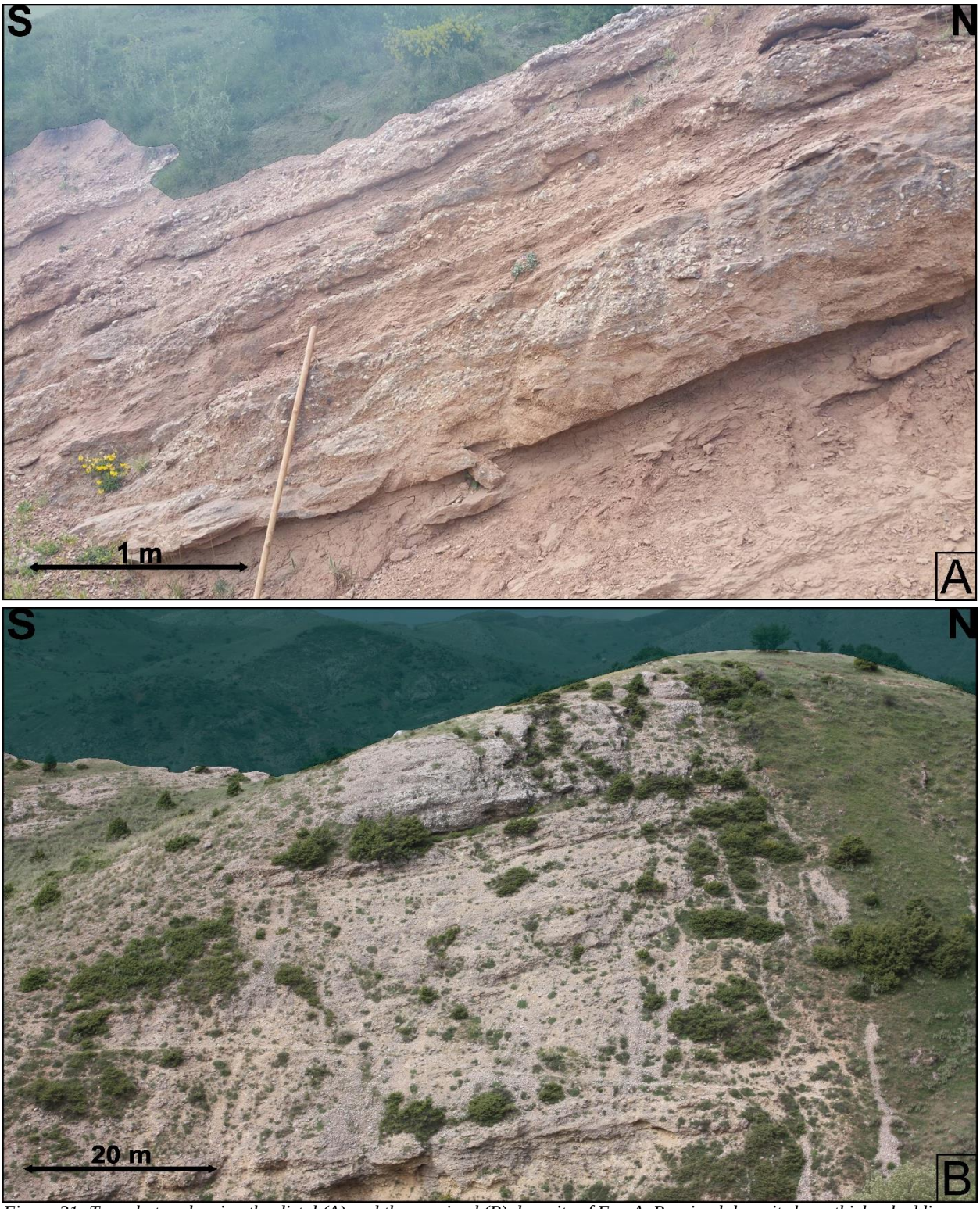

Figure 31: Two photos showing the distal (A) and the proximal (B) deposits of Fan A. Proximal deposits have thicker bedding, poorly defined bed contacts and has larger clast size. Distal deposits display better sorting, clearer bed contacts and thinner beds. This means that Fan A display a fining southward clast size, better clast organization southward and beds get thinner towards south. These observations support the theory of the fans being sourced from the uplifted footwall of the Dhoumena Fault and flowing southwards to the lower elevated areas of the Kerpini Fault Block.

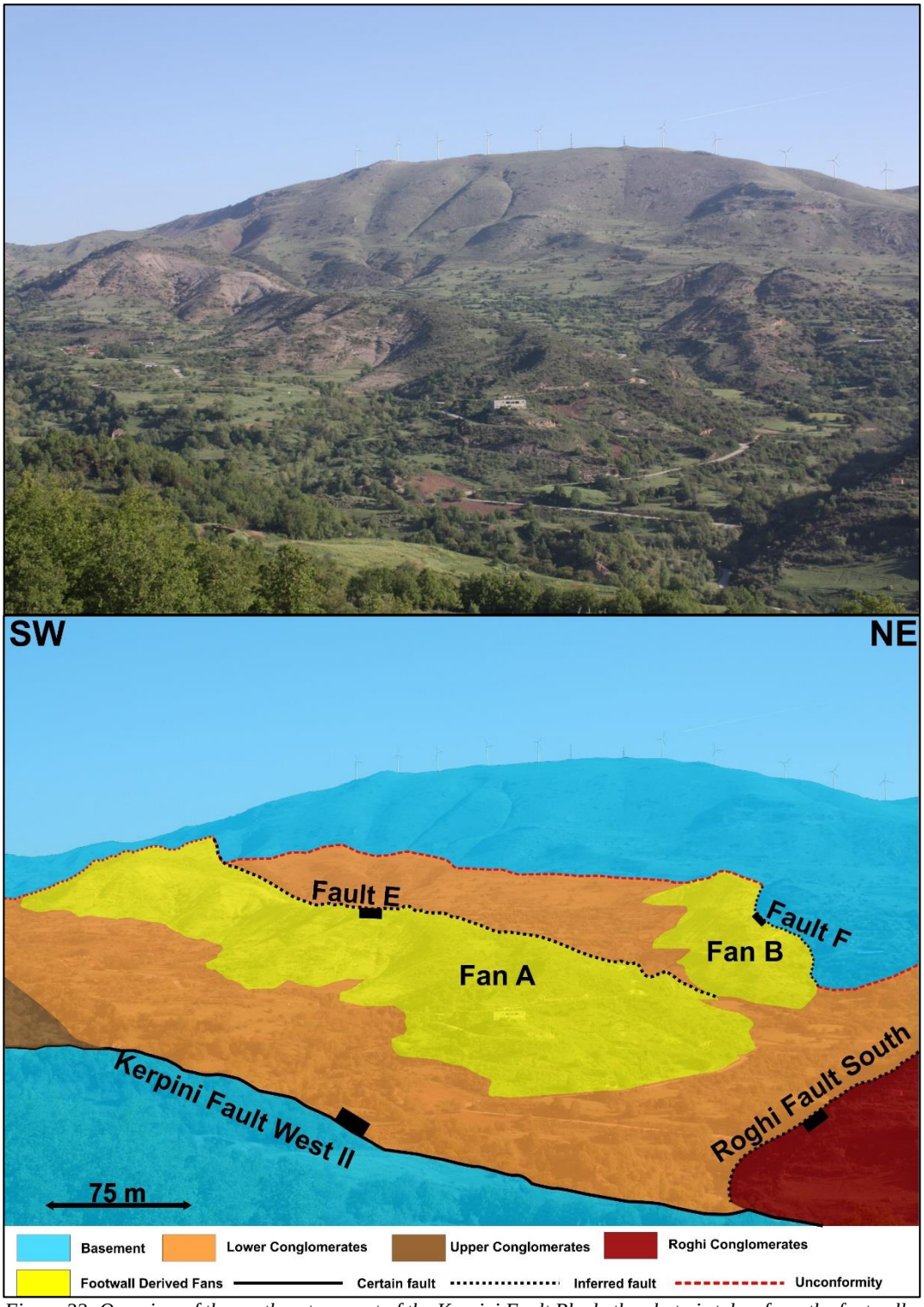

Figure 32: Overview of the northeastern part of the Kerpini Fault Block, the photo is taken from the footwall of the Kerpini Fault looking north. The figure shows Fan A and Fan B, and their bounding faults. One can observe that the Lower Conglomerates unit sits unconformable on top of the basement overlain by the Footwall Derived Fans. The uplifted footwall of the Dhoumena Fault is located north of the two fans.

5.1.8 Sub-horizontal Sediments – Kerpini Fault Block

The Sub-horizontal Sediments were studied in detail by Stuvland (2015) in his master thesis at the University of Stavanger. During his study, Stuvland (2015) identified a total of eight outcrops of Sub-horizontal Sediments located in the Kalavryta and Kerpini Fault Blocks. The two outcrops located in the Kalavryta Fault Block are outside the study area of this project and are therefore not taken into account. Two outcrops located within the Kerpini Fault Block coincide with the apex of the Footwall Derived Fans. These outcrops are therefore neglected as being Sub-horizontal Sediments, but rather a part of the Footwall Derived Fans. Three of the Sub-horizontal outcrops carried through to this project are located northwest of Kerpini village, while one outcrop is located at the northwestern extent of the Roghi Conglomerates. The sediments characterized as Sub-horizontal Sediments in this project, onlapps the Lower Conglomerates in the western part, and onlapps the Roghi Conglomerates and the Lower Conglomerates in the eastern part of the fault block. The Sub-horizontal Sediments consist of clast-supported pebble-cobble sized conglomerates with poorly sorted matrix (Stuvland, 2015). According to Stuvland (2015), the Sub-horizontal Sediments are deposited as a result of fluvial incision during either the late stages of the Kerpini Fault (late syn-Kerpini Fault deposits) or post the Kerpini Fault (post-Kerpini Fault deposition).

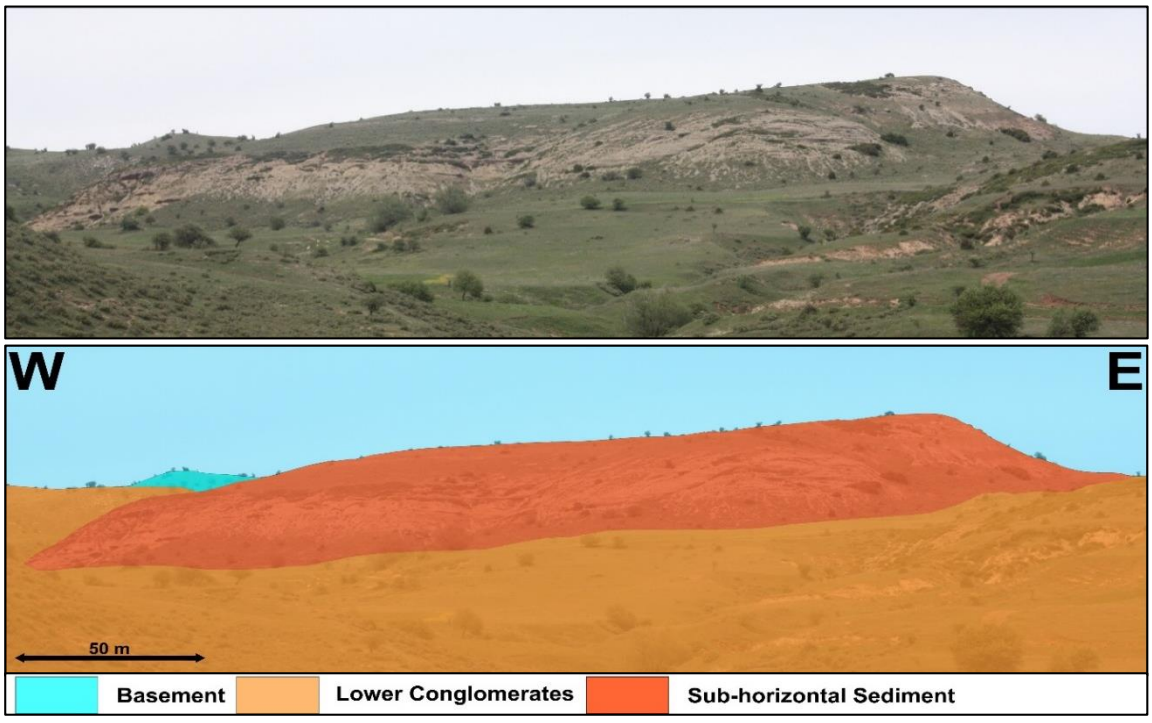

Figure 33: Overview photo of one of the Sub-horizontal Sediment outcrops. The contact between the Sub-horizontal Sediments and the Lower Conglomerates are not distinguishable due to vegetation, but it is believed, based on observations from Stuvland (2015) that there is a onlapping relationship between the two units.

5.2 Upper Conglomerates – Kerpini Fault Block

5.2.1 Introduction

The Upper Conglomerates form the main focus of this study, therefore the field observations for this unit are considerably more detailed. Facies and facies distribution have been investigated in addition to general texture and grain size, sedimentary structures and paleoflow directions. Facies are studied and classified based on Galloway and Hobday (1996) classification (Figure 7). Lateral and vertical variations in facies, geometry and texture are observed. Due to vegetation and poor exposed bedding, correlations along individual beds are difficult. Therefore, shorter representative logs will be presented for different outcrops. In the facies distribution section in the discussion chapter, complete vertical logs of the Northern Lobe will be presents. These logs are based on observations and correlation between areas of good rock exposure and poor rock exposure. The Upper Conglomerates are located in the southwestern part of the Kerpini Fault Block, just north of the Kerpini Fault and south of the Kerpini village. The unit stretches approximately 3 km in east-west direction and 1.5 km in north-south direction. There is a drop in elevation of 300 m from the highest point close to the Kerpini Fault to the lower areas south-east of Kerpini village. The elevation and thickness decreases towards the eastern part of the fault block which is believed to be the depocentre of the Kerpini Fault Block (Syahrul, 2014). Figure 34 displays the Upper Conglomerates in relation to the Lower Conglomerates and the Footwall Derived Fans, the picture is taken north-east of Kerpini village looking south. From the highest point (marked with a red square), the unit splits into two lobes (Northern and Southern Lobe) moving east. The texture and geometry of the westernmost part of the Upper Conglomerates differs from the eastern deposits. In the following subsections (5.2.2, 5.2.3 and 5.2.4), the Upper Conglomerate unit will be divided into the Northern Lobe, Southern Lobe and the Western Conglomerates.

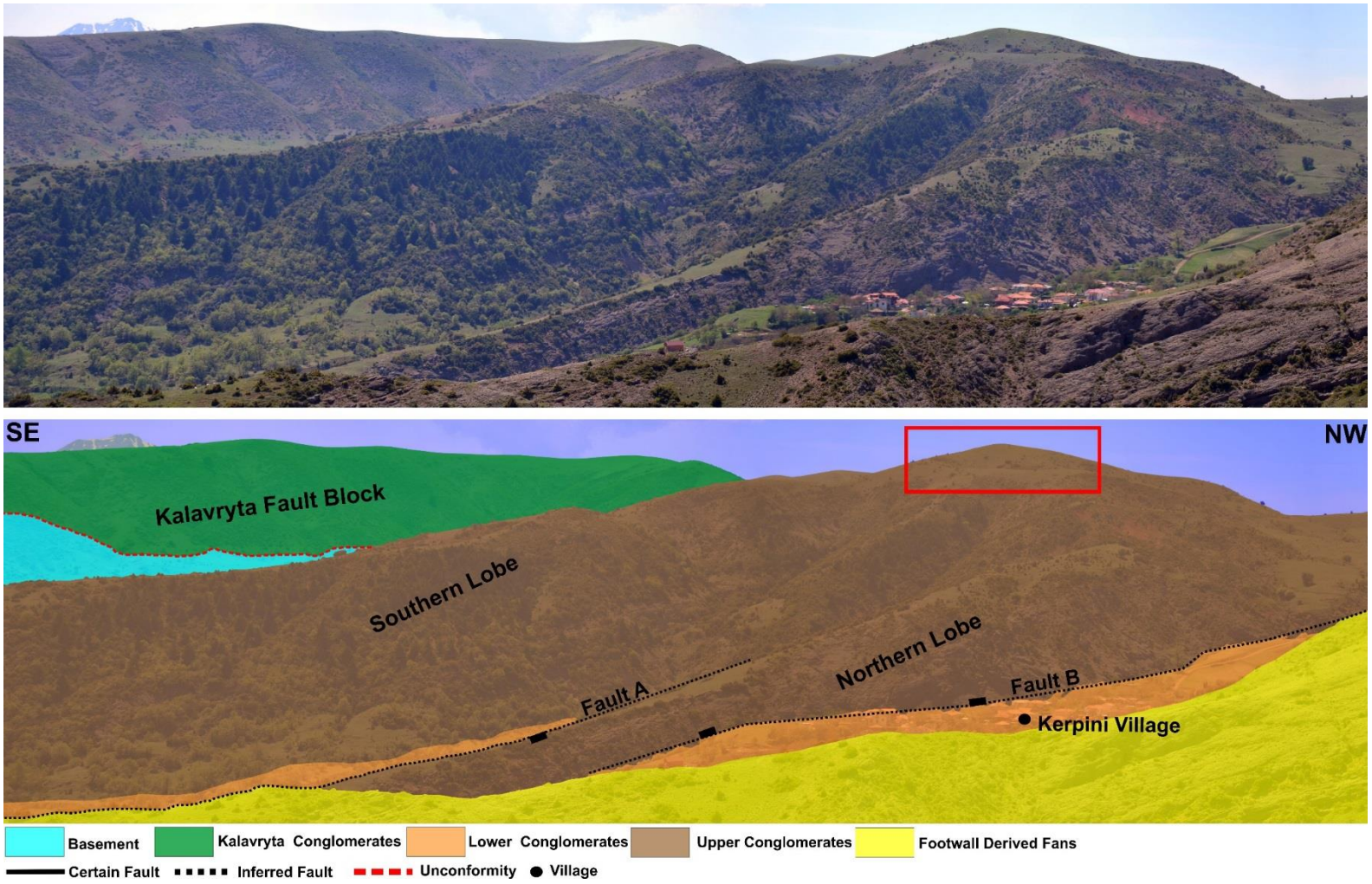

Figure 34: Overview photo of the Upper Conglomerate deposits looking south. The uplifted footwall of the Kerpini Fault is located south of Southern Lobe. In addition, two faults (Fault A and B) has been marked on the figure, further analysis of these faults are found in chapter 6. From the highest point on the figure (marked with red square) the Upper Conglomerate unit splits into two lobes going eastward. Photograph kindly provided by the University of Stavanger, Chris Townsend.

5.2.2 Texture and Geometry

Southern Lobe

The Southern Lobe, with its thick and continues sediments, is the dominating feature of the Upper Conglomerates. Vegetation covers most of the northern side of the lobe, but the southern side offers good rock exposure. Thus, most of the observations refer to the rock record on the southern side of the Southern Lobe. The Kerpini Fault marks the southern extent of the Southern Lobe, any clear contact between the sediments and the fault is not observed due to poor exposure of the fault plane. Nonetheless, the sediments are believed to be in direct contact with the Kerpini Fault.

There is an overall eastward grain size fining in the Southern Lobe, from boulder and cobble sized conglomerates close to the presumed apex to fine-grained marl at the eastern extent. Whether the change in grain size, in east-west direction, is gradual or abrupt is difficult to establish due to discontinuous bedding. Thinly bedded sandstones are more abundant from the center of the lobe and eastward. Unlike the Lower Conglomerates, where the sandstones appear as lenses, the sandstones within the Southern Lobe appear as "sheets" between coarser conglomerates. Grain size changes up section are different for the western and eastern part of the lobe. The western part displays only a slight fining upward trend while the eastern parts display a very clear fining upward trend.

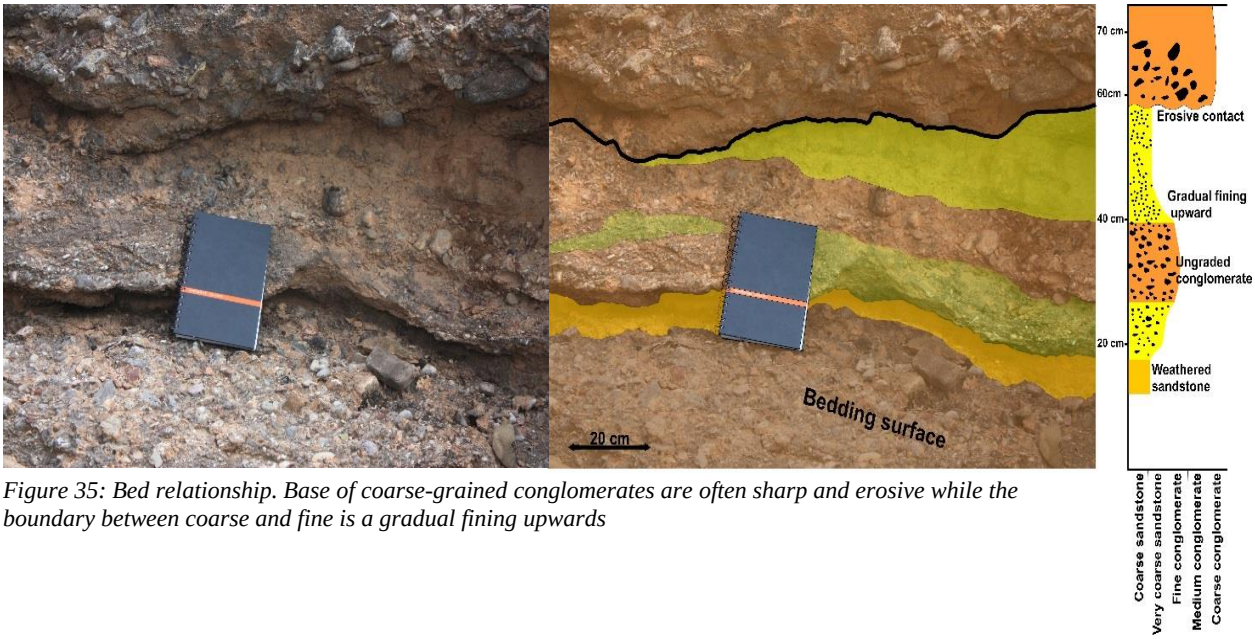

Figure 35: Bed relationship. Base of coarse-grained conglomerates are often sharp and erosive while the boundary between coarse and fine is a gradual fining upwards

Bedding and bedding surfaces are more prominent in the eastern parts of the lobe, while the conglomerates in the west appear more chaotic and unbedded. The bed thickness varies from decimeters to several meters, with the thickest beds normally at the base of the lobe. There are some exceptions in which thick beds of 1-2 m are observed at the top. Bed boundaries are often sharp erosive, especially the base of coarser conglomeratic beds (Figure 35). The transition from coarser conglomeratic beds to finer conglomerate beds or sandstone beds, are often gradual fining upward (Figure 35). As stated previously there is a general grain size decrease from west to east, most likely represented by the loss of depositional energy and distance from source point.

However, there are some features looking like massflows on the southern side of the lobe. The massflows appears to originate at the top of the lobe and are deposited on the side of the lobe. These features have a fan like shape, narrow at the top and wider at the base (Figure 37), at least three such features are observed at the southern side of the lobe. The massflows are dominated by chaotic and ungraded medium to coarse-grained conglomerates with little to no internal bedding, suggesting high-energy and rapid deposition. The texture and geometry of the massflow features breaks the general grain size and organizational (more organized towards east) trend. Figure 36 shows a location where two of these massflows meet at the base of a river valley.

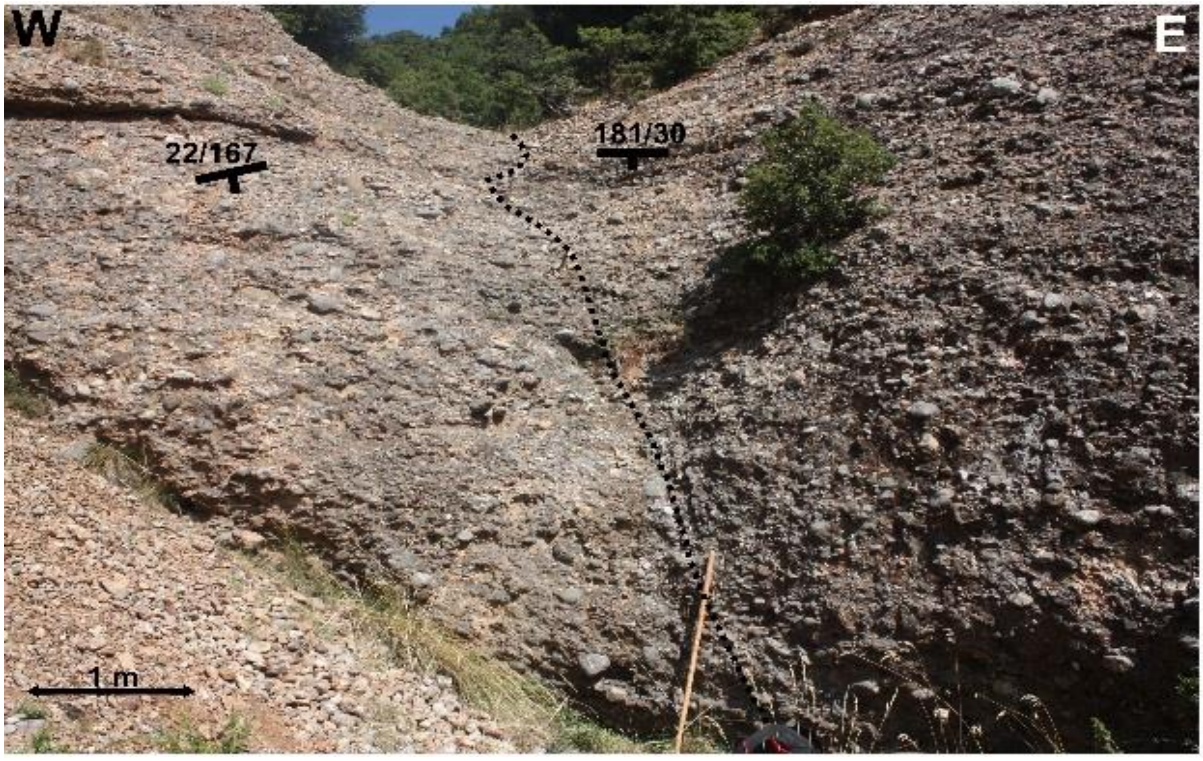

Figure 36: Two massflows meets in a river valley. Pay attention to the poorly exposed bedding that makes correlation across challenging. Dip angles and dip direction suggest two individual flows, where one erodes into the other.

Due to lack of bedding and clast organization, correlation across the river valley is not possible. Dip angle and dip direction measurements on each side of the valley suggests two individual massflow deposits exist in close proximity, but their relative timing is difficult to establish. Based on the above observations, these features are interpreted as being individual high-energy rapid deposits. As the fan is building eastward, heavy rainfall (large sediment supply) or tectonic movement could have triggered an avalanche like deposit downslope from the eastward building alluvial fan.

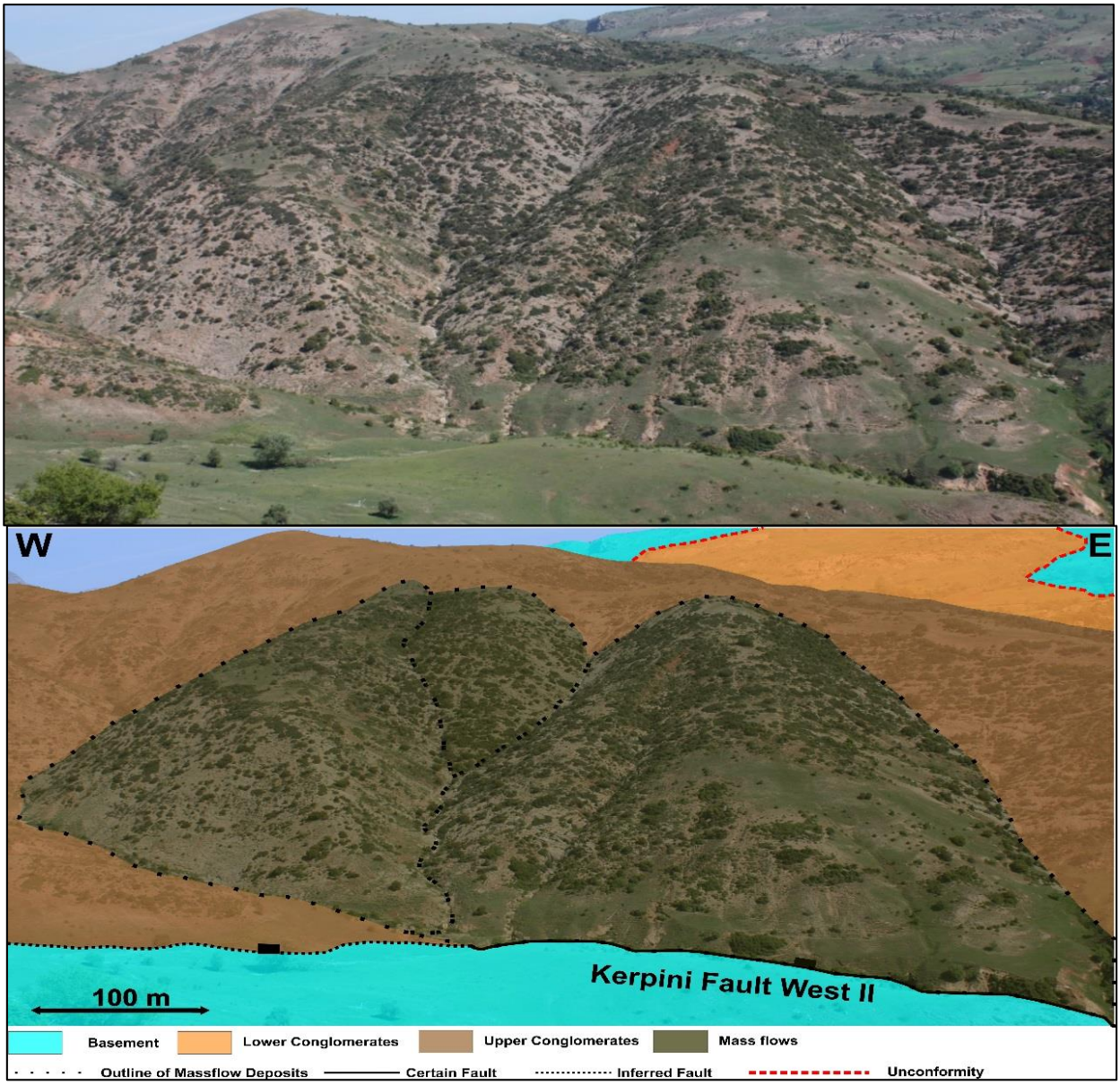

Figure 37: Photo taken from the Kerpini Fault footwall looking north onto the southern side of the Southern Lobe where the massflows deposits are located. The conglomerates within the massflows breaks up the fining eastward grain size pattern observed for the rest of the Southern Lobe. The geomorphology of these deposits could also support the theory that these deposits originates from massflows downslope of the Southern Lobe (towards the Kerpini Fault). Scale is relevant to massflows deposits

Northern Lobe

The Northern Lobe is located 80 m north of the Southern Lobe, separated by a north dipping Fault located in a river valley where basement and Lower Conglomerates are exposed. Compared to the Southern Lobe, the Northern Lobe is smaller in all directions. The height above the topography of the river valley is maximum 100 m in the western parts, and tapering out at its eastern extent. Good exposures occur on both sides of the lobe, however there is a steep drop of the northern side of the lobe which limits access. The drop is down into another east-west orientated river valley where a south-dipping fault has been interpreted, this river valley marks the northern extent of the Upper Conglomerates.

The eastward fining trend observed for the Southern Lobe is more pronounced in the Northern Lobe, from bouldary conglomerates in the west to sandstone and marl in the east (Figure 38). The more pronounced fining trend is better identified by the higher quality of exposures, less reworking of the deposits and no secondary massflow deposits. A fining upward trend is observed at the westernmost and easternmost parts of the lobe, while the central section has a more uniform grain size distribution up the succession.

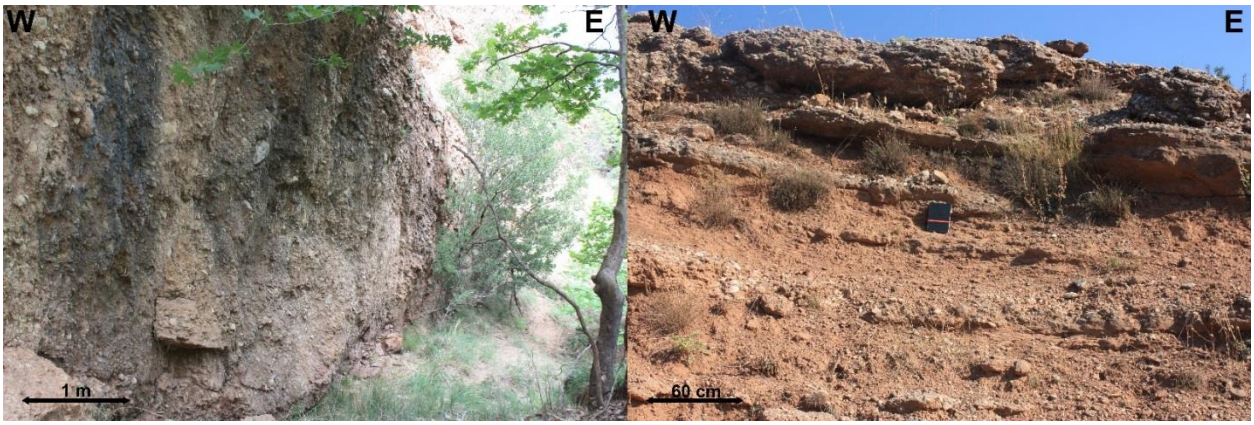

Figure 38: Left picture display a thick basal bed in the western part of the lobe. The right picture display a series of thinner alternating marl and conglomerate layers at the eastern extent of the lobe. These pictures illustrate the fining eastward trend of the Northern Lobe.

Bedding and bedding contacts are in places well exposed. Lower beds are often covered by vegetation, hence it is difficult to follow the continuity of the beds from west to east. The upper beds are better exposed and can be clearly followed from east to west. Some of the uppermost beds onlap the underlying beds. In the western part, the basal beds are very thick (8-12 m) with thinner (1-5 m) beds on top. Beds become thinner towards east, and at the eastern extent, beds are on average 20-40 cm thick. The thick and massive beds observed in the western part are not present in the eastern parts, or they are not exposed.

The position to which the thick basal beds extend marks a significant change in the topographic slope. East of the basal bed position, the topographic slope is approximately 10° and west of the basal beds the topographic slope is close to 20° (Figure 39). This implies that the thick basal beds have shaped the present day topographic profile of the lobe. In addition, the basal beds appear to have had some control of the later alluvial deposits.

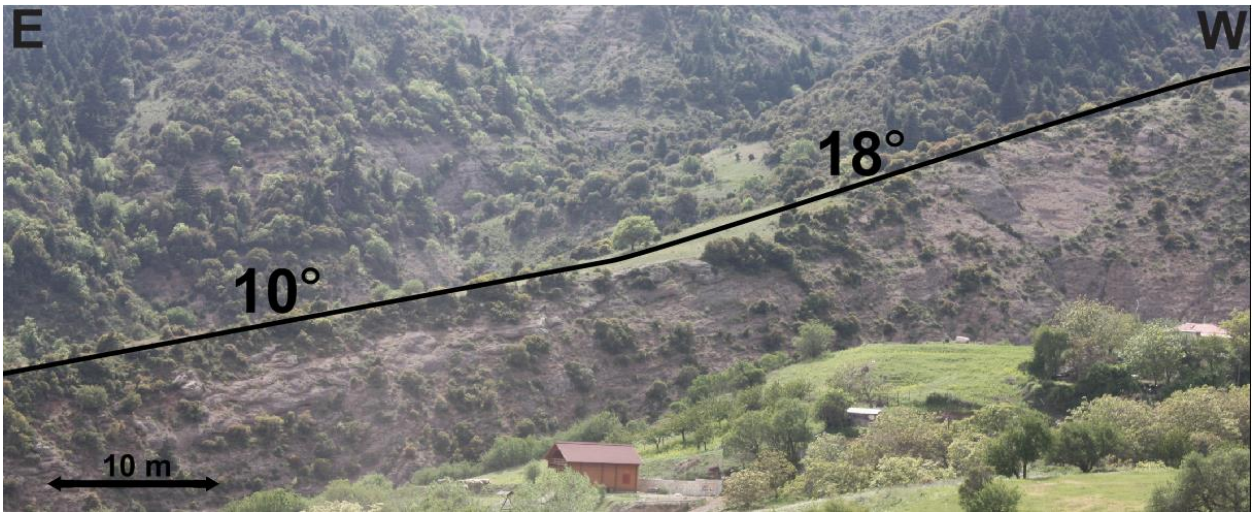

Figure 39: Figure showing the change in the topographic slope along the Northern Lobe at the locations where the thick basal beds ends. Scale is relative to the Northern Lobe deposits.

Western Conglomerates

The Western Conglomerates are located at the western extent of the Upper Conglomerates. The topographic expression of this area has the appearance of a smaller fan sourced from the higher grounds and deposited downslope towards west-northwest. The Western Kerpini Fault and Splay Fault I marks the southern extent of the Western Conglomerates. The conglomerates are overlying the Lower Conglomerates, it appears as the Lower Conglomerates unit is going below the Western Conglomerates. Initially, all the rocks south of Fault C were classified as belonging to the Upper Conglomerates. However, the Upper Conglomerates has not been observed to lie directly in contact with the unconformity hence, it has been interpreted that the Lower Conglomerates underlie the Western Conglomerates. In addition, there is no sandstone beds observed within the Western Conglomerates, while there are clearly exposed sandstone beds in the Lower Conglomerates at the location of Figure 40.

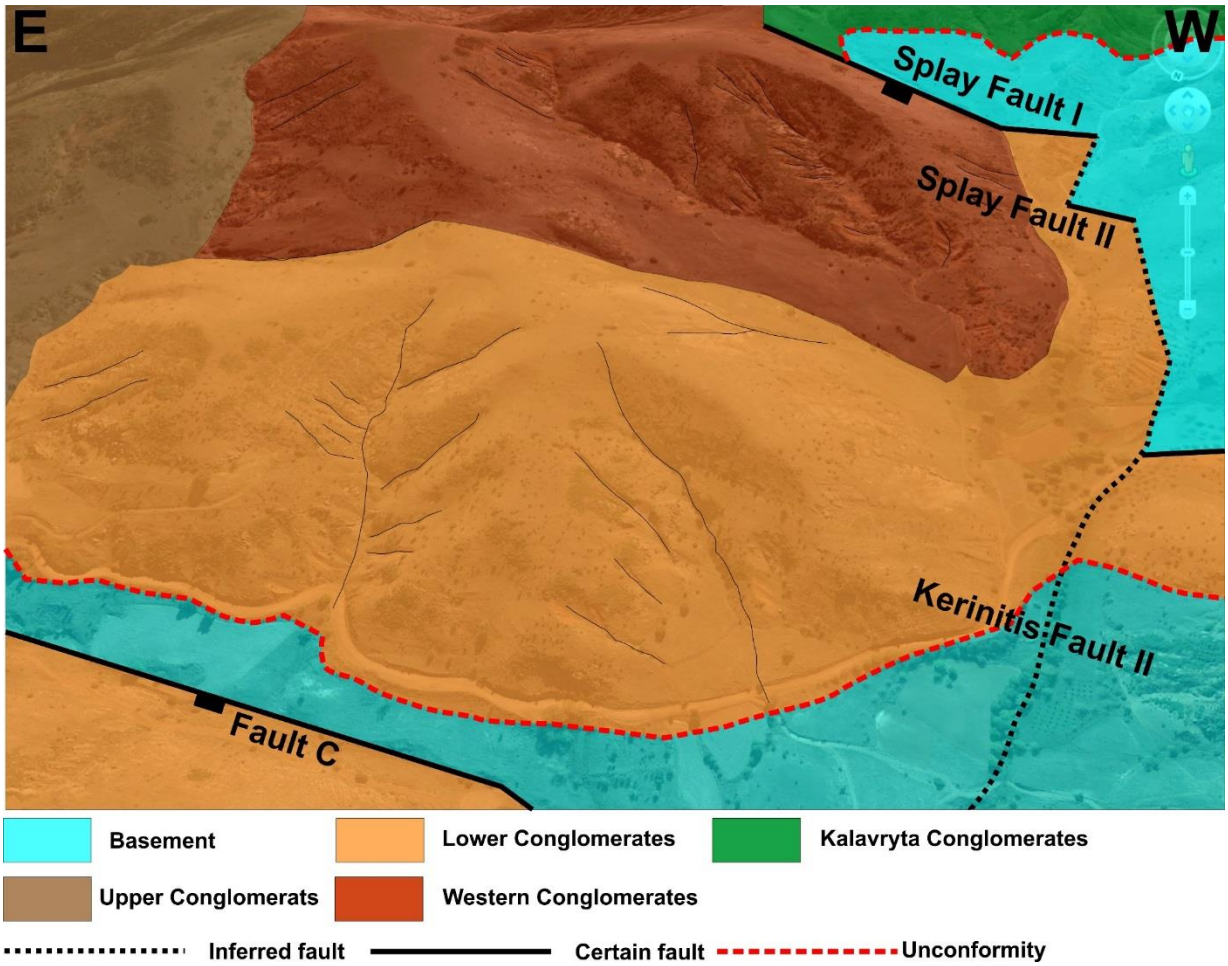

Figure 40: Overview of the Western Conglomerates (marked in dark red) from Google Earth. The Lower Conglomerates are underlying the Western Conglomerates. The elevation of the Lower Conglomerates is higher than in the rest of the fault block as a result of uplift from Fault C. The two splay faults located between segments II and III of the Kerpini Fault is also shown, a further description of these fault are found in subsection 6.1.3.

In contrast to the Southern and Northern Lobes, the clast size in the Western Conglomerates does not decrease in any particular direction (this includes fining up the succession). The whole volume of rock consists of cobble sized unsorted, ungraded conglomerates. Western Conglomerates are mostly clast supported, polymodal with very poorly sorted matrix.

Due to the chaotic and unorganized nature of the Western Conglomerates, bedding and bedding surfaces are not very prominent. The few beds present are in general thick to very thick, ranging from 50 cm to 1 m. All the beds are coarse-grained and most likely have an erosive base, this implies that original thickness, before deposition of beds on top, is thicker. The lack of exposed bedding surfaces makes dip angle/direction measurements challenging and less trustworthy (see subsection 5.2.3.3).

Figure 41: Outcrop example of the Western Conglomerates. Notice the lack of bedding and unorganized nature of the cobble sized conglomerates.

5.2.3 Dip Angles and Dip Direction

There will always be uncertainty related with geological measurements such as dip angle and dip direction, the measurements in this project is no different. If there is, any uncertainty exceeding the ordinary it will be mentioned in the appropriate subsection. Alluvial fan sediments, as those in the Upper Conglomerates, are deposited with a particular dip dependent on the setting and type of alluvial fan. Differentiating between structural and depositional dips in alluvial fan deposits can be challenging.

5.2.3.1 Southern Lobe

The Southern Lobe has reasonably well exposure of bedding surfaces, which makes the dip and dip direction measurements reliable. As Figure 42 display, the general dip direction for the Southern Lobe is south. There is variation in the dip direction readings from 210° to 160. These discrepancies can be explained by uncertainty in the readings and the natural variation in the dip direction data. Dip angle readings varies from 13° to 29°, with an average of 25°. Any trends in the dip angle data such as decreasing dip angle up-section is not observed. The variation in the dip angle data are not controlled by any east-west or up-section trend. Dip data for the Southern Lobe has been treated as structural dips, due to both sides (northern and southern) of the lobe dips southwards.

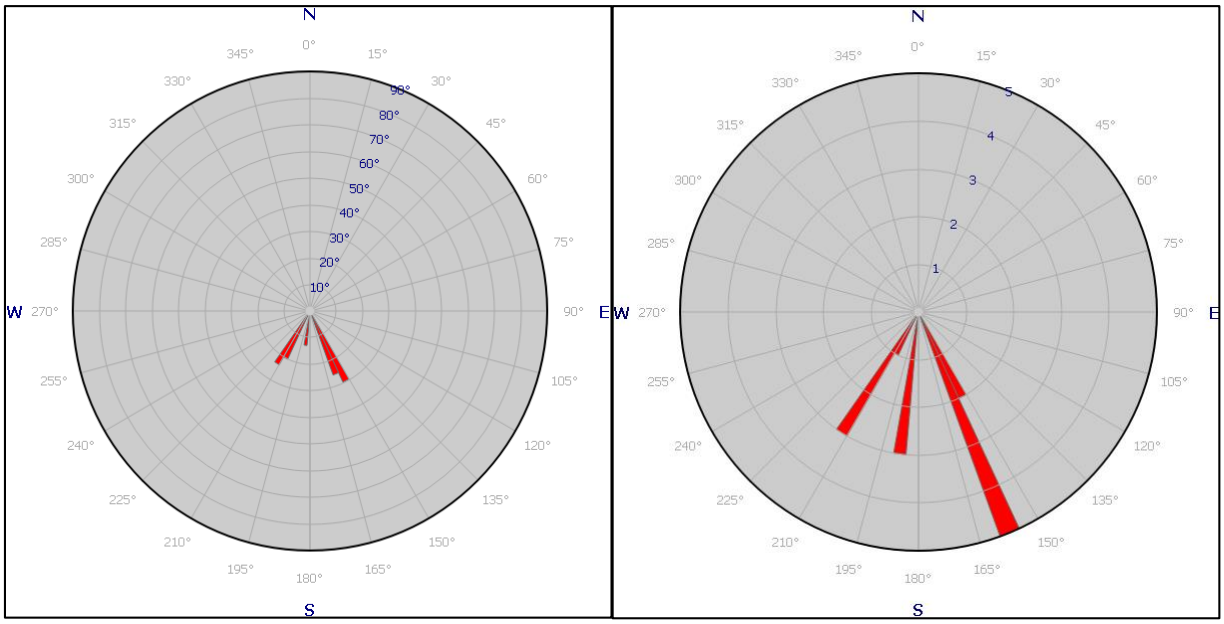

Figure 42: Dip and dip direction for the Southern Lobe.

5.2.3.2 Northern Lobe

The Northern Lobe has the best-exposed bedding of the three areas of the Upper Conglomerates. The dip measurements are considered accurate and reliable. Figure 43 show the rose diagram for the dip angle and dip direction measurements for the Northern Lobe. What really stands out for the Northern Lobe is the dominant north dipping conglomerates on the northern side. These north-dipping beds differ in dip direction from the rest of the Upper Conglomerates. Average dip angle for the south dipping conglomerates are 20°, and 24° for the north dipping conglomerates. Bedding dips tends to get shallower moving eastward, especially in the finer grained beds (alternating beds of marl and conglomerates in Figure 38) at the eastern extent of the lobe. Lower dip angles in the eastern part of the lobe could indicate that these sediments are deposited at a late stage of the alluvial fan development, and has experienced less of the structural rotation.

Figure 59 show a photo looking east in the river valley which marks the northern boundary of the Upper Conglomerates. In this figure, one can clearly see the north dipping conglomerates and an inferred fault that will be further described in subsection 6.3. Dip angles for the northern side of the Northern Lobe steepens down the section, implying that the Northern Lobe were deposited simultaneously as the development of Fault B. The south dipping conglomerates shows dip direction measurements ranging from E115S to S165E.

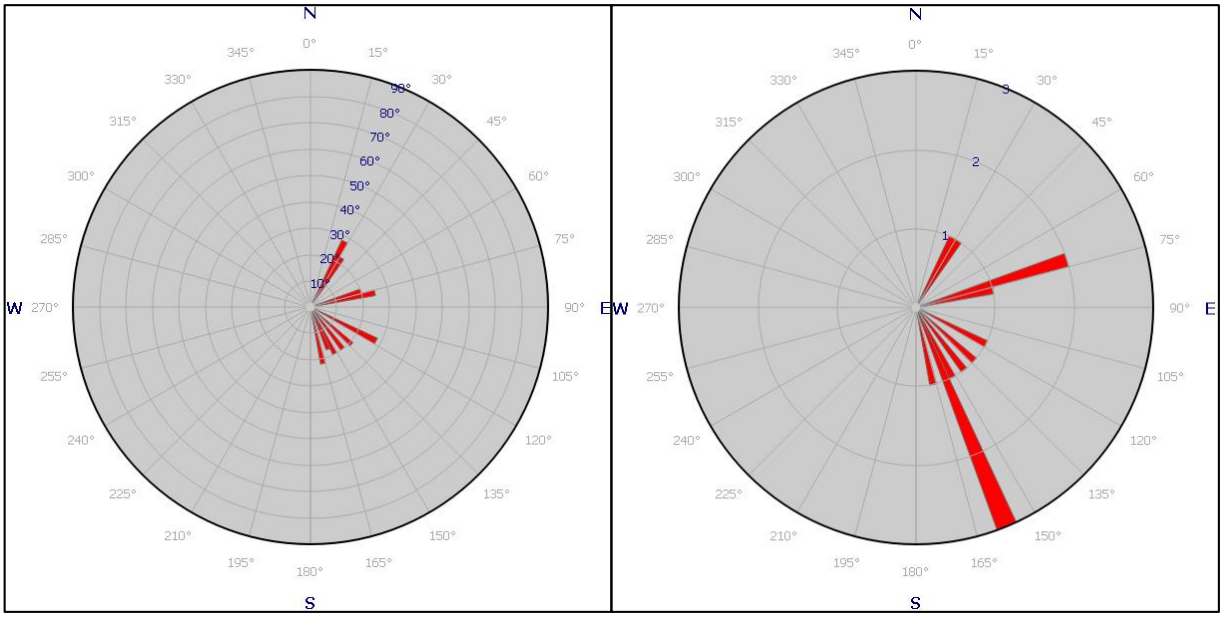

Figure 43: Dip angle and dip direction measurements for the Northern Lobe.

5.2.3.3 Western Conglomerates

The dip data for the Western Conglomerates has the largest variation. Bedding and bedding surfaces are poorly defined and hence the reading has to be treated with some uncertainty. All of the dip direction data are in the southern hemisphere. The large variation in dip direction might reflect the chaotic and unbedded nature of the Western Conglomerates. A more likely explanation is that the large variation in dip direction has to do with the structural complexity of the Western Kerpini Fault III, this will be further discussed in sub section 6.1.3. Dip angles vary between 15° and 30°, this difference in dip angle is large for measurements taken within such a small area. The southwest dipping bedding has in general the largest dip angle with an average of 24°, while the southeastern dipping beds has an average dip angle of 20°.

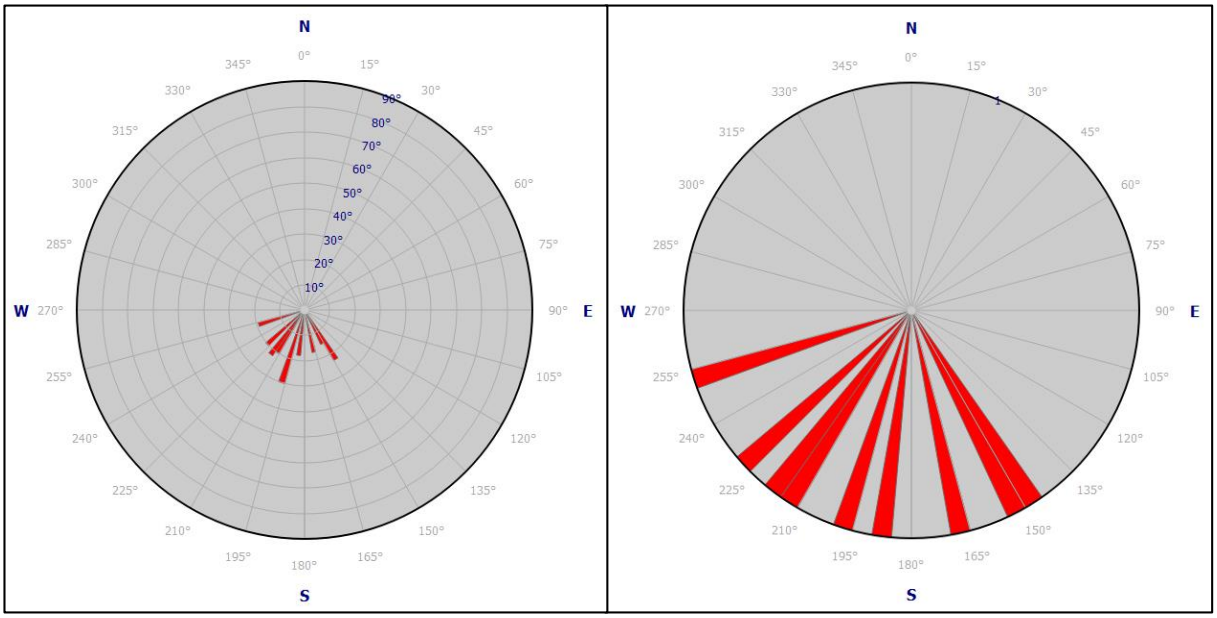

Figure 44: Dip angle and dip direction measurements for the Western Conglomerates.

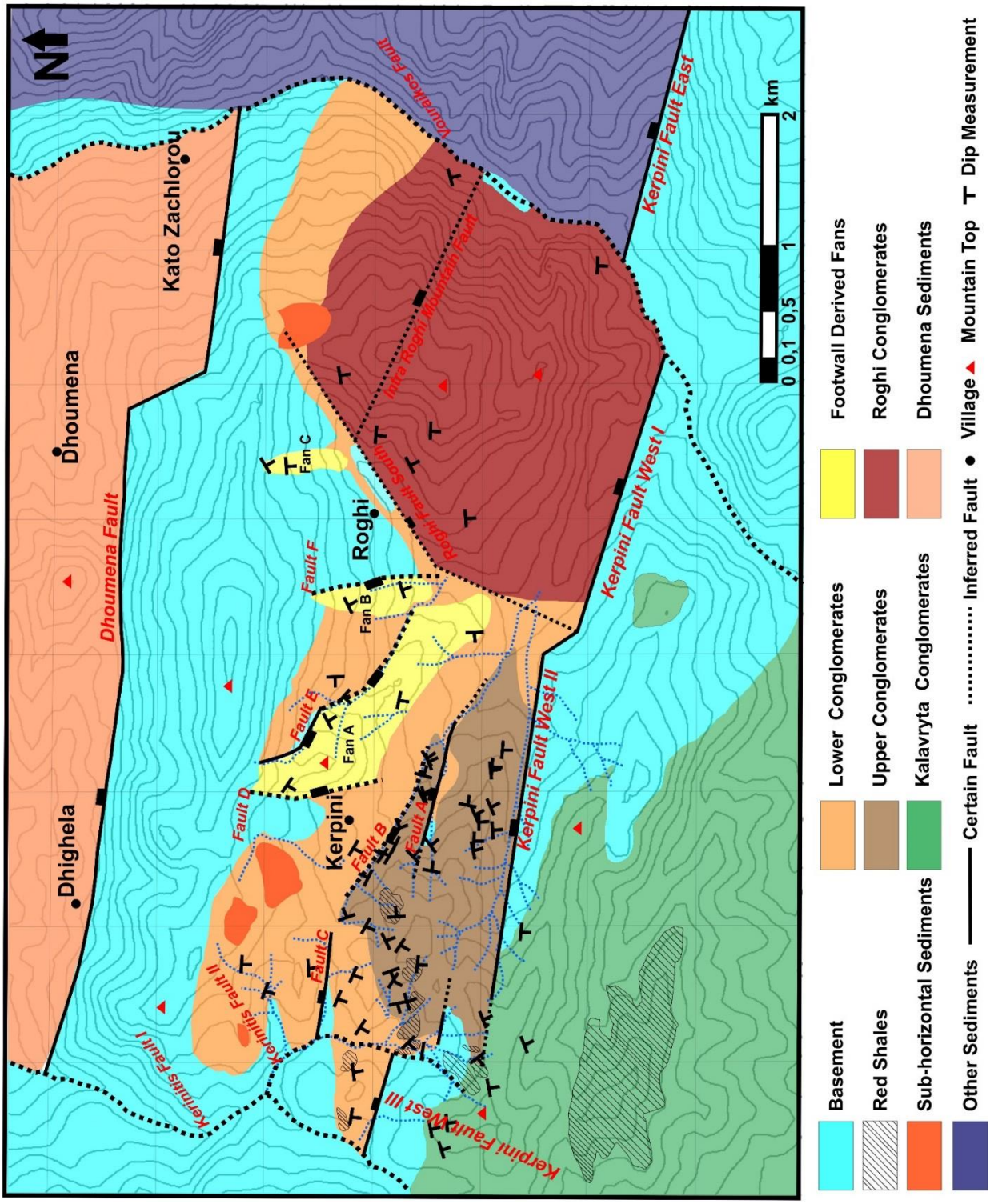

Figure 45: Map displaying the locations of the dip measurements for the different stratigraphic units within the Kerpini Fault Block, including the different parts of the Upper Conglomerates.

5.2.4 Facies

The following subsection will include a description of the different alluvial fan facies found within the Upper Conglomerates. Facies are defined as one or several processes operating in a depositional environment. As mentioned earlier the facies described for this unit is based on the triangular classification scheme (Figure 7) of Galloway and Hobday (1996). This classification scheme is based on the dominating processes of the alluvial fan deposits. As the following sections will show, the alluvial fan changes characteristics and dominating processes through time. In the texture and geometry section, grain/clast size and organization is not described, the reason being that these characteristics are dependent on the facies not the different parts of the unit. Thus, these characteristics will be described in the following subsection.

5.2.4.1 Debris-flow

Two types of deposits resulting from debris-flows are distinguished. The first type of deposits is found in the two lobes (Southern and Northern) where there seems to be more of a constant sediment supply. The second type is found in the Western Conglomerates and the massflows on the southern side of the Southern Lobe, these deposits are deposited in a rapid and chaotic manner with less fluid contribution. These two types of deposits will be described separately in the following section

Debris-flow deposits within the two lobes consist of cobble and boulder sized conglomerates, an average grain size is difficult to establish due to high matrix content. When disregarding the matrix, average clast size is medium to coarse cobbles (100-256 mm). Figure 46 is a photo taken from the river valley separating the two lobes looking north. This figure shows the debris-flow deposits of the Northern Lobe, where the largest clast are marked. From this figure, it is evident that clast size is clarge and it varies from finer to coarser vertically. At first glance the deposit looks unbedded (upper photo of Figure 46) and chaotic, but when marking the largest clasts a trend appears. There is a trend where the largest clasts (boulders) are deposited in the same beds, but the bed contacts are very poorly defined. This phenomenon can be explained by the depositional energy and erosive force of the flows. Before lithification of the previous flow (matrix and clasts), a new flow is deposited and erodes into the underlying deposits. This implies that the debris-flows are relatively frequently, before the previous deposits are lithified.

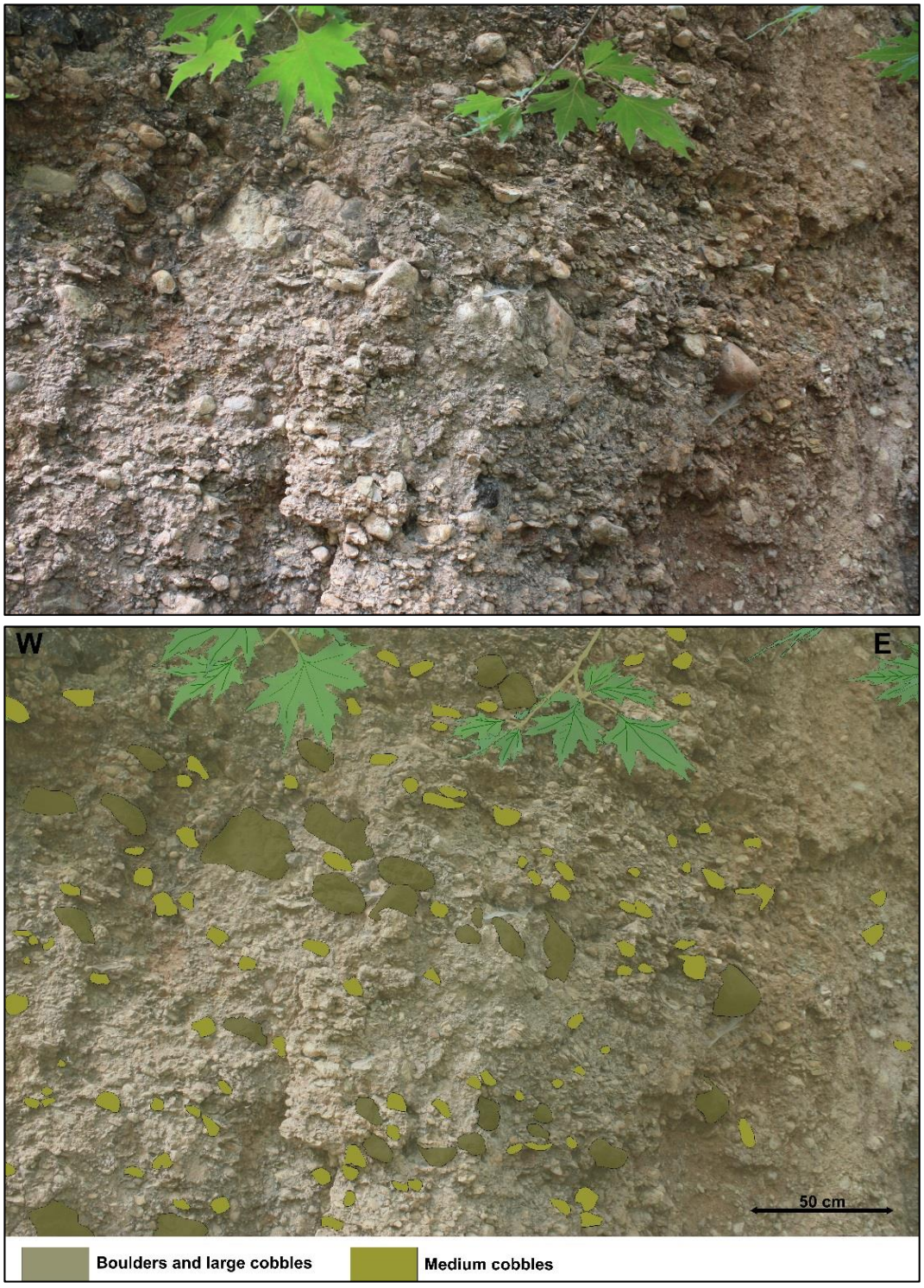

Figure 46: Debris-flow deposits of the Northern Lobe where the largest clasts are marked. The boulders and large cobbles are deposited in the same beds, with medium and fine cobbles between. In comparison to other conglomerate deposits in the fault block, these debris-flow deposits are matrix supported.

The clasts are sub-rounded to rounded, the largest clast have a tendency to be more angular than the small and medium clasts. Overall, the clasts display high sphereicity with some outliers displaying low sphereicity. Disregarding the matrix, the conglomerates are bimodal with large quantities of the clasts being limestone. Chert clasts are rare, but appear more frequently in the debris-flow deposits of the Southern Lobe than in the Northern Lobe, another difference between the clast content of the two lobe's debris-flows is the presence of sandstone clasts in the Northern Lobe. These changes in clast lithology could indicate changes in the source and possibly a difference in age.

Clasts are rarely in contact with each other, which mean the conglomerates are matrix supported. The matrix consists of poorly sorted, coarse to very coarse-grained sand, with no mud content. Coarse-grained matrix normally indicates a strong and stable matrix with low water content. The finer grained material, such as mud and fine-grained sand, is lost as the flows lose the fluid content downfan. Clay content is a large contributor to the matrix strength, low clay content in combination with large clasts (boulders and cobbles) indicates high competence flows.

Immediately east of the location were the photo in Figure 46 were taken, clast were organized in a matter that suggest a paleoflow towards the east (clast dipping west, indicating flow towards east). This kind of grain organization is rare within the debris-flow deposits, hence any trustworthy paleoflow pattern are not established based on these deposits.

These deposits described above are classified as debris-flows based on the large clast size, the unbedded nature of the deposits and the lack of grain orientation and sorting. The extent of these deposits is limited to the base of the lobes at their western margin. Debris-flow deposits are not observed further to the west or higher up the section. There is evidences of fluidized flows (high competence and matrix supported conglomerates), which leads to speculation that flooding or a period of heavy rain has triggered the downslope movement of these coarse-grained flows. The lack of any clear bedding might suggest a single flow event, while the organization of the largest boulders in layers might suggest episodic flow events. A paleoflow pattern is not observed within the debris-flow deposits, but the presumed flow direction (also supported by the single paleoflow indication) based on the fining eastward pattern is a flow from the apex area in the west towards the east.

The conglomerates of the Western Conglomerates and the deposits referred to as massflows earlier in the paper are also classified as debris-flow deposits. These deposits have a different characteristic than the debris-flow deposits of the Southern and Northern Lobe. Matrix content, clast size and clast organization is the biggest differences between the deposits.

Figure 37 shows a picture taken of the massflows located on the southern side of the Southern Lobe, the picture is taken looking north. Average clast size for these deposits is fine to medium cobbles (64-100mm), with low sand content. The variation in clast size is not big due to the absence of the finer-grained material. There is no organization of the clasts as Figure 47 displays, the larger clasts (marked in darker green) are distributed in a random manner. Organization of the larger clast shows no trend either in the vertical or horizontal direction. This characteristic substantiates the chaotic appearance of these deposits. Bedding and bedding contacts are absent which leads to the speculation of these deposits being an individual flow deposited within a short time period.

The clasts are sub-angular to subrounded with clasts showing both high and low sphereicity. There seems to be no correlation between the clast size and roundness/sphereicity. Limestone clasts are most abundant, with a considerable proportion of chert clasts. Sandstone clasts are rarely observed within these deposits. The chert clasts are in general smaller, more rounded and have higher sphereicity as shown in Figure 47. This does not necessarily mean the clast have been transported further, it is more likely that the chert clast are easierly eroded and reworked.

Figure 47: This figure shows the relationship between limestone (green), chert (red brown) and sandstone (yellow) clasts in the Western Conglomerates. Chert clasts are smaller and more rounded, while limestone clasts show lower sphereicity.

The light orange colored clasts displayed in Figure 48 are an attempt to display the organization of the clasts and the fact that these deposits are clast supported with low matrix content. Clast are frequently in contact with each other, when not, the conglomerates are supported by a coarse to very coarse-grained sandy matrix. Figure 48 also displays the unorganized nature of the conglomeratic deposits, where boulders and cobbles/pebbles are deposited in a random manner.

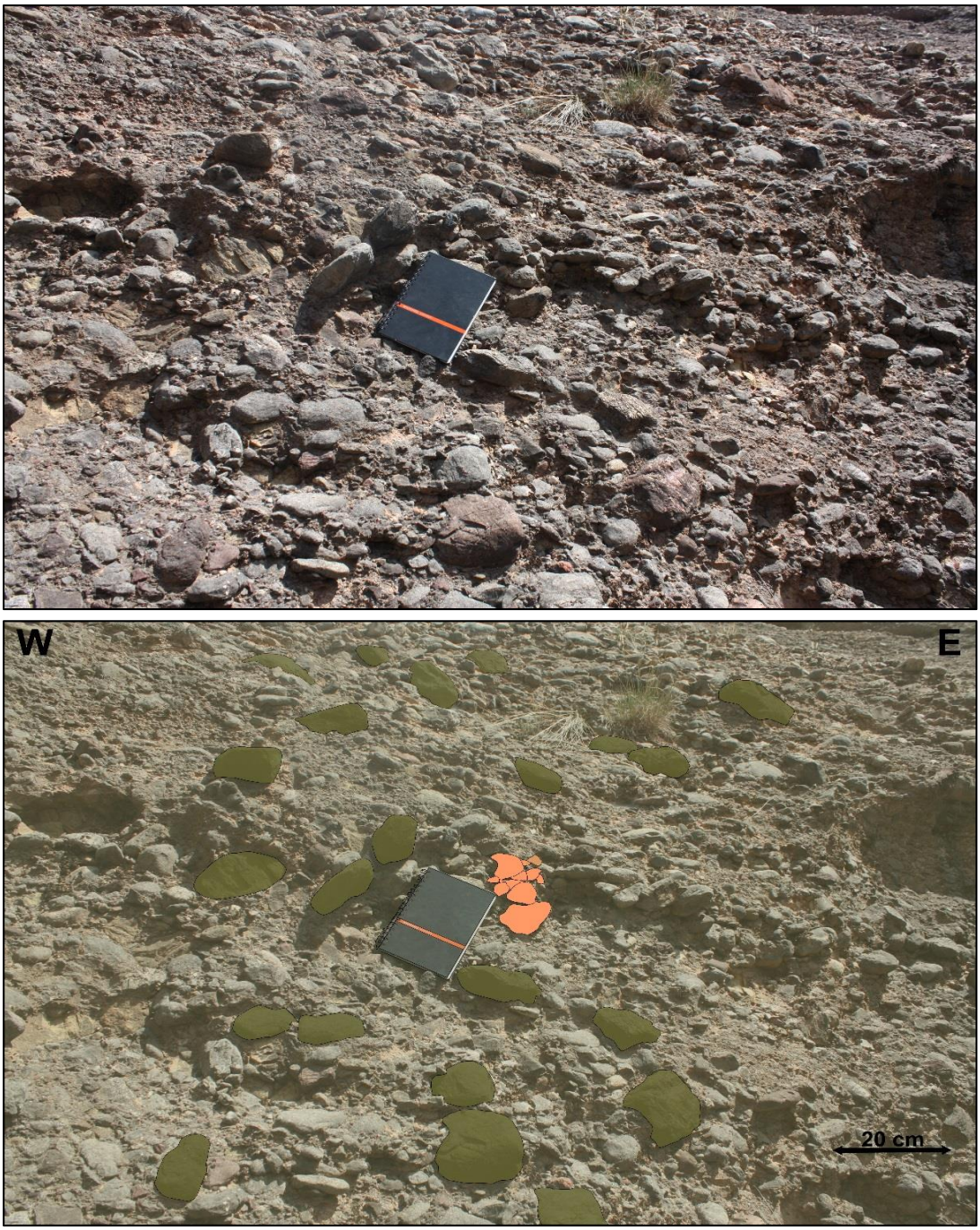

Figure 48: Massflows on the southern side of the Southern Lobe. This figure shows the large variation in clast size for the massflows and the chaotic and unbedded nature of these deposits.

Paleoflow indicators are not observed for the massflows on the southern side of the Southern Lobe. The overall unorganized, unbedded and chaotic nature of the deposits indicates a high velocity flow where the clasts are not organized and paleoflow indicators are absent. Even though the Western Conglomerates have the same characteristics (unbedded, unorganized and chaotic) as the massflows, some indications of paleoflow have been obtained. Dip of individual clasts and imbrication suggest a flow towards the north and northwest. The paleoflow direction for these debris-flow deposits are different from the ones obtained in the two lobes, where the few indications points towards a flow towards east.

As mentioned earlier, the biggest difference between the two types of debris-flow deposits is the clast size and the matrix content. Based on the observations described in previous paragraphs, the competence of the massflows are smaller due to the lack of big boulders and the overall smaller clast size of these deposits. The fact that these conglomerates are clast supported points toward low fluid content in the flows. Smaller grains, such as sand and mud is often transported by water in suspension and deposited as matrix between the clasts. Low fluid content could place these deposits somewhere between debris-flows and gravity-flows. Gravity flows have low to no water content and is not triggered by flooding or seasonal rain (therefore the low fluid content), but rather by tectonic movement (fault movement and/or earthquakes) leading to slope failure. Another explanation could be slope failure due to large sediment load.

The massflows are possibly a result of slope failure of the Southern Lobe, the slope fails and a fast flowing mass of clasts are deposited downslope in an avalanche like way. Whether the slope failure is caused by sediment overload or tectonic movement is difficult to determine. The Western Conglomerates are bigger and the volume of conglomerates significantly exceeds the massflow. Matrix content in these conglomerates is higher than the massflows but still the conglomerates are clast supported. Larger volume and higher matrix content could indicate some fluidized flow, but far from the amount of the debris-flows of the two lobes. It is possible that these conglomerates are deposited as the accommodation space towards the east was filled. With no accommodation space available, the flows were forced to the west even though the whole fault block is tilted to the east. Alternatively, the sediment supply exceeded the accommodation space and the additional sediments were deposited in the opposite direction as the two main lobes.

5.2.4.2 Sheetflood

Sheetfloods are the most abundant facies within the Upper Conglomerates and accounts for large portions of Southern and Northern Lobe, this facies is not found within the Western Conglomerates. It is challenging to describe the exact boundary between debris-flows and sheetfloods. Bedding, clast organization, clast size and matrix content are important parameters for separating the different type of deposits. The typical sheetfloods as described in subsection 3.1.2 are not observed within the Upper Conglomerates. Grain size and bed thickness exceeds the expected, so by using the classification scheme of Galloway and Hobday (1996) these deposits are somewhere between debris-flows and sheetfloods (Figure 49). This implies more mass movement and less channeled flow than the deposits classified as sheetfloods by Galloway and Hobday (1996).

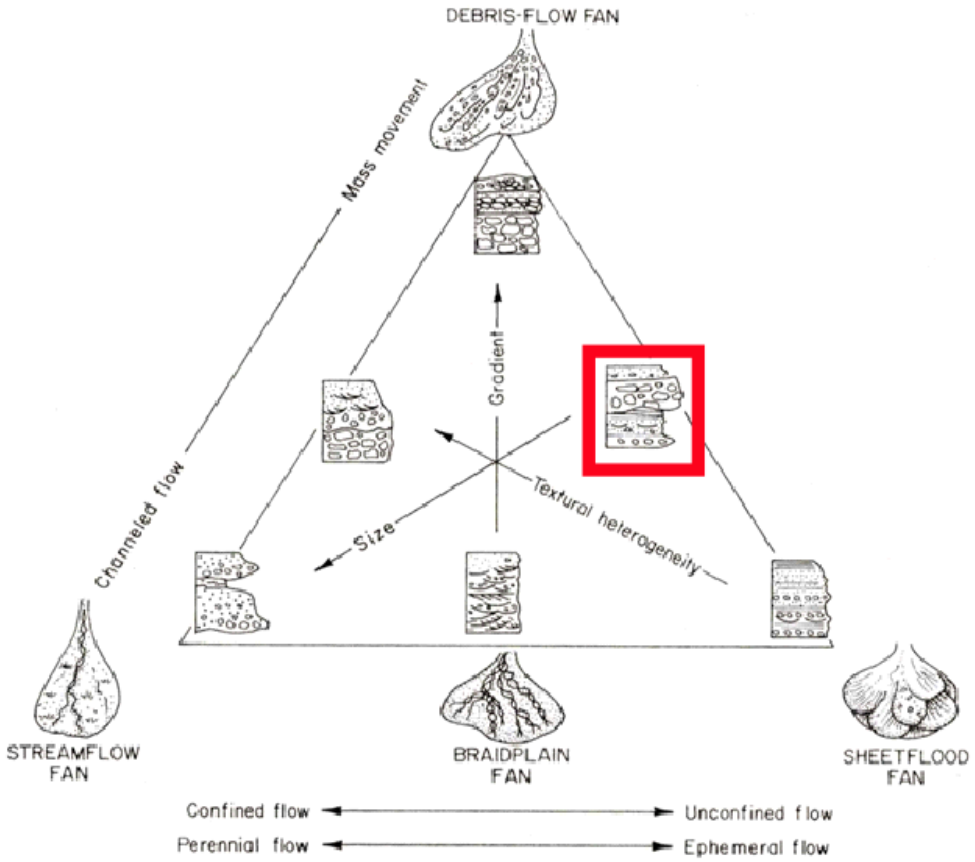

Figure 49: Red box shows the classification of the sheetflood deposits of the Northern and Southern Lobe. The grain size and bed thickness points towards more mass movement and higher gradient than deposits in the lower right corner of the Galloway and Hobday (1996) classification scheme. (Modified from Galloway and Hobday (1996))

Sheetflood deposits consist of coarse-grained sandstone to medium-grained conglomerates. Conglomerate clast size varies from small/medium cobbles (64-100mm) to pebbles (4-64mm), an average value is difficult to obtain due to large variation between different beds. Figure 50 shows an example of very thickly bedded sheetflood deposits on the southern side of the Southern Lobe. The yellow layers represent a coarse-grained sandstone bed between conglomerate beds. The bed thickness of the upper conglomerate bed is approximately 1m, while the conglomerate bed under the sandstone bed is 25 cm thick. Most of the sheetflood conglomerate beds observed fall within 20-100 cm thickness range. The finer-grained beds, such as the sandstones and the pebbly conglomerates are thinner. The sandstone bed in Figure 50 is 20 cm thick, this is in the upper range of fine-grained bed thicknesses. Bed contacts, especially the base of thick beds consistent of cobbles and boulders, are sharp erosive or sharp planar. Grey colored clast (largest clast in the bed) in Figure 50, below the sandstone bed, shows that the transition from conglomerates to sandstones is not gradual or transitional, but rather sharp erosive or sharp planar. This implies that the sheetflood deposits possess erosional forces, even though the grain size and overall depositional energy is lower than for debris-flow deposits.

Clasts are angular to sub-rounded with a significant variation in the sphereicity, the sand grains vary between very angular to sub-angular. As for the whole fault block, limestones clasts are the main clast lithology while chert clasts are the second most abundant clast lithology. Sandstone clasts are rarely observed, but when observed they are rounded with a high sphereicity. Chert clasts are on average smaller than the limestone and sandstone clasts, and occur more frequently in the sandy/pebbly beds than the coarser conglomerate beds. The chert clasts are angular to sub-angular with low sphereicity.

The sheetflood conglomerates are clast supported with relatively low matrix content, but the amount of matrix increases towards the east in what is believed to be the more distal parts of the alluvial fan. As for the debris-flows, the amount of matrix could potentially indicate the water content of the flows. It could also point towards a supercritical flow (high velocity flow), where only the coarse sediments (clasts) are transported and deposited. The finer grained beds, such as the sandstone bed in Figure 50 could be deposited by flows with lower velocity and Freud number. This implies that the beds observed in Figure 50 are individual beds from individual flows rather than a grading feature.

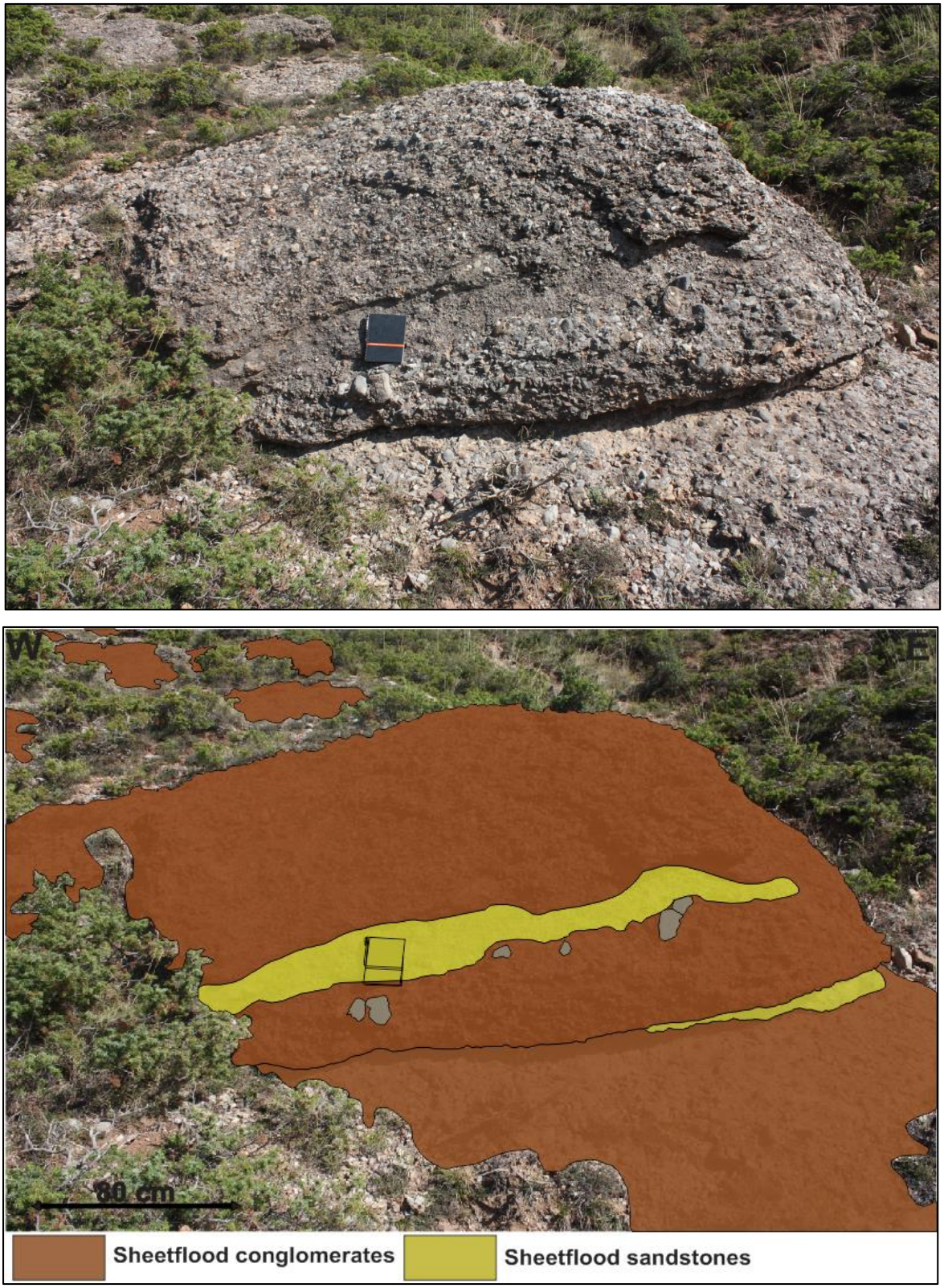

Figure 50: This figure displays a sheetflood deposit consistent of thickly bedded conglomerates and medium to thinly bedded sandstones. The grey colored clast is an attempt to show the sharp contact between the sandstone bed and the conglomerate bed.

The sheetflood deposits displayed in Figure 50 are located in the western part of the Southern Lobe, the sheetflood deposits in Figure 51 are located east of Figure 50 at more or less the same elevation. By comparing the two figures, it is evident that the beds thin eastward. The four conglomerate beds in Figure 51 are probably correlatable with the thicker sheetflood conglomerate beds in the west (Figure 50). Due to vegetation, it is not possible to follow individual beds, but it is clear that the beds are thinner in the east. This trend is also observed for the sheetflood conglomerates of the Northern Lobe.

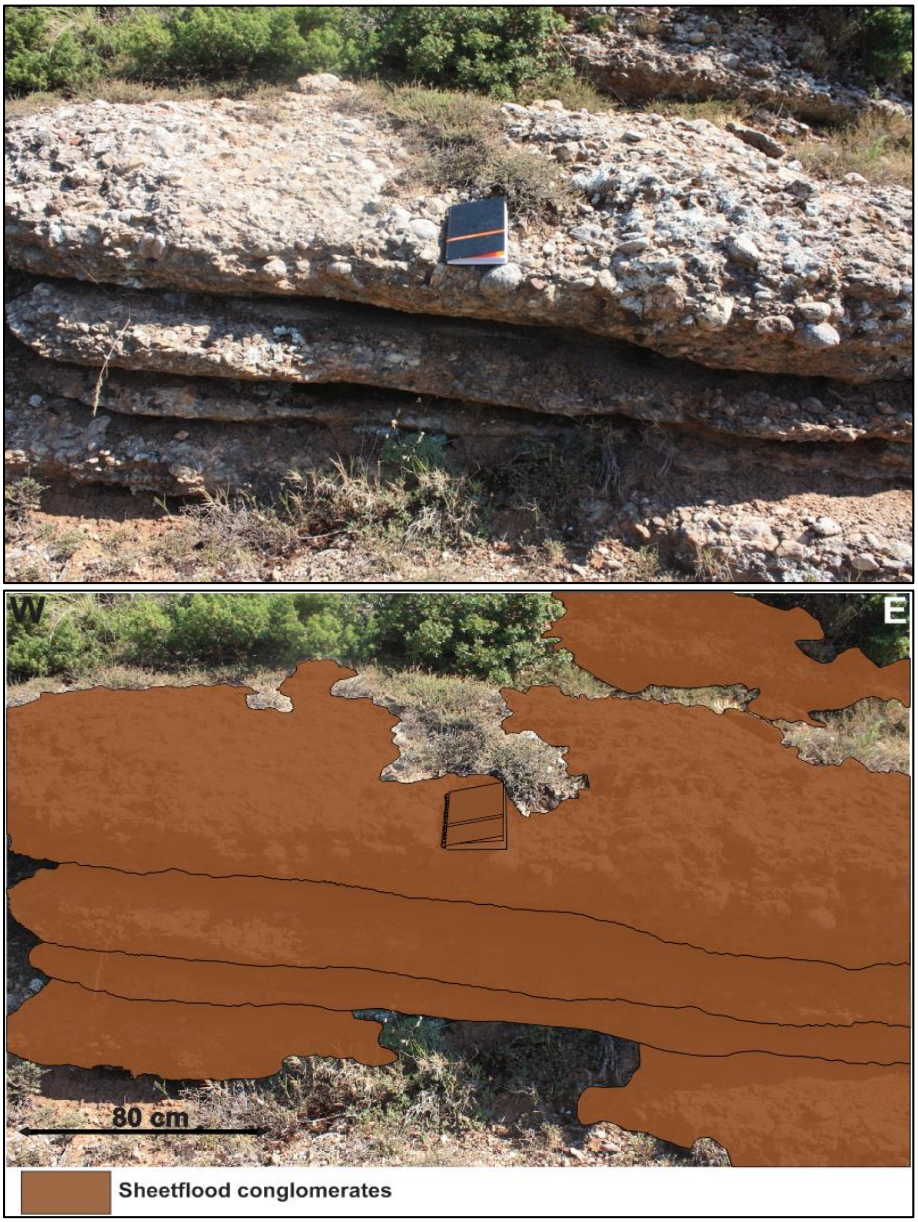

Figure 51: Sheetflood deposits east of the location of the sheetflood deposits in figure 50. These beds are clearly thinner than the ones in Figure 50, indicating a thinning eastward trend for the sheetflood deposited beds.

5.2.4.3 Streamflow

Streamflow deposits are found at the eastern extent of both the Southern and Northern Lobes, but this facies is not observed for the Western Conglomerates. Northern Lobe has better preserved streamflow deposits than the Southern Lobe. Streamflow deposits of the Southern Lobe are heavily weathered, and the streamflow conglomerates are often covered by fine-grained material from the marl/sand beds. The streamflow facies have different characteristics than the sheetflood and debris-flow facies, where the biggest difference is the grain size and the bed thickness. The classical examples of streamflow facies as described in subsection 3.1.3 is not observed within the Upper Conglomerates. Grain size, bed thickness and lack of clear channelization differ from what is normally expected in streamflow facies. The above characteristics points towards more mass movement and less channeled flow (Figure 52).

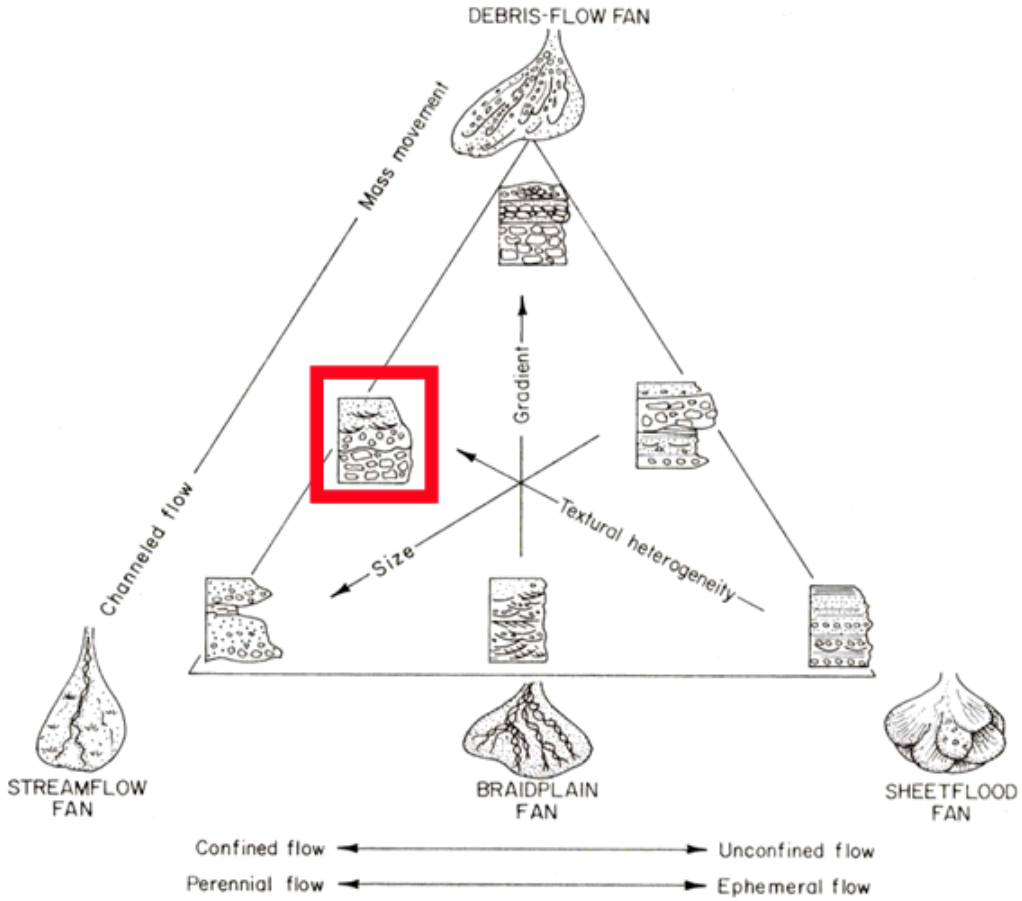

Figure 52: The streamflow deposits of the Upper Conglomerates are classified as shown in the figure. There is alternating layers of conglomerates and sand/marl, hence there is more mass movement and larger textural heterogeneity than for the streamflow deposits shown in the lower left corner of Galloway and Hobday (1996) classification scheme. (Modified from Galloway and Hobday (1996)).

Streamflow deposits are characterized by alternating beds of fine-grained conglomerates and marl/sand. The clast size of the conglomerates varies from pebbles (4-64mm) to small/medium cobbles (64-100mm). Cobbles up to 100mm are rarely observed and boulders are not present in the streamflow conglomerates. Average clast size is approximately 70mm, but there is variation for different beds. Grain sizes for the sandy layers are normally fine to very fine. In most beds, it is difficult to separate between marl and sand due to the very fine-grained nature of the deposits. Sand and marl beds are heavily weathered, which also makes grain size analyses challenging. As shown in Figure 53, beds and bed contacts are well defined. Marl/sand beds are on average thicker than the conglomerate beds, the thickness of the fine-grained beds normally varies between 5 and 60 cm. The conglomerate beds vary in thickness from 20 to 150 cm, the thick top layer in Figure 53 is the thickest bed observed within the streamflow deposits. Bed contacts are sharp and in most cases planar, at some locations it is evident that the conglomerates have eroded into the finer grained layers. Conglomerate beds are normally ungraded and unsorted, while it is hard to obtain any grain organization for the marl/sand beds due to the weathering.

Limestone clasts are the most abundant clast lithology for the streamflow conglomerates followed by chert clasts. Sandstone clasts are only observed sporadically. The limestone clasts are sub-angular to sub-rounded with relatively high sphereicity. Chert clast are more angular (angular to sub-angular) and have a lower sphereicity.

There are three thin conglomerate beds in the upper right corner of the lower picture of Figure 53 (marked with a red square), that seems to be onlapping onto a fine-grained sand/marl beds. This feature could indicate either the backstepping or the prograding of the streamflow deposits. It is evident, by studying the figure, the conglomerate beds are prograding eastwards. In the lack of clear and reliable paleo-flow indicators, this prograding observation indicates that the streamflow deposits are deposited towards east (flowing towards east).

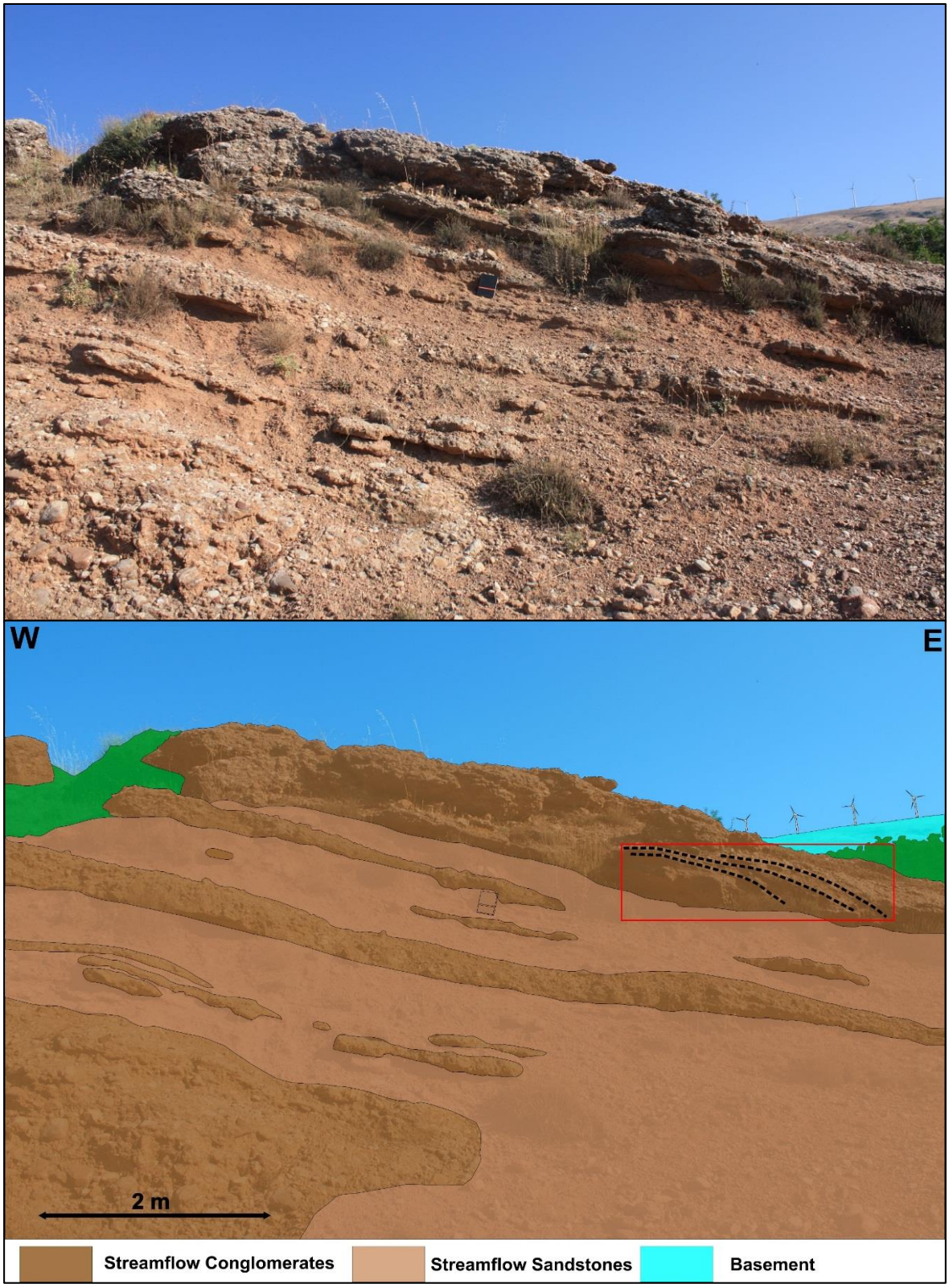

Figure 53: Outcrop example of streamflow deposits in the distal parts of the Northern Lobe. There is alternating beds of conglomerates and sandstone/marl, implying high textural heterogeneity. Fine/medium-grained conglomerates also indicate mass movement instead of channelized flow.

Chapter 6: Structural Observations

The Kerpini Fault Block is the main study area of this thesis, hence the Kalavryta and Dhoumena Faults and fault blocks has not been as thoroughly studied. In addition to the Kerpini Fault, several intra-block faults have been investigated. Some of these intra-block faults were identified by previous University of Stavanger master thesis projects (Stuvland, 2015; Syahrul, 2014). These faults were investigated in further detail, which in some cases led to modification and adjustment of particular faults. Stuvland (2015) was the first to identify Fault C, while Syahrul (2014) identified Fault D, E and the Roghi Fault South. Faults have been identified based on basement outcrops (uplifted footwall), lithology/facies changes and the dipping relationship of sediments. The Kerpini Fault marks the southern boundary of the fault block, and Dhoumena Fault marks the northern boundary. North-south striking transfer faults have been interpreted to be located in Vouraikos and Kerinitis valleys (Dahman, 2015), the presence of these transfer faults will be further discussed in the following chapter. Solid black lines in figures for Chapter 6 represent the fault trace, while the dashed black lines are an inferred fault or the continuation of a fault that is not clearly visible.

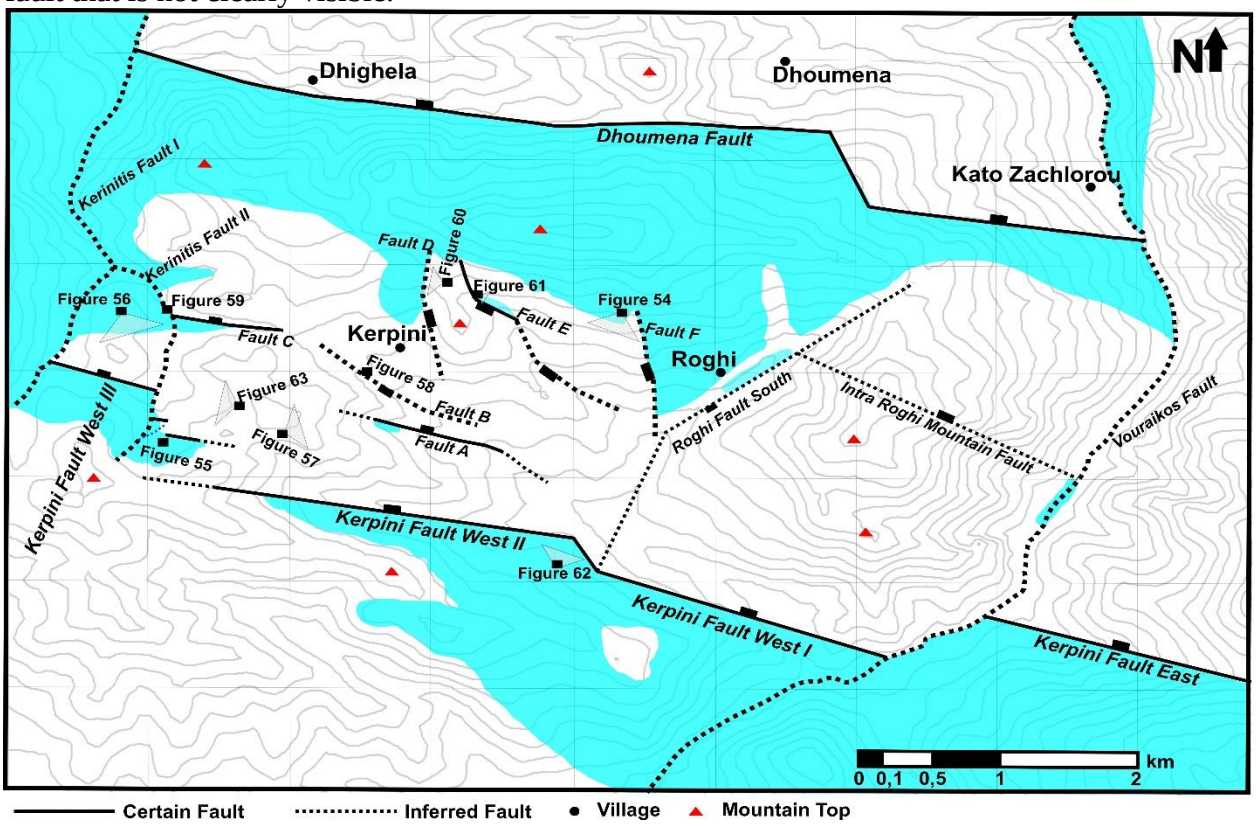

Figure 54: Structural map of the Kerpini Fault Block. There are two main strike directions for the faults, east-west and north-south. All faults are given a specific name. Basement locations within the Kerpini Fault Block are shown alongside faults because these outcrops helped identify the presence of faults.

Fault	Location	Type	Strike	Dip	Dip Direction	Max Displacement (m)	First Observation	Footwall Unit	Hanging wall Unit
Kerpini Fault East	East of Vouraikos Valley, north of Souvardho village.	Normal Fault	N105°E	40-45°	North	1400 (Ford et al., 2013)	Unknown	Basement	Coarse alluvial conglomerates. (Ford et al., 2013)
Kerpini Fault West I	Eastern part of Kerpini Fault Block. South of Roghi Mountain	Normal Fault	N107°E	40-45°	North	1750-2000	Unknown	Basement	Roghi Conglomerates
Kerpini Fault West II	Central part of the Kerpini Fault Block.	Normal Fault	N100°E	40-45°	North	1000	Unknown	Basement and Kalavryta Conglomerates	Lower Conglomerates and Upper Conglomerates
Kerpini Fault West III	Western part of the Kerpini Fault Block	Normal Fault	N110°E	40-45°	North	400	Unknown	Basement	Lower Conglomerate Unit
Fault A	Between Northern and Southern lobe. South of Kerpini village	Normal Fault	N105°E	40-45°	North	300	Hadland, 2016	Basement, Upper and Lower Conglomerates	Lower Conglomerate Unit and Upper Conglomerate Unit
Fault B	Immidiately north of the northern lobe. South of Kerpini village	Normal Fault	N120°E	45°	South	N/A	Hadland, 2016	Lower Conglomerates	Upper Conglomerates
Fault C	Western part of the Kerpini Fault Block. 1 km east of Skepasto Mountain	Normal Fault	N97°E	40-45°	North	350	Stuvland, 2015	Basement and Lower Conglomerates	Lower Conglomerates
Fault D	East-northeast of Kerpini Village. West of Fan A	Normal Fault	N350°E	30-50°	East	N/A	Syahrul, 2014	Basement and Lower Conglomerates	Footwall Derived Fan. Fan A
Fault E	East-northeast of Kerpini Village. East of Fan A	Normal Fault	N310E	30-50°	West	N/A	Syahrul, 2014	Basement and Lower Conglomerates	Footwall Derived Fan. Fan A
Fault F	West-northwest of Roghi Village. East of Fan B	Normal Fault	N350°E	30-50°	West	N/A	Hadland, 2016	Basement (Lower Conglomerates)	Footwall Derived Fan. Fan B
Roghi Fault South	East of Roghi village. Eastern boundary of the Roghi Conglomerates	Transfer Fault (normal displacement)	N30°E (Syahrul, 2014)	Close to vertical (Syahrul, 2014)	Southeast	400	Syahrul, 2014	Basement and Lower Conglomerates	Roghi Conglomerates (Sub-horizontal Sediment)
Intra Roghi Mountain Fault	Northeast of Roghi Mountain. Within the Roghi Conglomerates	Normal Fault	N115°E	40-45° (Syahrul, 2014)	North-northeast	100	Syahrul, 2014	Roghi Conglomerates	Roghi Conglomerates
Vouraikos Valley Fault	Eastern extent of the Kerpini Fault Block	Transfer Fault	North-South	Close to vertical	N/A	Transfer Fault	Dahman, 2015	Transfer Fault	Transfer Fault
Kerinitis Valley Fault	Western extent of the Kerpini Fault Block	Transfer Fault	North-South	Close to vertical	N/A	Transfer Fault	Unknown	Transfer Fault	Transfer Fault

Table 2: Summary of the different faults located within the Kerpini Fault Block. The data shown in the table are based on field observations, cross-sections and previous work.

6.1 Kerpini Fault West

The Kerpini Fault has been separated into two parts, the Western and Eastern Kerpini Fault. The Eastern Kerpini Fault is located east of the Vouraikos Valley outside the area of interest of this thesis project. Eastern and Western Kerpini Fault is separated by a 750 m left step in the Vouraikos Valley. The Western Kerpini Fault can further be subdiveded into three distinct segments, segments I, II and III. The three segments have slightly different strike, segment I strikes N107°E, segment II strikes N100°E and segment III strikes N110°E. Two distinct steps separates the different segments of the fault, both steps relocate the displacment northwards (right stepping). The step between segments I and II coincides with the north-south striking Roghi Fault South (subsection 6.9.2), Roghi Fault South is belived to controll the step between segments I and II. The step between segment II and III is quite complex, where the second segment of the Kerpini Fault splays into two smaller normal faults (Splay Fault I & II). Displacment along these two smaller normal faults are belived to be in the range of 500-600 m. Poor fault plane exposure makes fault dip measurements challenging, but a dip angle similar to other basin bounding faults in the region (40-45°) has been asssumed for all the segments. Segment I of the Kerpini Fault (south of Roghi Mountain) exhibits the largest diaplacement of the three segments (Figure 70). Displacment decreases as one moves westward. The fault tip (the position of zero displacment) is not observed for the Western Kerpini Fault. As the fault reaches the Kerinitis Valley, the fault truncates in the valley with large displacment (410 m based on cross-section A). Another explenation of the western end of the Kerpini Fault is that there is a rapid loss of displacment, 410 m of displacment is lost over a distance of 450 m (based on the location of cross-section A).

Figure 55 shows an interpreted and an uninterpreted overview picture taken from the north looking south of the Kerpini Fault West, segments I and II. Some intra-block faults have also been included in the figure. The Kalavryta Conglomerates located in the footwall is marked with green color, bounded by the Kalavryta unconformity (dashed red line). The step in the fault is located where the Roghi Fault South truncates the Kerpini Fault West.

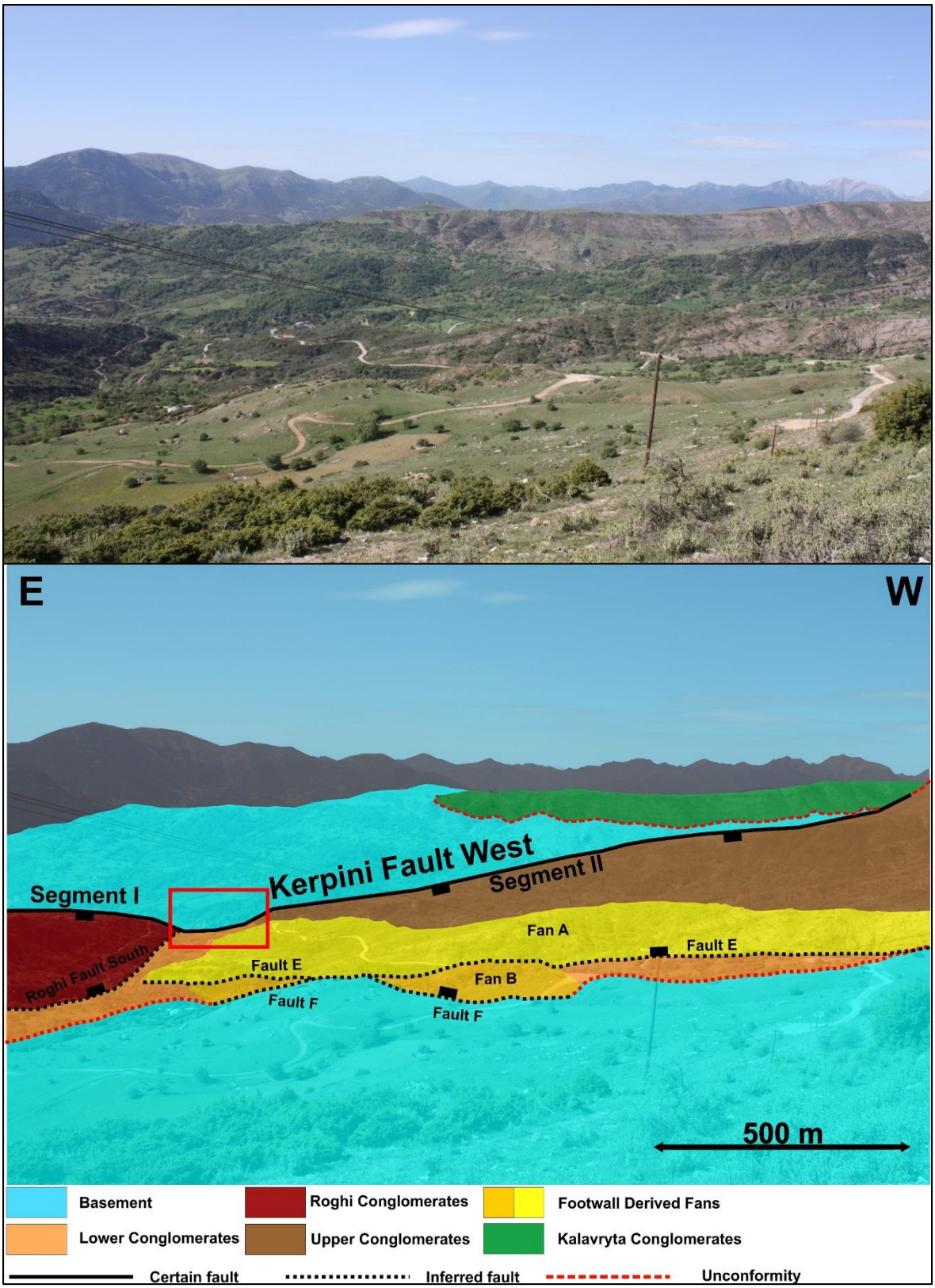

Figure 55: Overview picture of the Western Kerpini Fault, photo is taken looking south. Most of the Kerpini footwall is composed of basement, in addition there is approximately 150 m of Kalavryta Conglomerates (green color). Some of the stratigraphic units in the Kerpini Fault Block are also marked in the figure. The red box shows the location of the step between segments I and II Scale is relative to Kerpini Fault West trace.

6.1.1 Kerpini Fault – Segment I

Segment I is the easternmost segment of the Western Kerpini Fault, the length of the segment is roughly 2 km. The eastern end is marked with a significant left step, where the Eastern Kerpini Fault is located 750 m to the north along the Vouraikos Valley. Roghi Conglomerates are located in the hanging wall of the segment I, while basement is located in the immediate footwall of segment I. Based on cross-section E (Figure 70), the displacement of the Kerpini Fault (segment I) is between 1500-1750 m. This implies that the displacement of the Western Kerpini Fault is largest in segment I. There is not observed a significant change in the displacement along segment I, this mean that the displacement of the Western Kerpini Fault is large when it north-steps to the Eastern Kerpini Fault. As described in the previous paragraph, the western end of segment I is where the Roghi Fault South intersects the Western Kerpini Fault resulting in a northwards step in the Western Kerpini Fault.

6.1.2 Kerpini Fault – Segment II

Segment II is the central segment of the three, it stretches for 3 km between the two steps. Upper Conglomerates are displaced against basement in the eastern part of the segment, while Upper Conglomerates are displaced against Kalavryta Conglomerates in the immediate hanging wall of the western part of segment II. An interesting observation is the 150 m of Kalavryta Conglomerates in the immediate footwall of the Kerpini Fault. This implies that the sediments deposited syn-Kalavryta Fault were displaced by the Kerpini Fault, and must therefore have existed within the Kerpini Fault Block prior to the Kerpini Fault development. The Kalavryta Conglomerates are most likely located below the Upper Conglomerates, and could outcrop further north in the fault block. The displacement of Western Kerpini Fault within segment II decreases westward, this statement is based on the throw calculations from cross-sections B, C and D (Figure 67, 68 and 69). The easternmost of segment II cross-sections (Figure 69) display a throw of 1000m, while the two central and western cross-sections (Figure 67 and 68) display a throw of approximately 700m. This implies that the displacement is decreasing westwards towards the step between segments II and III.

6.1.3 Kerpini Fault – Segment III

The Kerpini Fault has by previous authors (Collier and Jones, 2004; Ford et al., 2013; Syahrul, 2014) been interpreted to only have one step, the step between segment I and II. Based on field mapping, basement-sediment contacts, this study introduces the possibility that the Kerpini Fault splays into two smaller normal faults (Figure 54 and Figure 57) before it terminates in the Kerinitis Valley. Red Shale deposits at the location where the two smaller normal faults has been identified, complicates the overall picture of the area. The Red Shales lie on top of the basement and on top of the Upper Conglomerates. Based on the contact between the Red Shales and the basement it is believed that the Red Shales have been mobilized recently (relative), and the red shale-basement contact is a soil profile (Figure 56) not an unconformity contact.

Figure 56: Photo showing the Red Shales overlaying the basement. Based on the irregularity and inconsistency of the shale-basement contact, it has been classified as a soil profile. Scale is relevant to red shale outcrop.

Figure 57 shows an overview picture of the eastern part of segment III, where the two splay faults are marked. The picture is taken with an angle such that Splay Fault I seem to be curvy when it is actually a straight feature. Kerpini Fault II steps/splays northwards into the easternmost fault marked in Figure 57, Splay Fault I. From there, the displacement is again shifted northwards to another normal fault, Splay Fault II. The final step, along the Kerinitis Fault II, is shown in Figure 57 with a dashed black line. The Kerinitis Fault II is interpreted as a

transfer fault (see subsection 6.7). Red Shale and vegetation makes it difficult to place the basement-sediment contact accurately. The final stage of the Kerpini Fault (northern dashed black line) is also shown in Figure 57, the exact fault trace is located south of the hill. It is in the step from segment II to III it is suggested that the Upper Conglomerates are sourced from and deposited in the hanging wall.

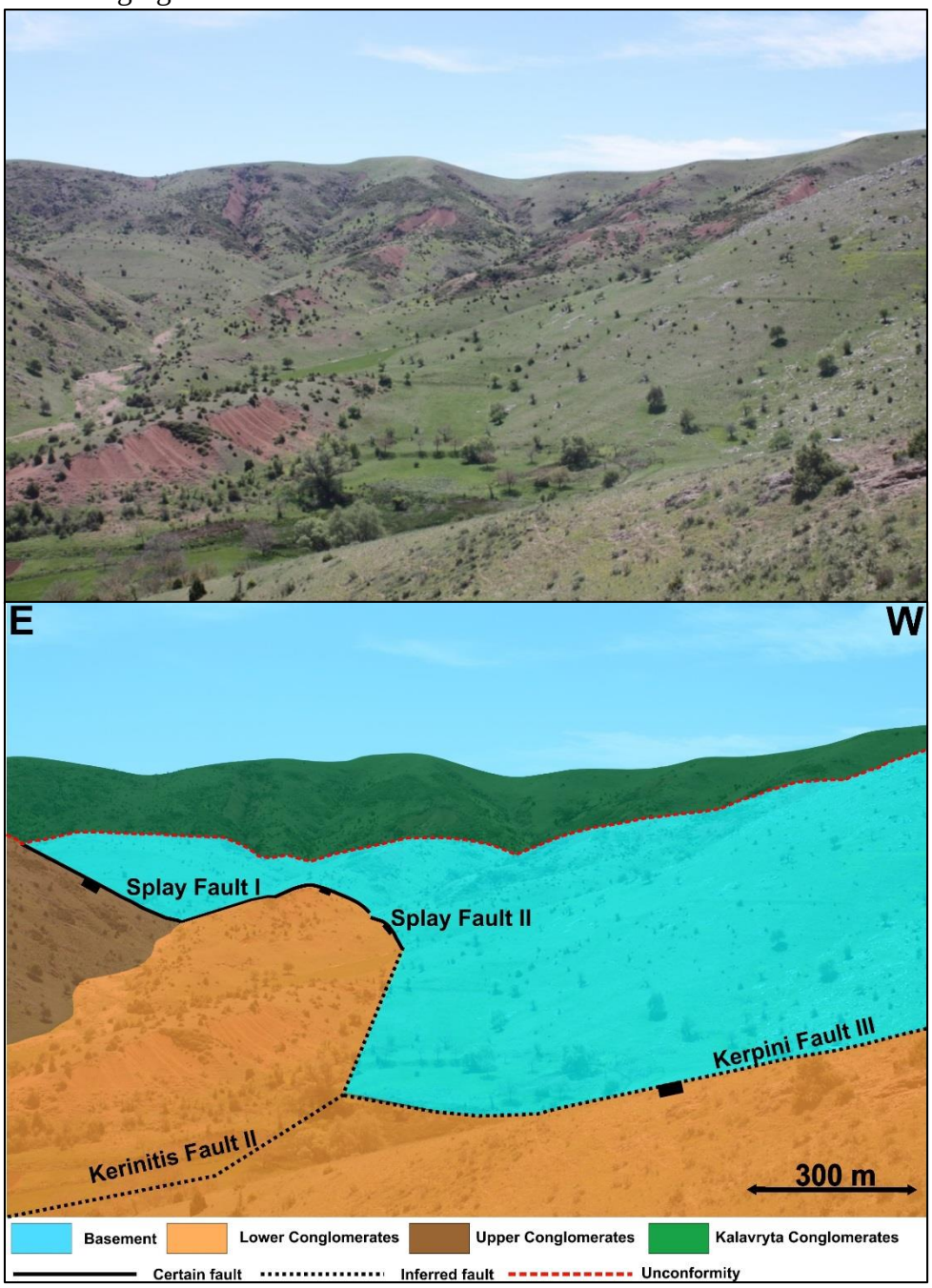

Figure 57: Western Kerpini Fault. The figure shows the structurally complex step of the Kerpini Fault between segments II and III, where the two splay faults are marked. The exact position of the Kerinitis Fault II is difficult to interpret due to vegetation and the presence of Red Shales. Scale is relevant to the area with the two splay faults.

6.2 Fault A

Fault A was identified by an anomalous elevated outcrop of basement cherts lying between the two lobes of the Upper Conglomerates, it is also located south of Fault B. The fault is striking N105˚E and dipping towards the north, this means that Fault A has a very similar strike as the Kerpini Fault. A similar dip as the Kerpini Fault (45˚ -50˚) has been assumed since the fault plane is not exposed.

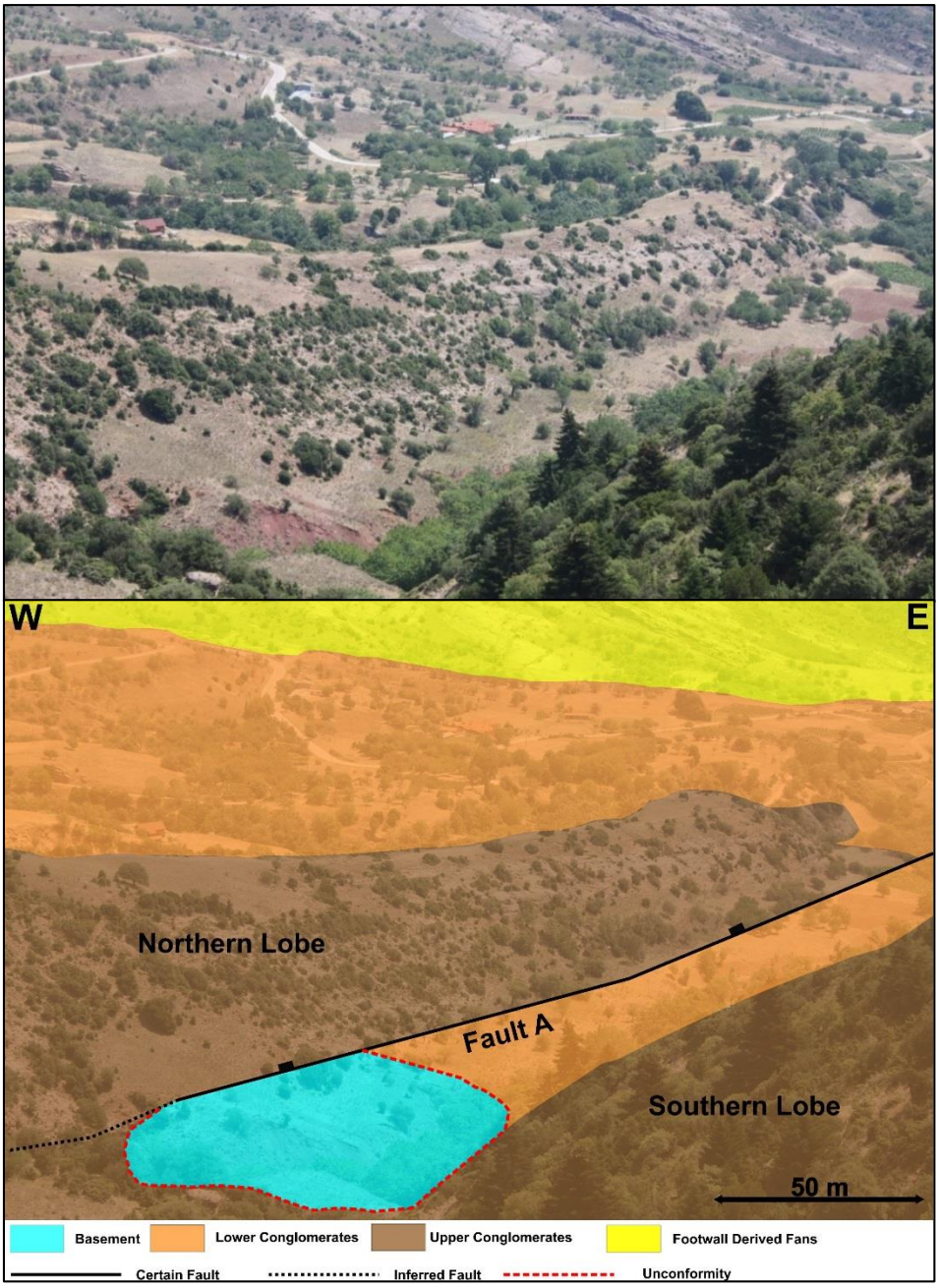

Figure 58: Overview photo of the north-dipping Fault A. The basement in the footwall is marked with a light blue color. It is believed that the fault continues towards the west (dashed black line). The fault also continues eastward where a rapid facies change is observed on each side of a river valley. Scale is relevant to basement outcrop.

Figure 58 display an interpreted and an uninterpreted overview picture of Fault A. At the western extent of the fault, basement-chert is uplifted and exposed in the footwall. The basement-chert is only exposed in a small 80x50 m outcrop, the rest is covered by the Upper Conglomerates. The fault is most likely continuing towards the west, but is fully covered by the Upper Conglomerates and is therefore difficult to map. At the eastern extent of the fault marked in Figure 58, there is an east-west river valley that separates the Northern and Southern Lobe. It is likely that Fault A continues a distance in this river valley. The reason for carrying the fault eastward is that there are conglomerates in the Northern Lobe (in the hanging wall) and fine-grained marl/sand in the footwall. At such short distance (approximately 30 m), it is not likely that the lithology change across the river valley could be explained by a single facies change. Therefore, a faulted contact explains the abrupt change in lithology across the river valley.

Together with the south dipping fault (Fault B), Fault A creates a graben. The fault is most likely older than the Kerpini Fault and this fault may represent a propagation of the active fault into the hanging wall of the Kerpini Fault. This implies that the displacement of the Kerpini Fault has propagated northwards and formed Fault A. Fault A creates accommodation space for the Upper Conglomerates to fill, so the deposition shifts from the accommodation space close to the Kerpini Fault into the accommodation space created by Fault A.

6.3 Fault B

Fault B is located immediately north of the Northern Lobe, south of Kerpini village, in a deep river valley. As for the previous intra-block faults, the fault plane is not exposed. Strike of this fault has been measured to be N125˚E, the dip of the fault is unknown due the fault plane is not exposed. A south dipping fault has been placed at this location to explain the dip relationship of the conglomerates across the river valley, the conglomerates are dipping in opposite direction (north and south).

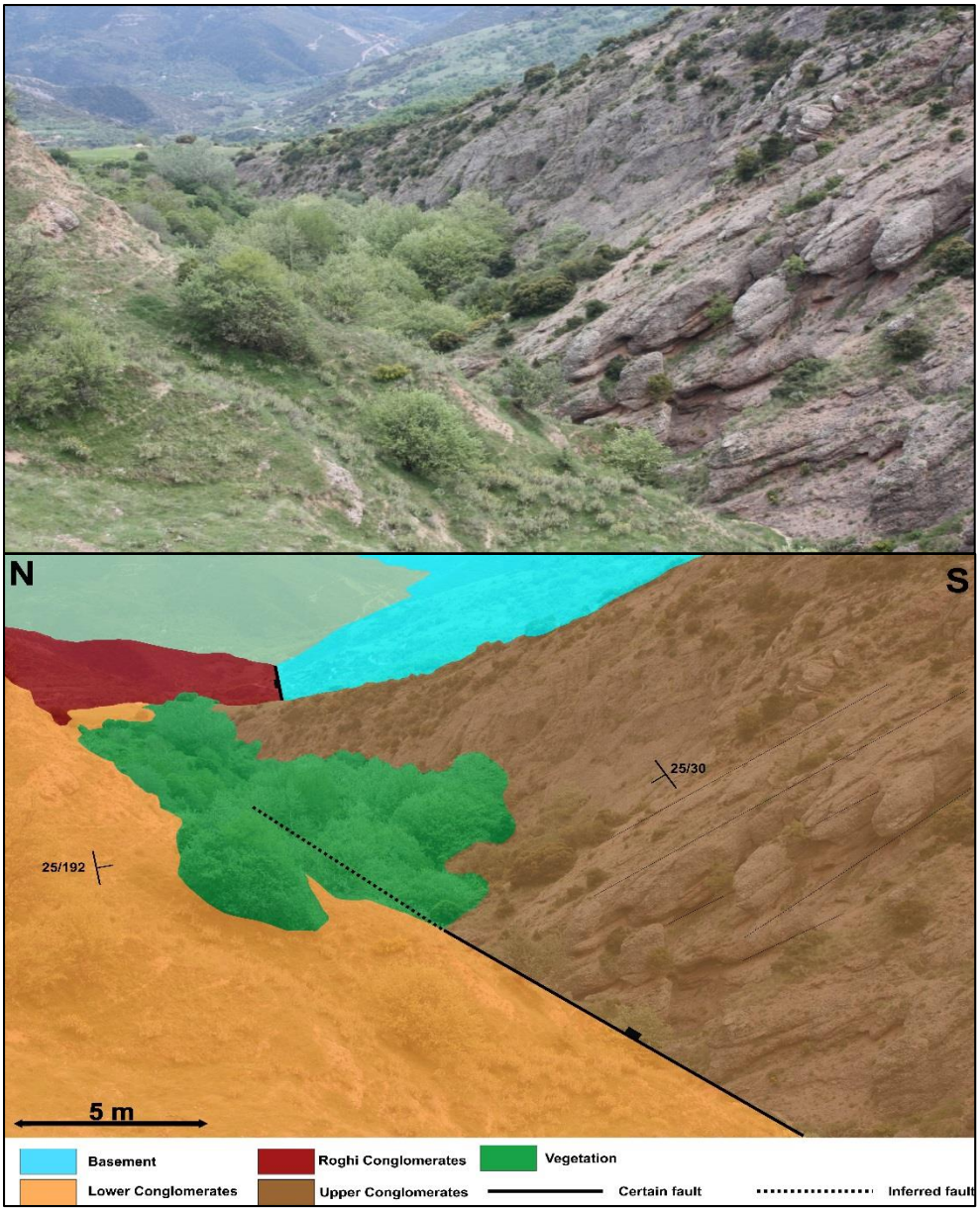

Figure 59: This photo is taken in of the river valleys looking east. The north dipping conglomerates are located in the hanging wall of the fault, while the south dipping conglomerates are located in the footwall of the fault. The fault continues to the eastern extent of the Upper Conglomerates. Scale is relevant for front of figure.

North dipping conglomerate beds are marked in Figure 59 in the hanging wall of the fault. The south dipping conglomerates in the footwall is poorly exposed at the location where this picture is taken. There is no exposed basement observed in the footwall of the south dipping fault. North dipping conglomerate beds of the Northern Lobe is observed southeast of Kerpini village and carries on for 1,3 km to the southeast. It is therefore believed that the fault has the same length, approximately 1,3 km. The green area marked in Figure 59 is a heavily vegetated area in the river valley, which makes it hard to place the exact location of Fault B towards the east. Depositional dips could in principle explain the north dipping conglomerate beds, but if restoring the section an angle of 25˚-30˚ has to be added to the bedding dip. By restoring the section and adding the rotation of the unconformity, the basal north-dipping conglomerates were deposited in an angle of 45˚-50˚. These large angles would most likely exceeds the frictional angle, which makes a south dipping fault a more reasonable explanation for the north dipping beds.

6.4 Fault C

Fault C is located in the western part of the Kerpini Fault Block (Figure 54), separating basement to the south from conglomerates in the north. The fault plane is not exposed and most of the basement in the footwall is covered by vegetation. The strike has been measured to be N100˚E with a small change in strike, 5˚ -10˚ towards the east.

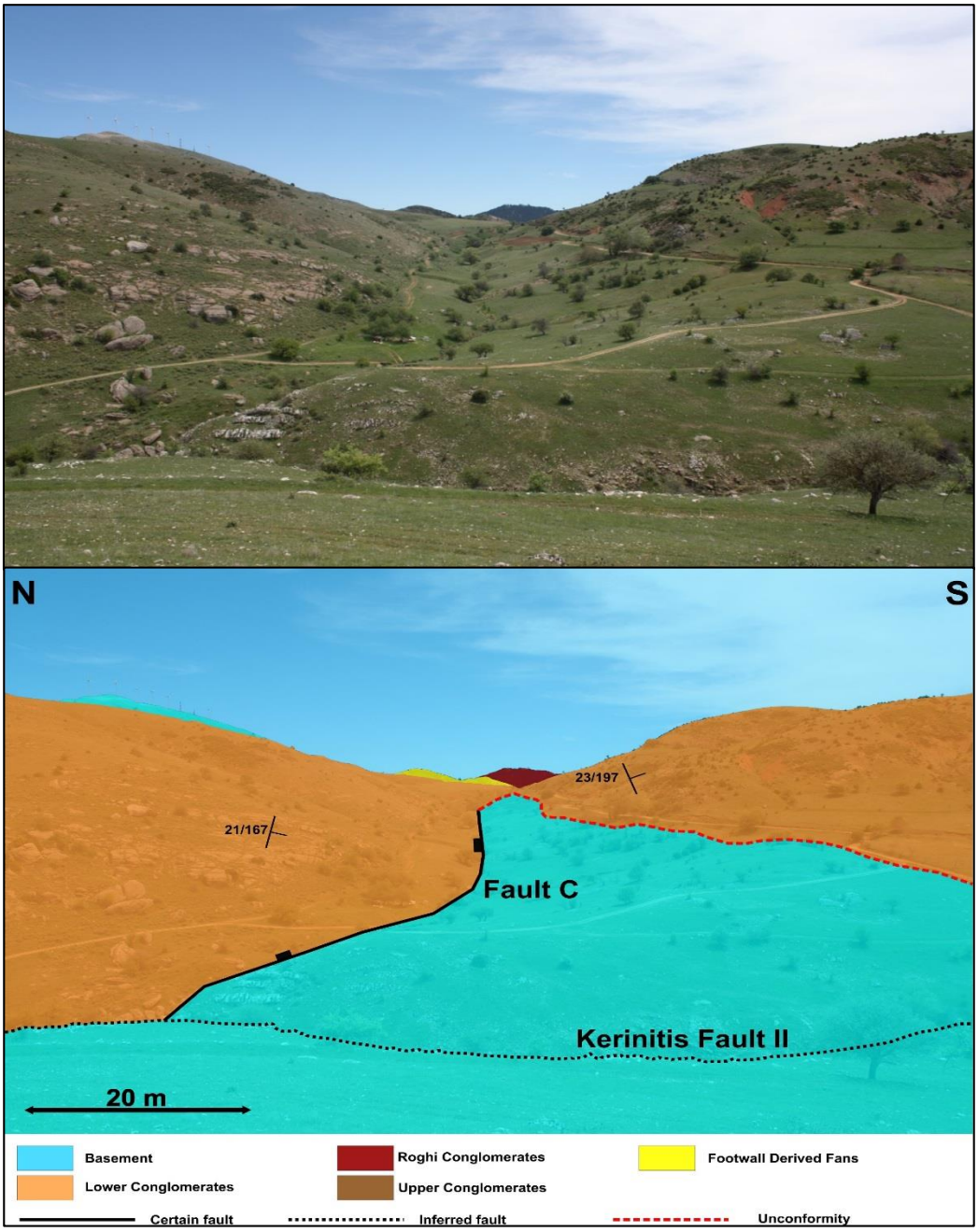

Figure 60: Photo of Fault C looking east. The displacement of the fault is largest at the western end of the fault, but the displacement stops abruptly in a north-south orientated river valley. There has to be something within the river valley that accommodates the displacement, possibly the Kerinitis Fault II. Scale is relevant to center of figure.

Since the fault plane is not exposed, any dip measurements were not taken, but a similar dip trend to the Kerpini Fault (45˚ -50˚) is assumed. The fault is dipping north-northeast, and is approximately 800 m long. Figure 60 shows an interpreted picture and a clean uninterpreted picture of Fault C. The angle in which the picture in Figure 60 is taken, might suggest a bigger change in strike than what is truly observed. Most of the basement seen in the footwall of the fault is covered by vegetation, but in the western end of the footwall (on the east side of Kerinitis Fault II) the basement is clearly exposed. The elevation of the exposed basement is highest towards the west and it is therefore assumed that the maximum displacement is at the western end of the interpreted fault in Figure 60. The dashed line in the figure represents a river valley in which the fault ends. At this point, the fault still has displacement that leads to the speculation of a possible transfer fault (Kerinitis Fault II) in the river valley. A displacement pattern observed for this fault is not reasonable with high (relative) displacement on the eastern side of the river valley, and no displacement on the western side of the valley. The transfer fault will in this case accommodate the displacement and transfer it elsewhere. Transfer faults and their presence in the study area will be further discussed in subsection 6.7. Conglomerates in the hanging wall of the fault are dipping 21˚ south-west into the fault plane, while the conglomerates in the footwall are dipping 23˚ south-southeast.

6.5 Fault D and E

The westernmost footwall derived fan, Fan A, is bounded by two faults (Fault D and E), one fault on both sides of the fan. The faults are dipping in opposite directions, and will be referred to as Fault D and E. This means that the two faults form a graben were the Footwall Derived Fans have filled the accommodation space. Figure 61 shows an interpreted and an uninterpreted picture of Fault D.

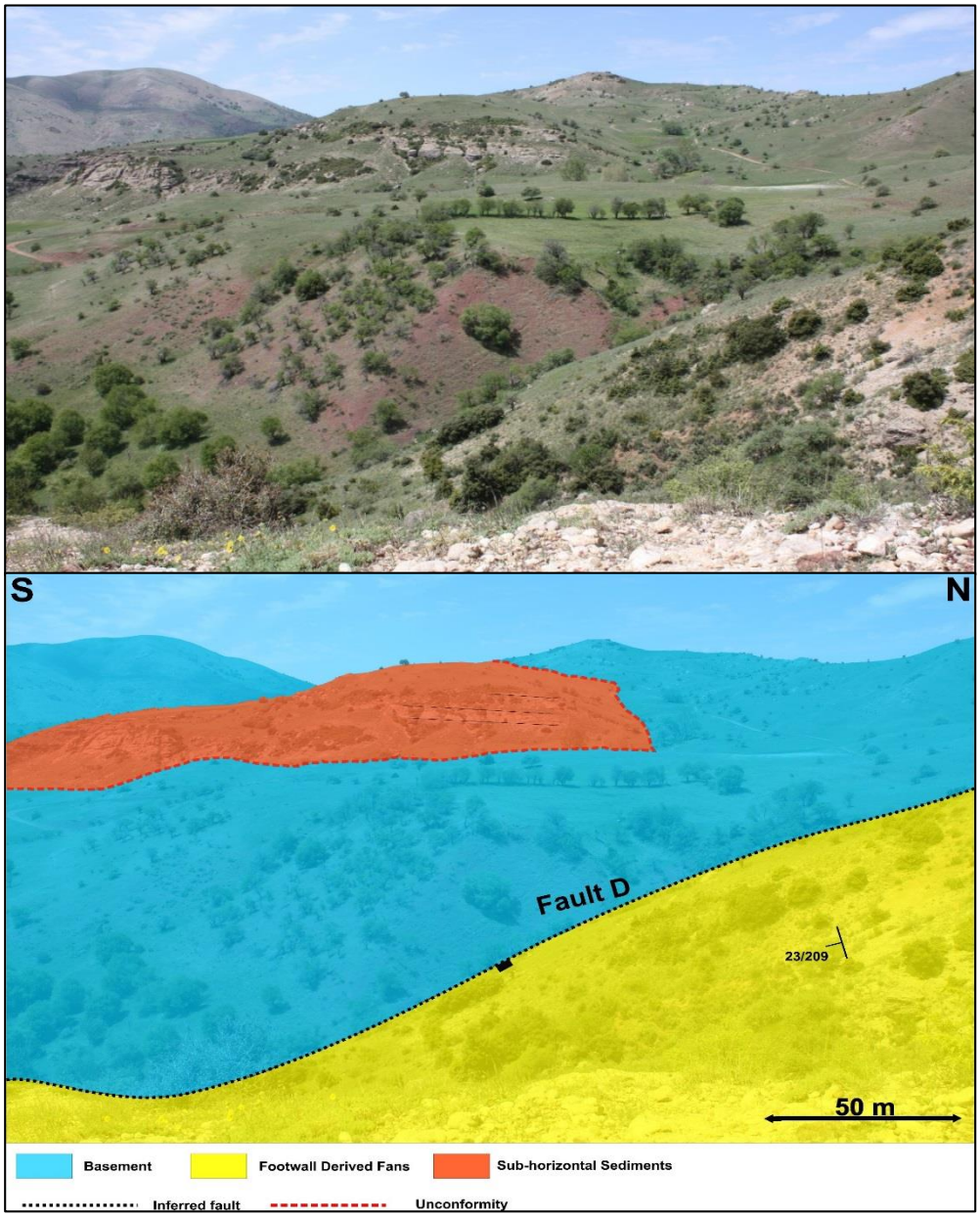

Figure 61: This photo is taken standing on top of Fan A, looking west. The figure clearly shows the red chert basement in the footwall of the fault. There is a sharp and high angled contact between the fan sediments and the basement, this implies the presence of a fault. Scale is relevant for immediate footwall (basement).

The fault is dipping towards the east, with basement exposed in the footwall. Like all the other intra-block faults, the fault plane is not exposed. The lack of fault plane exposure makes dip angle measurements of the fault difficult. A fault has been interpreted at this location due to the uplifted and exposed basement west of the fan. The northern fault tip is assumed to be located close to the apex of the fan, and the fault dies out (southern fault tip) somewhere southeast of Kerpini village. Even though the fan continues further towards the southeast, there are no evidences for continuing the fault towards the southeast. The conglomerate beds on the western side of footwall derived fan (bedding dip shown in Figure 61) dips in a south-southeast direction. This means that the sediments are not rotated into the fault plane. The most likely explanation for this is that the eastern fault (Fault E) has a bigger displacement, therefore the conglomerates are rotated more towards this fault.

Fault E strikes approximately N45˚E and dips towards the west, with basement exposed in the northern end of the fault (Figure 62). Further to the south, Fan A is displaced against the Lower Conglomerates unit. The reason for interpreting a fault on the eastern side of the fan is the exposed basement in the northern end of the footwall, along with a relatively sharp boundary between the Lower Conglomerates unit in the bottom of a river valley. As the map in Figure 54 shows, the northern part of the fault (where the basement is exposed in the footwall) is interpreted as a certain fault while the southeast continuation of the fault is inferred. Figure 62 shows an interpreted and a uniterpreted figure of Fault E. The figure shows that the conglomerates are displaced against basement in the northwest while further towards the southeast the Fan A-conglomerates are displaced against the Lower Conglomerates unit. Where the certain fault ends in Figure 62 (solid black line), the fault curves and gets a more southward strike. Conglomerate beds in the proximity to the fault dips in an east-southeast direction, which is more towards the inferred part of Fault E.

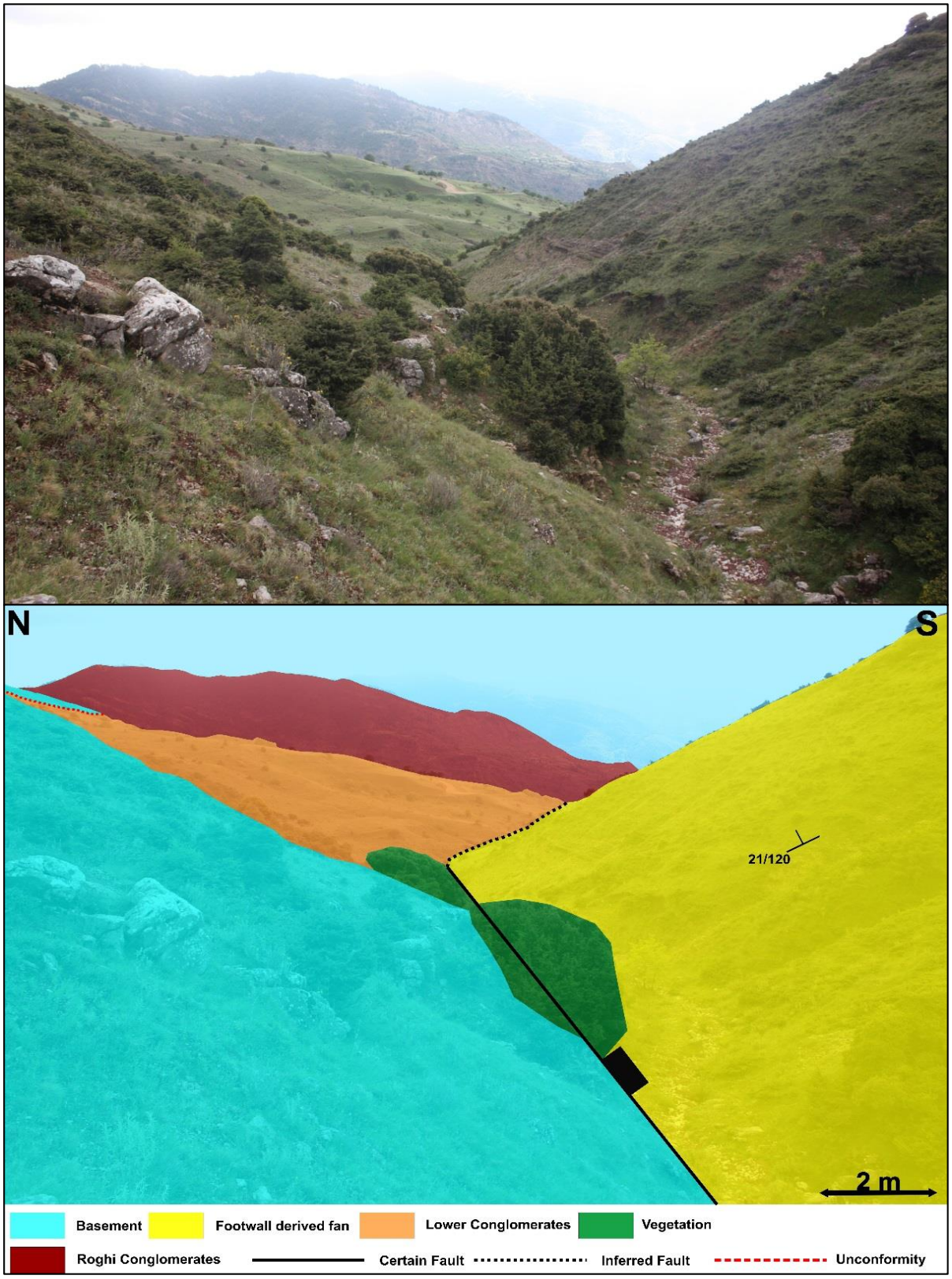

Figure 62: The photo is taken on the east side of the Fan A, looking southeast. As for Fault D, there is a high angled contact between the fan sediments and the basement. The dashed black line represent the approximate position of where the fault changes strike, to a more south-southeast strike. Scale is relevant to front of figure.

6.6 Fault F

Fault F is the bounding fault of Fan B, the fault is located east of the fan. It is a N30˚E striking fault that dips towards the west. Fault dip is unknown due to the lack of fault plane exposure, a dip in the range of 40˚-50˚ is assumed when making the cross-sections.

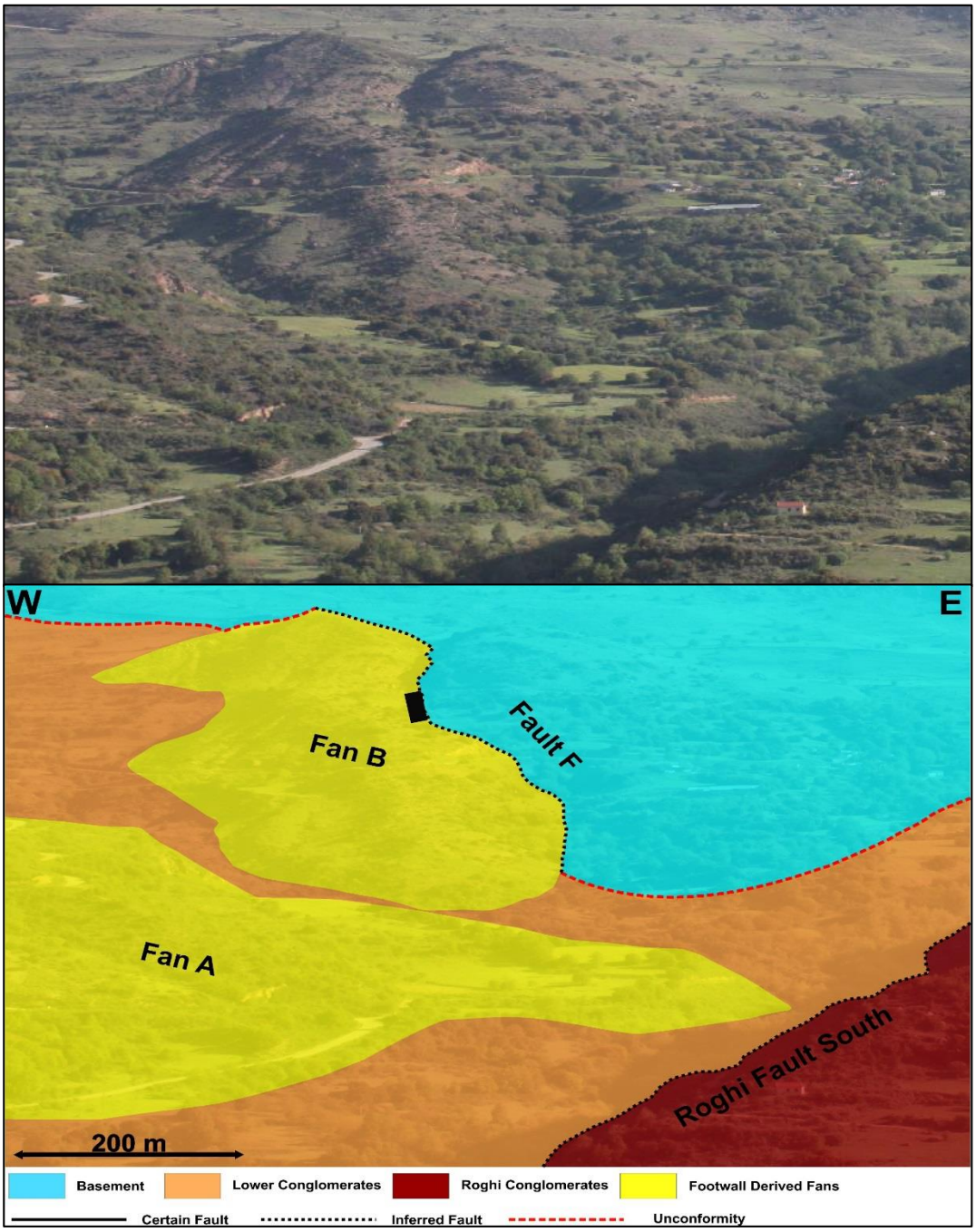

Figure 63: This is a zoom-in photo of the northern part of the Kerpini Fault Block. The figure shows Fan B, and its west dipping bounding fault. Even though the fault trace appears curvy, it is just the angle of which the photo is taken. It is possible that the fault extends to and connects with the Roghi Fault South. Scale is relevant to Fan B.

West of the fan, the elevation of the unconformity gently decreases down the slope. At the position where the fault has been interpreted, the unconformity suddenly drops in elevation along a north south-orientated river valley. The sudden drop in unconformity elevation has been interpreted to be caused by a fault. The northern extent of the fault is located at the apex of fan, while the fault ends where the fan sediments ends, with a possibly extension to the Roghi Fault South. Figure 63 shows an interpreted and an uninterpreted picture of Fault F taken from the footwall of the Kerpini Fault. The picture is taken in an angle such that fault seems to have some sharp bends, in reality the fault is more a straight feature. Fan B conglomerates located in the hanging wall of the fault dips towards the south, the expected dip against the fault is not observed. A possible explanation for the dips could be that conglomerates filled the accommodation space at a late stage, which means that the dips represent depositional dips.

6.7 Transfer Faults

There are two north-south orientated river valleys, Vouraikos and Kerinitis, which marks the eastern and western extent of the Kerpini Fault Block. Some of the major faults in the Corinth rift system either terminates against or steps in these river valleys. Therefore, one can speculate that the river valleys represent north-south orientated transfer faults that segment the whole rift system.

6.7.1 Vouraikos Fault

Both the Kerpini and Dhoumena Faults steps in the Vouraikos Valley. When doing simple fault projection exercises in the field, it is clear that the faults cannot be traced across the valley. In addition, by projecting the Kerpini Fault across the Vouraikos Valley the lithology changes from conglomerate (west side of valley) to basement (east side of valley). This means that the fault is most likely stepping, in this case of the Kerpini Fault it steps northwards. The same argument (lithology change) is not valid for the Dhoumena Fault, were the lithology change is not as clear across the valley. However, the thickness and texture/facies of the sediments on each side of the valley is very different. Therefore, one can argue that the Dhoumena Fault also steps in the Vouraikos Valley. It is also clear that the unconformity on each side of the Vouraikos Vally is at different elevations, the unconformity sits in the base of the valley on the western side. While on the eastern side, the unconformity sits in the middle of the slope (approximately 100 m higher).

The fault plane of the possible Vouraikos Fault is not exposed, but the dip is assumed to be close to vertical. The indications of a transfer fault in the Vouraikos Valley are as followed:

- Fault projection across the valley is not possible
- Different lithologies and facies across the valley
- Large difference in unconformity elevation across the valley

6.7.2 Kerinitis Fault

While the Kerpini Fault is marked by a northwards step at the eastern extent, an abrupt ending of the fault against Skepasto Mountain marks the western end of the fault. Skepasto Mountain is a large mountain consistent of basement. Figure 64 shows an interpreted and an uninterpreted picture of the western end of the Kerpini Fault. The conglomerates on the north side of the fault is dipping 30˚ south, and by projecting the unconformity (with the same dip as the conglomerates) into the fault one gets a throw of 410 m. 200 m west of where the picture in Figure 64 is taken, the Kerpini Fault has truncated against the Skepasto Mountain. 410 m of displacement has gone to zero displacement over a distance of 200 m. This displacement profile is unreasonable, it seems like there is some feature in the river valley that transports the displacement elsewhere.

Moving northwards along the Kerinitis Fault (river valley), the Dhoumena Fault steps northwards. By doing the projection exercise across the river valley in the field, it is obvious that the Dhoumena Fault does not propagate across the river valley. On the west side of the river valley, there is basement in the footwall of the Dhoumena Fault and sediments in the hanging wall. By projecting the fault across the river valley, one would have basement in both the hanging wall and in the footwall. Therefore, it is believed that the Dhoumena Fault steps northwards. Indications of a transfer fault in the Kerinitis River Valley are as followed:

- Abrupt ending of the Kerpini Fault against the Skepasto Mountain
- Different lithologies across the river valley

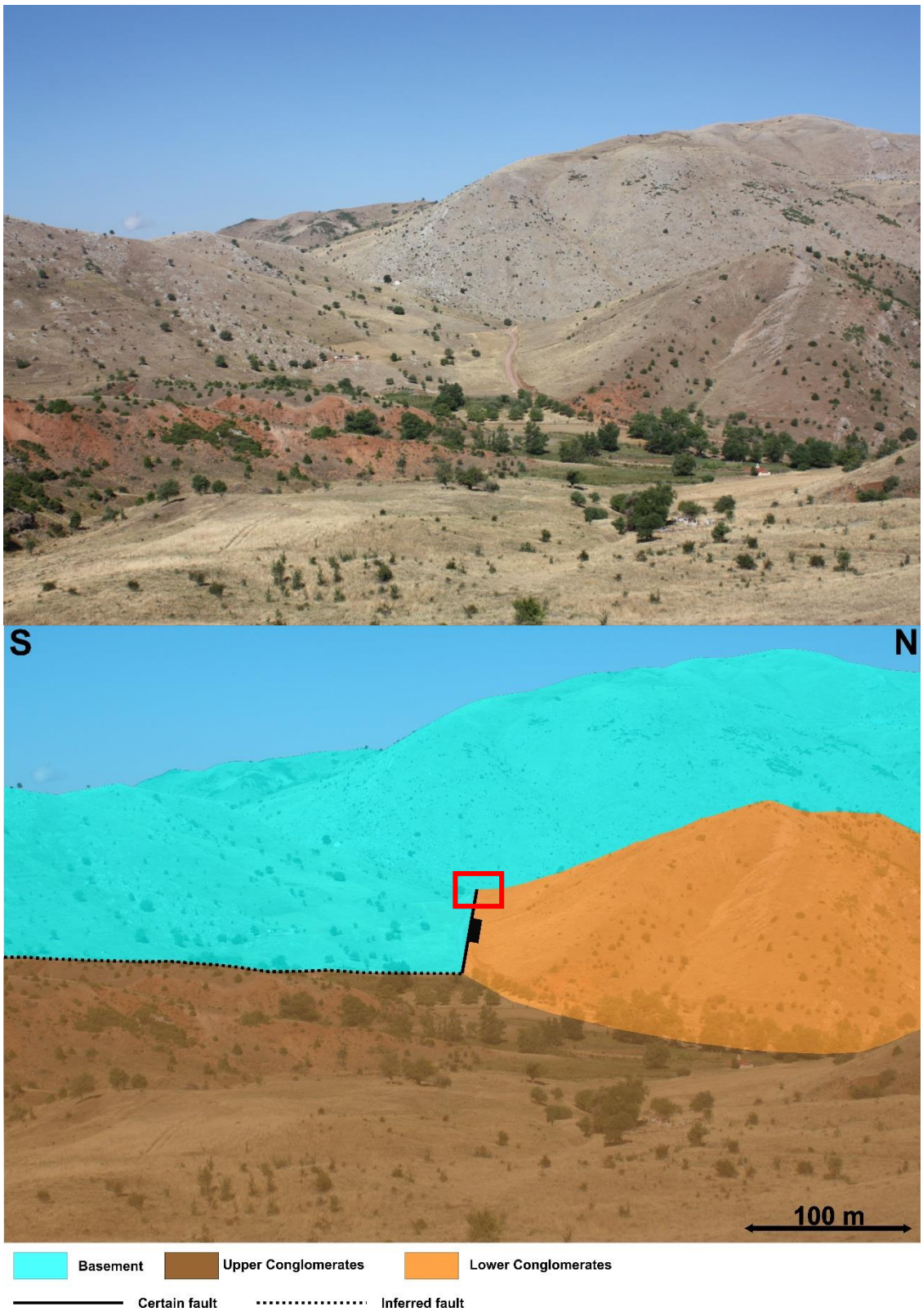

Figure 64: Kerpini Fault segment III. This is the final step of the Kerpini Fault, there is approximately 400 m of displacement on the fault where it is marked with a solid black line. At the end of the fault (marked with red square), the displacement has gone to zero.

6.8 Roghi Mountain Faults

The Roghi Mountain and its massive conglomerates have not been studied in detail in this thesis, which includes the structures that bound the mountain and faults within the mountain itself. Syahrul (2014) have interpreted two faults related to Roghi Mountain, the Roghi Fault South and the Intra Roghi Mountain Fault. His observations will be carried into this study.

6.8.1 Roghi Fault South

The Roghi Fault South is located east of Roghi village, in a small river valley. Syahrul (2014) interpreted this fault based on lithology changes across the valley. This change of lithology has not been observed during this study, conglomerates have been observed on both sides of the valley. However, the characteristics (bed thickness and clast size) of the conglomerates change across the valley. This observation might suggest a northeast-southwest orientated fault in the river valley. Another observation that might strengthen the presence of this fault is a small basement outcrop on the western side of the river valley. Syahrul (2014) interpreted the fault to have a N30˚E strike and a close to vertical dip angle. The additional observations made during this study is believed to strengthen the presence of the Roghi Fault South, hence it has been included in the final map (Figure 54 & 18).

6.8.2 Intra Roghi Mountain Fault

Intra Roghi Mountain Fault is the second fault identified by Syahrul (2014) in the Roghi Mountain area. This fault were identified based on a small basement outcrop in the Vouraikos Valley, this basement outcrop is believed to be in the footwall of the Intra Roghi Mountain Fault. Figure 28 also shows a change of dip angle between beds in the Roghi Mountain, were the beds change from 25˚ to 20˚ across the fault. The basement observation on the eastern side of the mountain combined with the sudden change in bedding dips are the evidences for the presence of a fault.

Roghi Mountain has several interesting features that have not been studied during this thesis. There are different areas were bed thicknesses and bedding dips change rapidly. This could indicate the presence of more normal faults within the massive conglomerate deposits. Only the Roghi Fault South and Intra Roghi Mountain Fault have been taken from previous work.

6.9 Cross-sections

The following subsection will include five different cross-sections, five in a north-south direction and two in east-west direction. Some assumptions are made with the Kalavryta unconformity, at one cross-section location the unconformity does not outcrop (Cross-section B). The Kalavryta unconformity at this location is placed based on interpolation from the last known location of the unconformity. Some faults are not perpendicular to the cross-sections, hence the dip angle in the cross-sections does not represent the real dip angle.

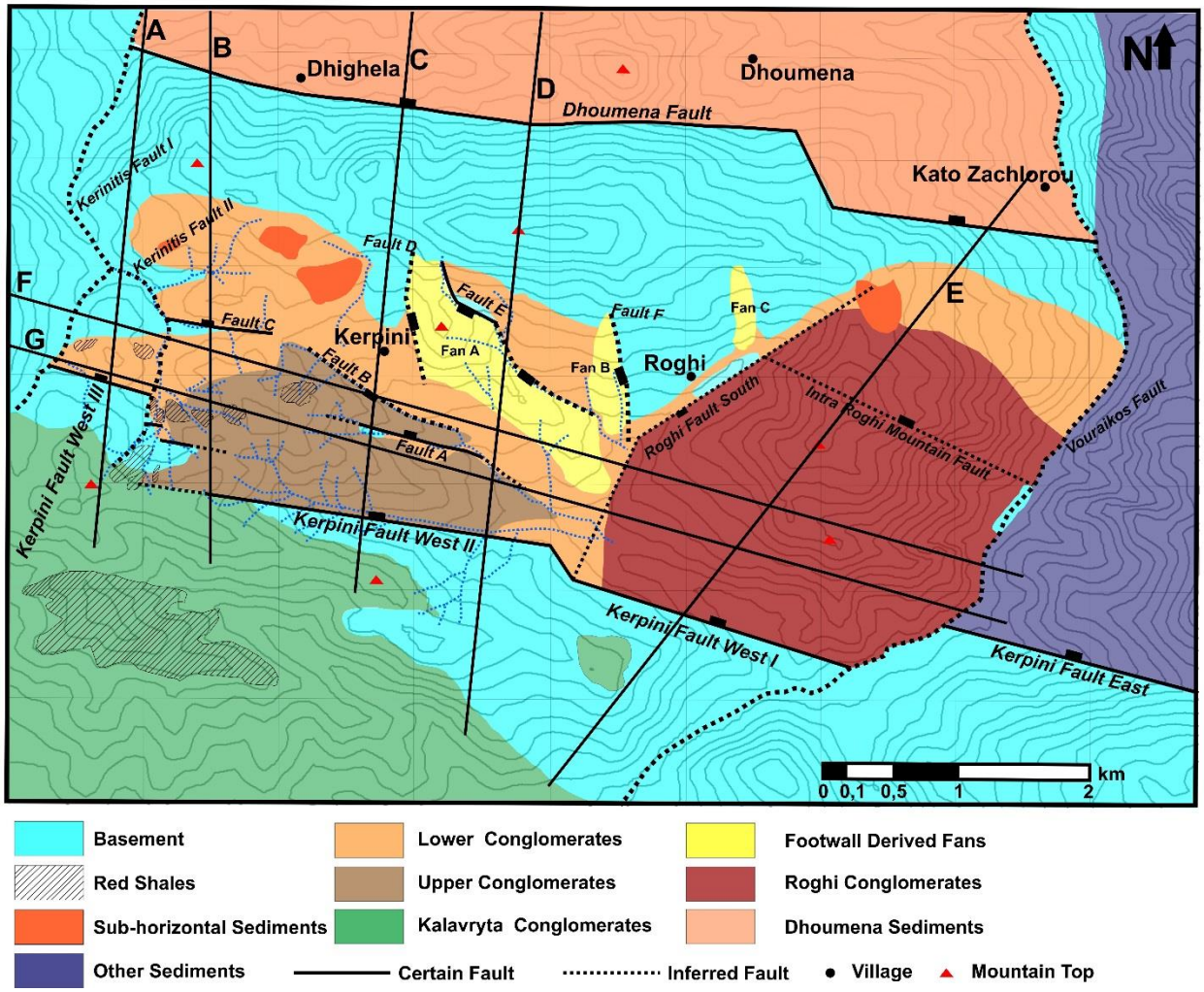

Figure 65: Map showing the locations of the cross-sections. Cross-section A until E are north south orientated, while cross-section F and G are east west orientated. The different faults and stratigraphic units are marked so comparison between the map and cross-sections can be done.

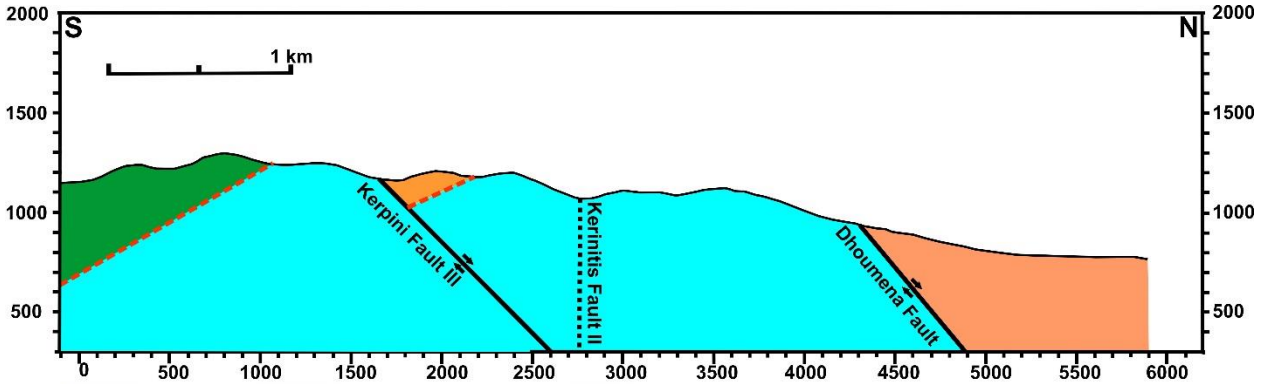

Figure 66: Cross-section A, the westernmost cross-section. This section display the displacement of Kerpini Fault III, this segment has the least displacement of the three segments. At this location, the Kerpini Fault has a displacement of 410m. Kerinitis Fault II is located at the base of a river valley, at the location of this cross-section there is not any clear evidences of putting a transfer fault at this location with basement located on both sides of the fault.

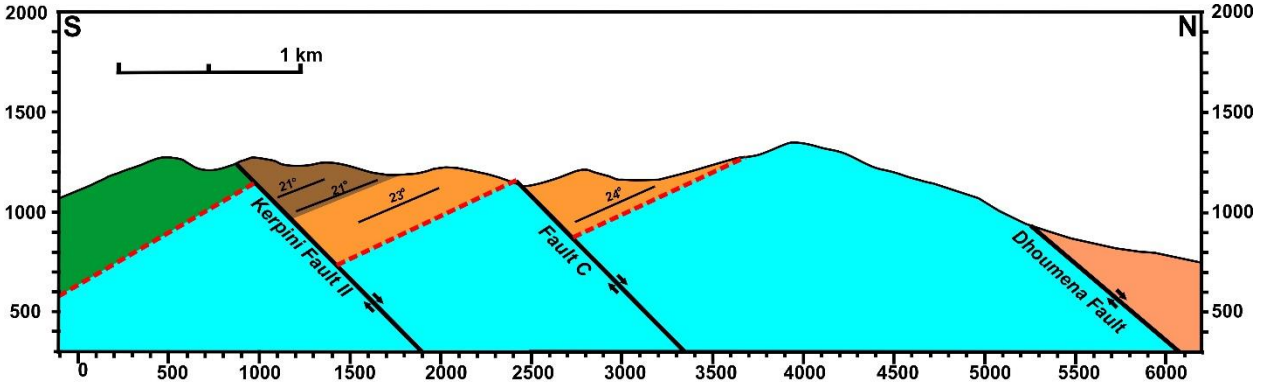

Figure 67: Cross-section B. The Kalavryta unconformity is not exposed at the location where the cross-section is made, this means that the elevation of the unconformity is interpolated from the last located where it is exposed. At this location the Kerpini Fault has a displacement of 430 m and Fault C has a displacement of 280m. The Lower Conglomerates units sits unconformably on top of the basement in both hanging walls.

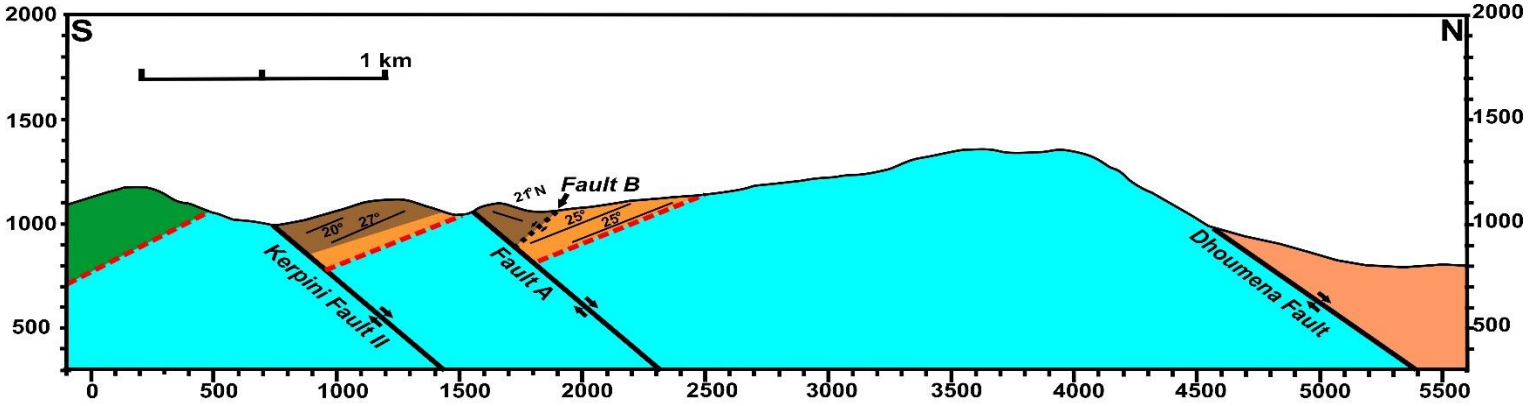

Figure 68: Cross-section C. This north-south cross-section shows both the Northern and the Southern Lobes. From south to north the faults are: Kerpini Fault II, Fault A, Fault B and Dhoumena Fault. Thickness of the Lower Conglomerates unit is thinner below the Southern lobe, this is most likely due to extensive erosion by the alluvial fan deposits during deposition. The north dipping beds of the Northern lobe is also seen in the cross-section, these beds have been rotated by the south dipping Fault B.

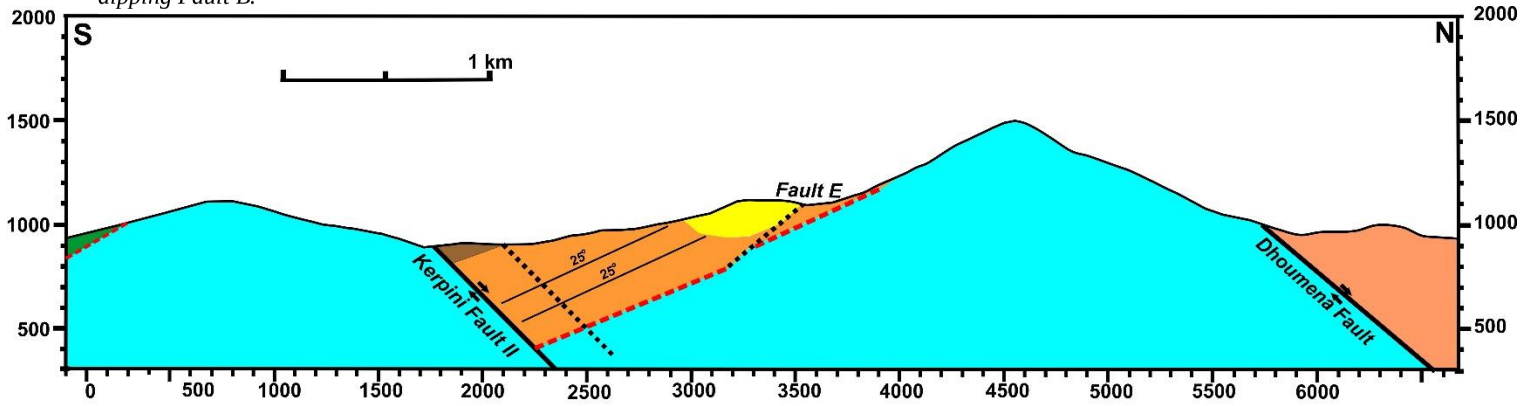

Figure 69: Cross-section D. The position of the cross-section is at the easternmost extent of the Southern Lobe, hence the Upper Conglomerates are so thin. Southern dashed black line represents the possible extent of Fault A, while the northern dashed line represents the Fault E. Fault E controls the deposition of Fan A. The Lower Conglomerates are very thick at the eastern part of the fault block, due to the displacement of Kerpini Fault II is larger at its eastern extent.

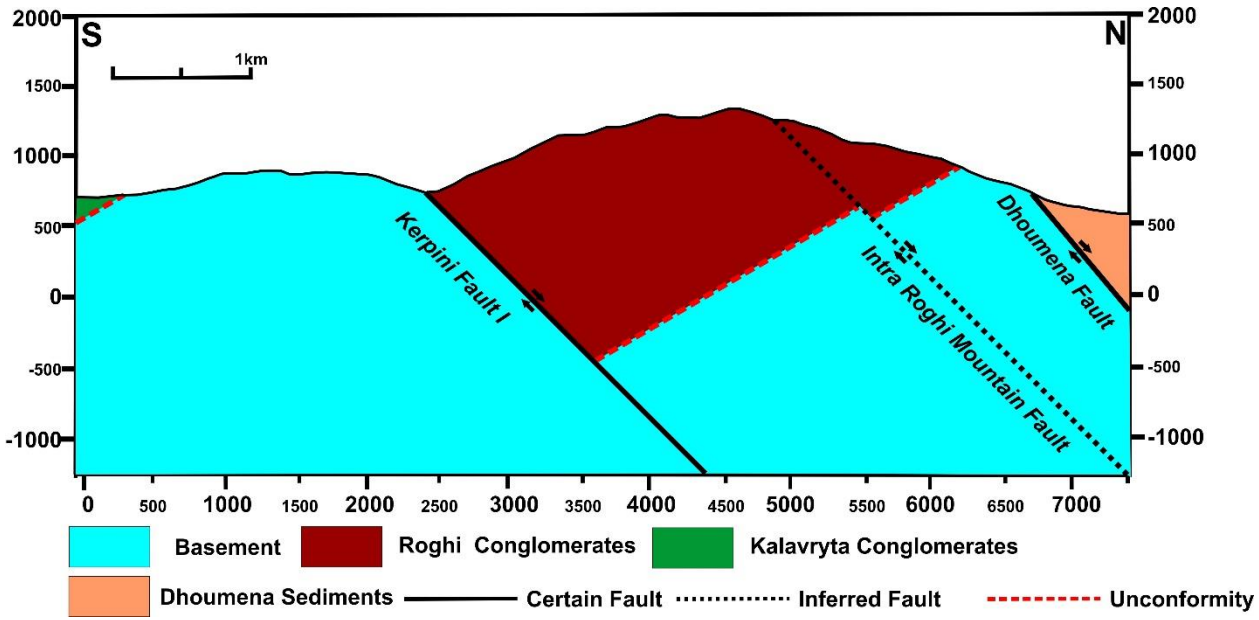

Figure 70: Cross-section E. This is the easternmost of the north-south striking cross-sections. The cross-section display the displacement of Kerpini Fault I, this is the segment where the Kerpini Fault has its largest displacement. This is evident by looking at the thickness of the Roghi Conglomerates in the hanging wall of the Kerpini Fault. Maximum thickness of the unit based on the cross-section exceeds 1500m, this is much thicker than any other unit within the Kerpini Fault Block.

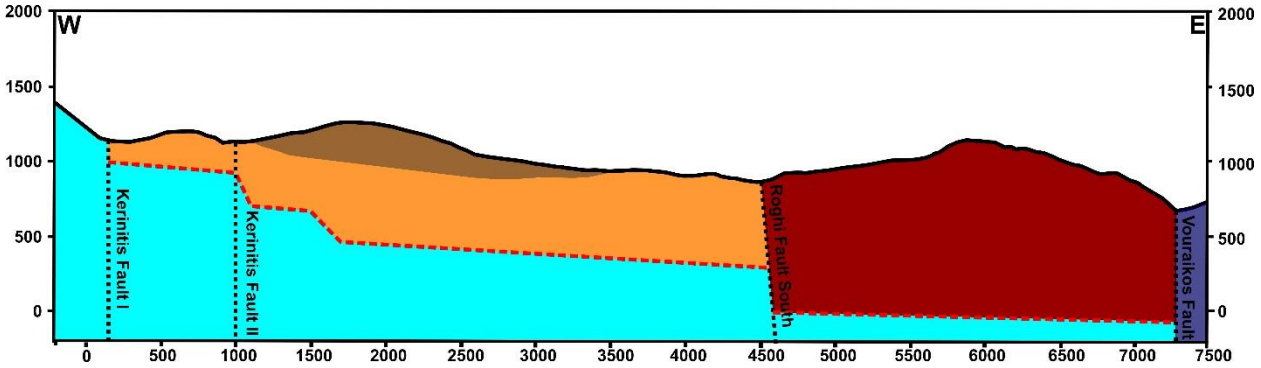

Figure 71:Cross-section F: This is the southernmost of the two east-west cross-sections. Three possible transfer faults have been marked by dashed black lines. The unconformity within segment II drops down several times from west to east, this is because the Kerpini Fault is stepping. One can also observe that the Roghi Fault South has clearly offset the unconformity between segment I and II.

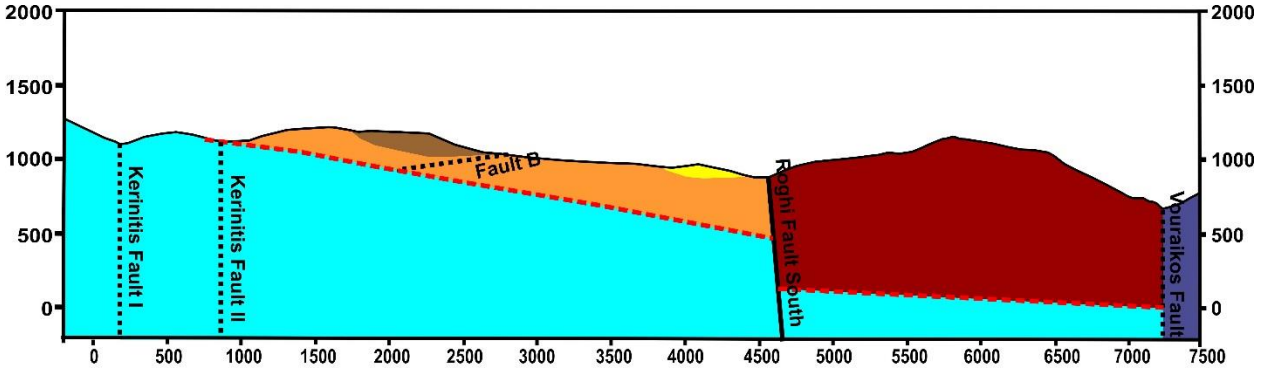

Figure 72: Cross-section G. This cross-section shows only the Northern Lobe of Upper Conglomerates. The section is taken oblique to the south dipping fault, this means that the dip represented in the cross-section is the apparent dip. The overall thickness of the sediments within the Kerpini Fault Block increases towards east, and decreases northwards.

Chapter 7: Discussion

This chapter will summarize and discuss the most important observations described in the previous chapters. Chapter 5 and 6 has described the different stratigraphic units, facies and faults in the study area. This chapter will attempt to link the different observations together to answer the problems addressed in this project:

1. Confirm the presence of the southwestern fan (Upper Conglomerates) identified by Syahrul (2014).
2. Determine the relationship between the Upper Conglomerates and the other stratigraphic units situated in the Kerpini Fault Block.
3. Determine the relative age of the Upper Conglomerates with regards to the Kerpini Fault.
4. Map facies changes in order to identify evidences for the Upper Conglomerates being an internal alluvial fan.
5. Determine if the Upper Conglomerates are likely to have been sourced from a step in the Kerpini Fault, and thus confirm their relationship.

This study is based on previous University of Stavanger master projects (Rognmo, 2015; Stuvland, 2015; Syahrul, 2014). The observations made during this study contradict some of the previous interpretations and evolutionary models. Observations made during this study will be synthesized into a new evolutionary model for the Kerpini Fault Block.

7.1 Facies Distribution – Upper Conglomerates

The main aim of this study was to confirm the presence of an alluvial fan in the southwestern part of the Kerpini Fault Block, as proposed by Syahrul (2014). Moreover, determine the relationship between the alluvial fan and the step between segments II and III of the Kerpini Fault. The Upper Conglomerates have been studied in detail and there is little doubt that they form a fan structure. Based on its position within the Kerpini Fault Block and the proximity to the mountaintop Kalandzi, the alluvial fan will be referred to as the Kalandzi Fan.

The facies of the Kalandzi Fan becomes more immature towards its southwest corner and the Kerpini Fault. This is evident from the decrease in conglomerate clast size and the thinning of the beds towards east. In addition to the lateral facie changes, vertical facies changes are observed for both the Southern and Northern Lobes of the Kalandzi Fan. The immaturity of the facies towards the southwest corner of the Kalandzi Fan suggests that the apex coincides with the step between segments II and III of the Kerpini Fault. Therefore, it appears that the step in the fault somehow contributed to the location of the Kalandzi Fan and possibly controlled its deposition.

The proportion of sheetflood deposits compared to debris-flow and streamflow deposits implies that the alluvial fan can be classified as a sheetflood-dominated alluvial fan. Rapid and episodic deposits linked with seasonal floods and heavy rainfalls (see subsection 3.1.2) often characterize this type of fan. Due to rapid deposition and lack of constant fluid supply (channels and streams) clay content of deposits are limited, which could explain the massive and chaotic appearance of the conglomerates.

During the fieldwork, the facies of the Kalandzi Fan and their lateral extent were mapped, resulting in the facies distribution map seen in Figure 73. Some areas of the unit are heavily vegetated, which means that the facies might not have been physically observed at the location. In these cases, facies were correlated with areas with better exposure. The facies map (Figure 73) represents the locations were the facies are observed and exposed. The facies map (Figure 73) show that there is a relation between the distance from the apex and the observed facies. The depositional energy, flow velocity, flow capacity, conglomerate clast size and bed thickness decreases away from the apex. This implies that facies characterized by mass movement, high gradient and textural heterogeneity, debris-flow and sheetfloods are distributed in the proximity to the apex.

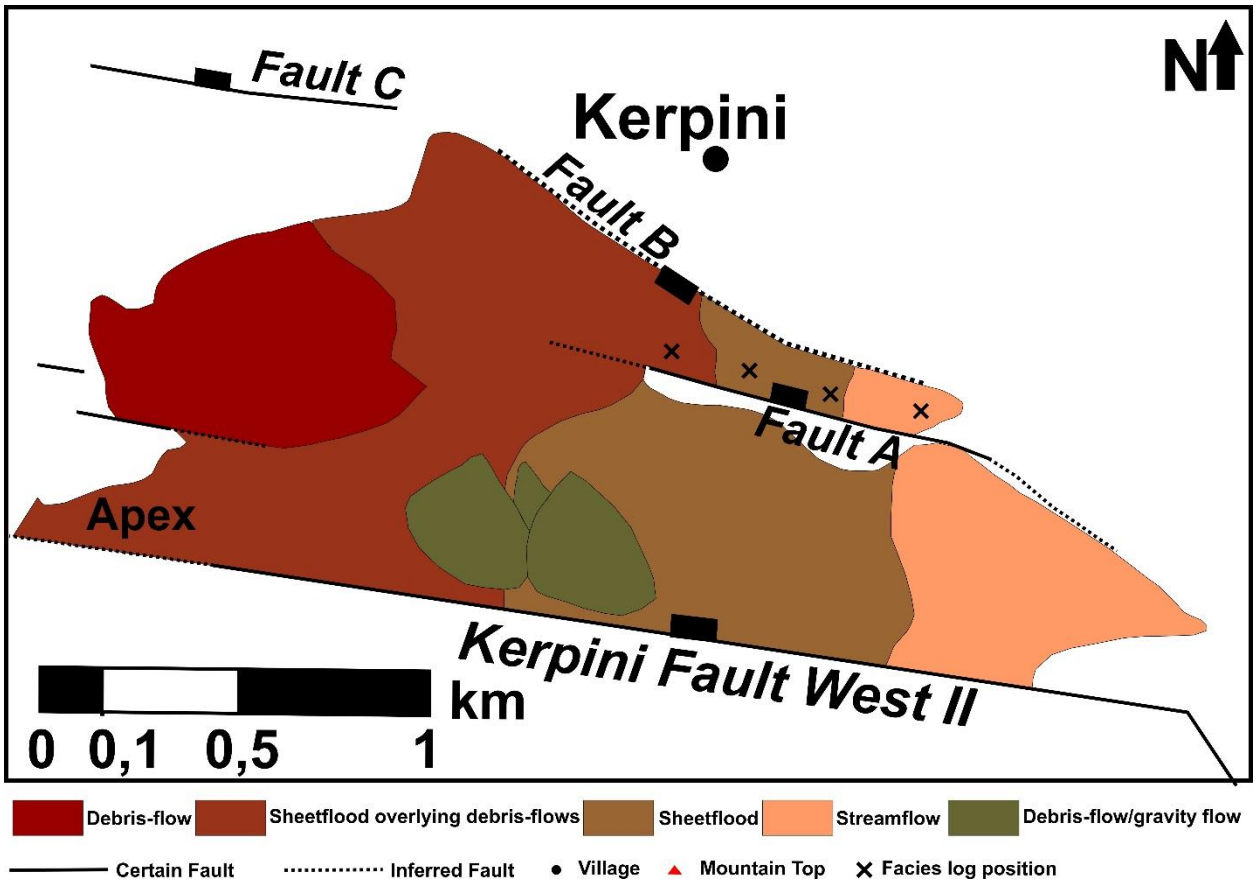

Figure 73: Facies map of the Upper Conglomerates. The apex is marked in the southwestern part of the map. Debris-flow and sheetflood facies characterizes the areas in the proximity to the apex. Moving eastward (Southern and Northern Lobes) the depositional energy, clast size and bed thickness decreases. Facies changes from debris-flow and sheetflood to sheetflood and streamflow moving eastward.

Sheetflood deposits, which have been classified based on bed thickness and conglomerate clast size, are distributed over large areas of the Kalandzi Fan. They occur in both areas close to the apex and eastward towards the eastern limit of the unit. Conglomerate beds with sheetflood characteristics are often found to be overlying separated by finer grained beds (coarse sand and/or pebble sized conglomerates). This implies that the sheetflood deposits are deposited in an episodic and rapid manner. The rapid and episodic deposition is likely linked to flooding events. Finer grained beds were most likely deposited as the rapid, episodic flows have settled, and a more channeled flow developed, transporting the remaining finer sediments downslope. The result is a fining upward sequence with a sharp (erosive) contact between cobble/boulder sized conglomerates and pebbly conglomerates/coarse sandstone. Debris-flow and sheetflood facies make up most of the rock volume of the Kalandzi Fan.

Streamflow facies are only present at the easternmost extent of the two lobes, these deposits represent the most distal part of the Kalandzi Fan. Streamflow deposits are most likely a result of loss of depositional energy and flow competence. As the higher-energy flows (debris-flows and sheetfloods) lose their competence downslope, the finer sediments (marl and sand) are transported further as suspended load.

The massflows on the southern side of the Southern Lobe has a massive and chaotic appearance, but differs from other debris-flow deposits observed, in their matrix content. The massflows have lower matrix content, hence they appear as clast supported conglomerates. This might suggest that they are gravity-flows resulting from slope failures of the Southern Lobe, rather than debris-flows.

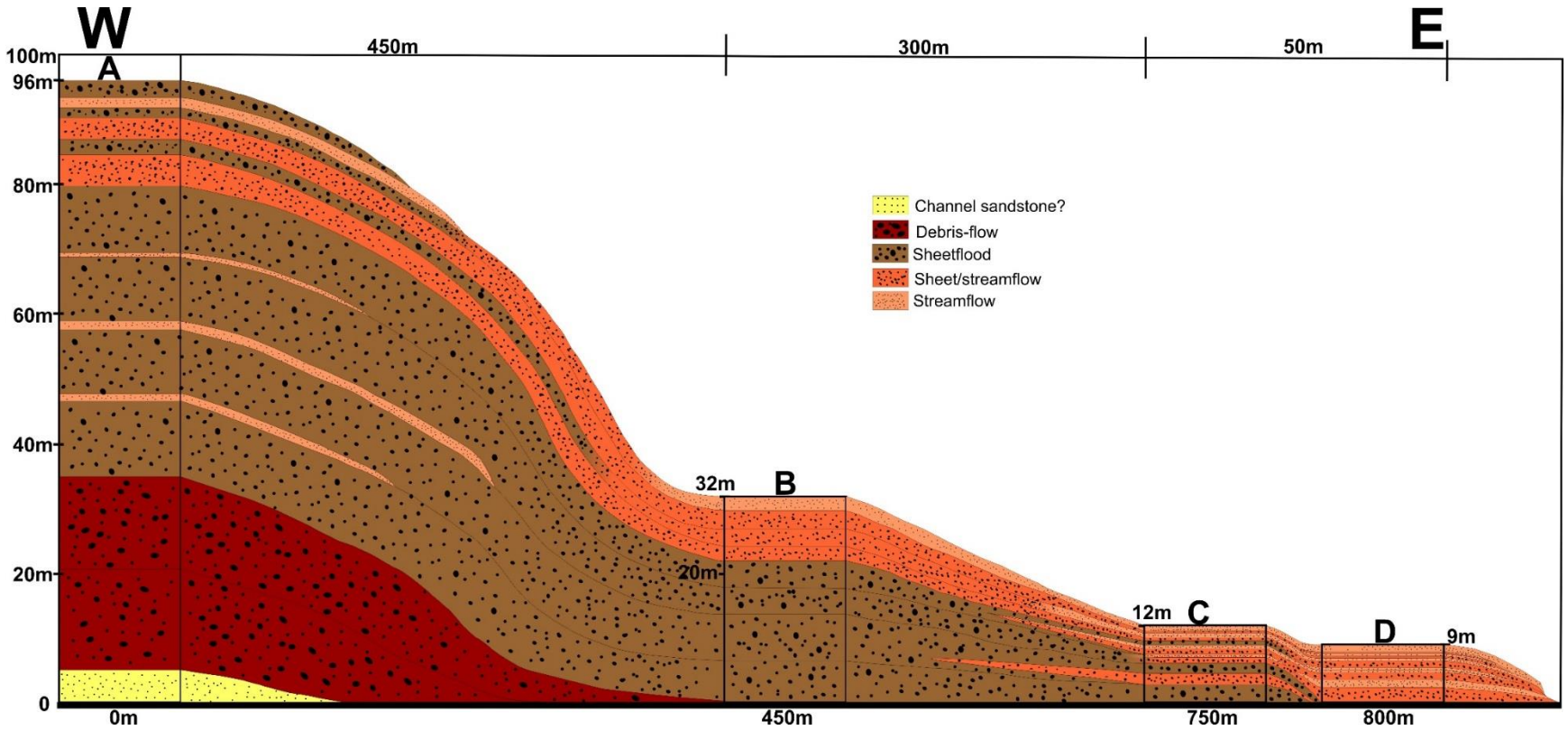

Figure 74: Facies correlation of the Northern Lobe based on four facies logs based on outcrop data. The logs (rectangles with scale) represent the vertical facies changes. Subsection 5.2.4 describes the different facies, it is these observations that are used to classify the facies observed in this figure. Logging vertical successions of the Northern Lobe proved easier than following individual beds latterly. Due to dense vegetation and recent weathering/erosion, beds cannot be followed laterally. Therefore, correlation between the vertical successions has been performed. The western log (A) display thick debris-flow deposits at the base, bed thickness and conglomerate clast size decreases up the section. Laterally from log A to B, the topographic slope changes as the debris-flow deposits pinch out. There is also a general fining eastward trend, this implies more sheetflood/streamflow deposits are present at the eastern part. From log B to C, the bed thickness continues to decrease and more streamflow characteristics are observed. At the eastern extent (log D) streamflow deposits are dominant as the grain/clast size has changed to marl/sand/pebbles. The correlation clearly states that facies are changing in both vertical and lateral direction. The NorthernLlobe display a fining upward and eastward trend. The same pattern applies for the Southern Lobe.

7.2 Stratigraphic Units

7.2.1 Pre-Kerpini Fault Strata

Kalavryta Conglomerates and Lower Conglomerates

The Kalavryta Conglomerates is considered the oldest sediments in the Kalavryta Fault Block, while the Lower Conglomerates unit is considered the oldest sediments in the Kerpini Fault Block. Both units sit unconformable on top of the basement in their respective fault blocks. Stuvland (2015) defined all the conglomerates (except the Sub-horizontal Sediments) within the Kerpini Fault Block to be of pre-Kerpini Fault origin. His interpretation was based on the lack of growth strata and the paleo flow directions. Syahrul (2014) on the other hand interpreted all the conglomerates within the Kerpini Fault Block to be of syn-Kerpini Fault origin, he explained the lack of growth strata with periodic movement of the Kerpini Fault. Observations made during this study suggest that the Kerpini Fault Block stratigraphy consists of a combination between pre and syn-Kerpini Fault strata.

The Kalavryta Conglomerate unit sits unconformable on top of the unconformity in the Kalavryta Fault Block, where approximately 150 m of conglomerates are present at the northern margin. They are clearly sitting in the immediate footwall of the Kerpini Fault, and should therefore be located in the hanging wall of the Kerpini Fault. The Lower Conglomerates unit sits unconformable on top of the basement in parts of the Kerpini Fault Block, and is therefore the likely northern extension of the Kalavryta Conglomerates. This implies that a large alluvial fan, most likely sourced from the Kalavryta Fault, were present before the Kerpini Fault was active. Apart from that both the Kalavryta Conglomerates and the Lower Conglomerates sits unconformable on the basement, their sedimentary texture is similar. This could further support presence of a large alluvial fan deposited prior to the Kerpini Fault. Conglomerate clast size is larger for the Kalavryta Conglomerates than for the Lower Conglomerates, this could indicate a northwards fining of the alluvial deposits. Both units appear massive, chaotic, unsorted and unbedded. Based on the field observations, the Kalavryta and Lower Conglomerates are deposits related to a large alluvial fan with an established channel system (sandstone lenses) propagating across a large area. The exact extent of the alluvial fan is not known, but it is believed to have propagated at least to a position north of Kerpini village where the northernmost outcrop of the Lower Conglomerates in the Kerpini Fault Block is located (Figure 18).

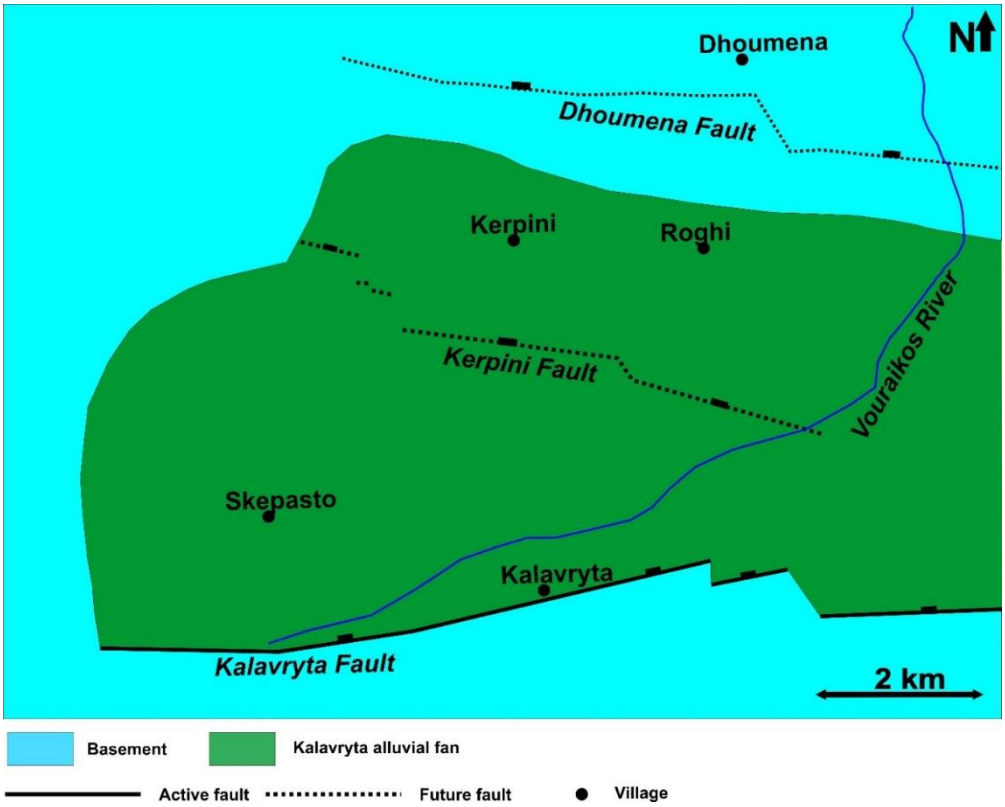

Figure 75: This figure shows the extent of Kalavryta Fan. The fan was deposited while the Kalavryta Fault was active. The northern and eastern extent of the alluvial fan is uncertain, Ford et al. (2013); Wood (2013) suggests the fan to continue northwards into the Dhoumena Fault Block. The northernmost outcrop position of the Kalavryta Fan (Lower Conglomerates unit) in the Kerpini Fault Block is north of Kerpini and Roghi villages as seen in the figure. Areas east of the Vouraikos River have not been studied in detail, but a quick interpretation could suggest the alluvial fan to be present east of the Vouraikos Valley.

The theory of a large alluvial fan (referred to as the Kalavryta Fan in this thesis) sourced from the south is a well-established theory within the Gulf of Corinth rift system, both Ford et al. (2013) and Wood (2013) supports the theory. Their work is rather simplistic and puts the Kalavryta Fan as a single package across the several fault blocks (Kalavryta, Kerpini and Dhoumena Fault Blocks). Both authors believe the large scaled alluvial fan expanded to the Dhoumena Fault Block. The Dhoumena Fault Block has not been studied in this thesis, therefore the extent of the alluvial fan has been limited to the Kerpini Fault Block.

7.2.2 Syn-Kerpini Fault Strata

Upper Conglomerates

The Upper Conglomerates were deposited on top of the Lower Conglomerates, and are not observed to be sitting unconformable on top of the basement within the Kerpini Fault Block. As described in previous chapters, the Upper Conglomerates are separated into three distinct parts, Northern Lobe, Southern Lobe and Western Conglomerates. The different parts of this unit have been interpreted to be deposited during different structural phases of the Kerpini Fault Block, which will become evident in the evolutionary models (subsection 7.4). Classical syn-fault characteristics such as growth strata and decreasing dip angle up section are not observed in either the Southern Lobe or the Western Conglomerates. A lack of clear syn-fault characteristics for the Western Conglomerates can be explained by rapid deposition or possibly related to depocenter development created by rapid fault movement. The unsorted, massive and chaotic appearance of the conglomerates points towards rapid and high-energy deposition. The same reasoning cannot be applied to the Southern Lobe, where the deposits show better developed bedding, sorting and clast organization, which suggests continuous and sustained deposition. The lack of clear syn-fault characteristics for the Southern Lobe can be explained by periodic movement of the Kerpini Fault, as suggested by Syahrul (2014). Periodic fault movement would create different syn-fault packages with a particular dip angle as the sediments are deposited flat before being rotated by an episode of fault movement. Syahrul (2014) expected an angular unconformity between the different syn-fault packages with the episodic fault movement model, such a relationship is not observed for the Kalandzi Fan. Evidences for syn-fault deposition of the Southern Lobe conglomerates and marls are sparse. However, the alluvial sediments of the Southern Lobe originate from the footwall of the Kerpini Fault, close to the step between segments II and III. In order for continuous sedimentation to originate from the fault step, either the fault was active during the deposition or the fault had recently moved and formed a depocenter for the Kalandzi Fan to be deposited in. The facies changes from west to east of the Southern Lobe indicates the Kalandzi Fan sediments to be deposited in the accommodation space created by the Kerpini Fault. Dip measurements suggest that the sediments in the Southern Lobe has experienced rotation related to the Kerpini Fault, this excludes the possibility of the Kalandzi Fan being deposited post the Kerpini Fault. Even though the classical syn-fault characteristics

(growth strata and decreasing dip angle up section) are missing for the Southern Lobe, there are other indicators suggesting syn-Kerpini Fault deposition.

The Northern Lobe is interpreted to be deposited as the displacement of the Kerpini Fault has propagated into the hanging wall, and Fault A and B are active. This implies that the Northern Lobe was deposited as the displacement of the Kerpini Fault shifted northwards to Faults A and B. There is no clear steepening of the dip angle of the south dipping conglomerates of the Northern Lobe, but the conglomerates dipping north into Fault B show decreasing dip angles up the section. This implies that Fault B was active during the deposition of the Northern Lobe.

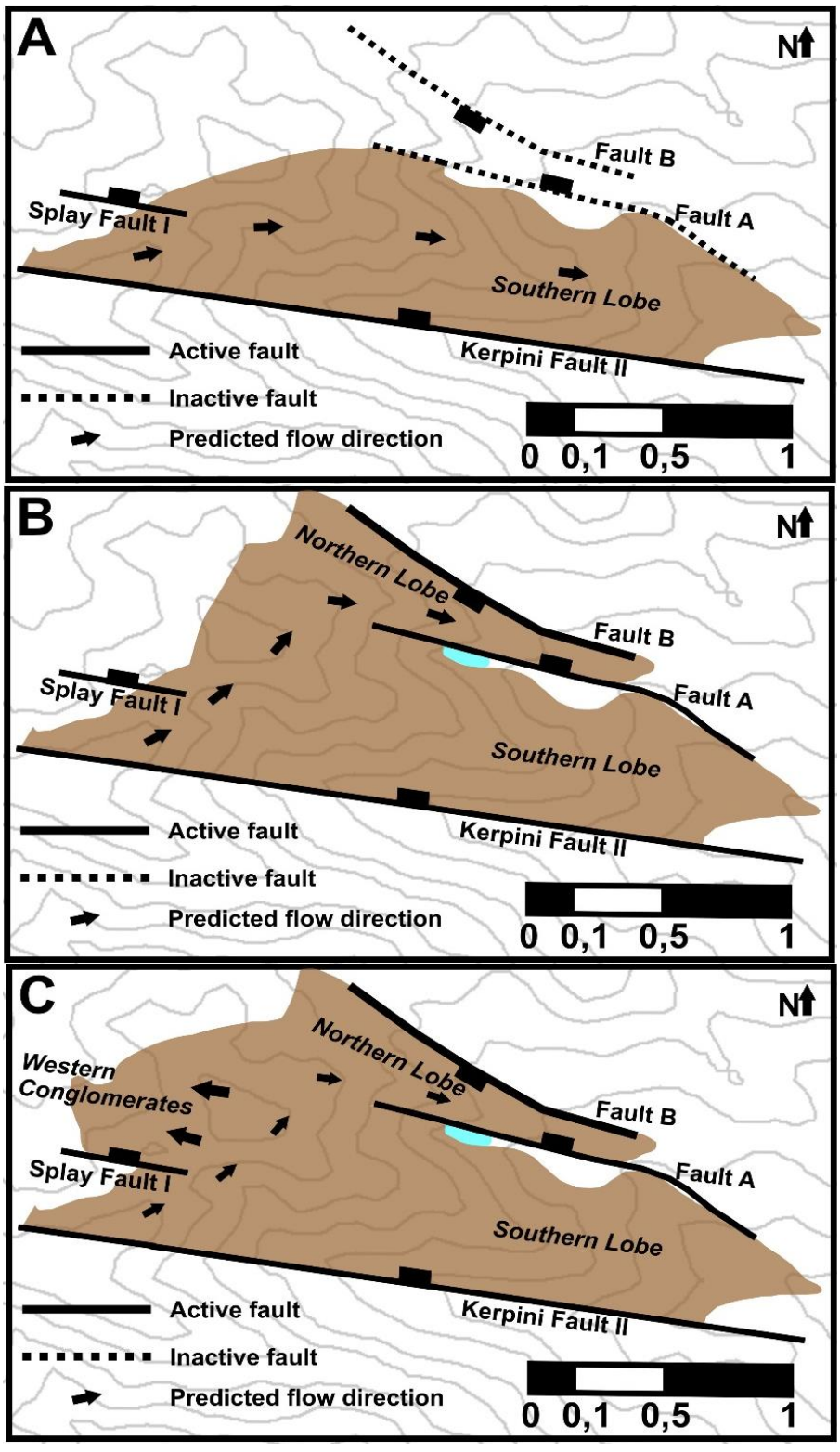

Figure 76: This figure proposes a relationship between the different parts of the Kalandzi Fan and the faults. Segment II of the Kerpini Fault were active as the Southern Lobe were deposited (A), then the displacement propagated into the hanging wall and Fault A and B became active (B). The accommodation space close to the Kerpini Fault was firstly filled followed by the accommodation space of Faults A and B. The Western Conglomerates were deposited as the accommodation space of the Kerpini Fault II and Faults A and B were filled (C).

7.2.3 Late syn-Kerpini Fault Strata/Post-Kerpini Fault Strata

Footwall Derived Fans

The Footwall Derived Fans (Fan A, B and C) have not been studied in detail during this project, but their presence has been acknowledged and their role in the evolution of the Kerpini Fault Block needs to be discussed. The Footwall Derived Fans are sourced from the uplifted footwall of the Dhoumena Fault. This implies that the Dhoumena Fault had started its displacement before the Footwall Derived Fans were deposited. As the fans now have a fairly steep southward dip it is likely the Dhoumena Fault continued to move after the deposition of the fans. If the age relationship between the Footwall Derived Fans and the Kalandzi Fan can be determined, the relative fault movement age between Kerpini Fault and Dhoumena Fault can be better constrained. There are two different fault movement possibilities that could explain the deposition of the Footwall Derived Fans: 1). Dhoumena Fault was active at the same time as the Kerpini Fault or 2). The displacement shifted northwards from the Kerpini Fault to the Dhoumena Fault. The relative age between the Kerpini and Dhoumena Faults will remain a question to answer after this project. The fans are in some locations situated on top of the Lower Conglomerate unit, which means they are younger than the sediments sourced from the Kalavryta Fault (the Kalavryta Fan in subsection 7.2.1). If the displacement of the Kerpini Fault shifted northwards to the Dhoumena Fault, the Footwall Derived Fans are categorized as post-Kerpini Fault deposits. If the displacement were distributed over both the Kerpini and Dhoumena faults, the Footwall Derived Fans will be classified as syn-Kerpini Fault strata. From a sedimentological /facies point of view, the Footwall Derived Fans are different from the Upper Conglomerates. There is more pronounced channelization, sandstone lenses and fining upward sandstone sequences, and overall smaller clast size. By using Galloway and Hobday (1996) classification scheme (Figure 7), the Footwall Derived Fans would be classified as a mixture between sheetflood and streamflow deposits. This implies a constant fluid supply over a relative long period of time rather than episodic events such as heavy rainfall or flooding seasons. A constant fluid supply/channelization suggests that the Footwall Derived Fans developed in the early stages of the Dhoumena Fault, before the footwall were extensively uplifted and the fluid supply would shift to lower elevated areas, confining the structural dip interpretation.

7.3 Structural

7.3.1 Introduction

Several faults have been described in the structural observation chapter (Figure 54). Some of these faults were identified by previous projects (Stuvland, 2015; Syahrul, 2014), and others were firstly introduced in this project. The Kerpini Fault and the interaction between the transfer faults (Vouraikos, Kerinitis I & II and Roghi Fault South Faults) and the Kerpini Fault will be considered in this subsection. In order to properly discuss the interaction between the transfer faults and the Kerpini Fault, block diagrams (Figure 77) and throw profiles (Figure 78) have been generated. The block diagrams (Figure 77) display a three dimensional view of the Kerpini Fault Block where the syn-rift sediments have been stripped of to show how the geometry of the unconformity surface, and how this has been effected by the transfer faults. The throw profiles are generated based on the estimated throw at the cross-sections locations (Figure 66 to 70), where the elevation of the hanging wall and footwall cut-offs, have been used to calculate the throw of the Kerpini Fault. The elevation of the cut-offs has been plotted against the distance to the western end of the fault block (0m represents the Kerinitis Valley). The throw of the Kerpini Fault at locations of cross-sections B and C has been calculated to be the accumulated throw of the Kerpini Fault plus the faults in the hanging wall (Fault A and C).

7.3.2 Kerpini Fault and Interaction with Transfer Faults

From Figure 77 it is evident that the Kerinitis and Vouraikos Faults mark the western and eastern boundary, respectively, of the Kerpini Fault Block. It is also evident that the Roghi Fault South and the Kerinitis Fault II coincides with steps in Kerpini Fault West. Roghi Fault South offsets the Kerpini Fault and creates a step between segment I and II, which suggests that the transfer fault controls the step in the Kerpini Fault. Figure 77B shows that the elevation of the unconformity is significantly offset by the transfer fault. There is approximately 300m difference in the elevation of the unconformity surface between the immediate hanging wall and footwall of the Roghi Fault South. The reason for the large difference in elevation is that the dip of the unconformity surface east of the transfer fault is steeper than west of the transfer fault. In addition, west of the Roghi Fault South the unconformity is at an elevation of approximately 1000m while east of the fault the unconformity is at an elevation of 550m. This implies that the displacement of the Kerpini Fault is largest along segment I, this is also evident in the throw profile (Figure 78) and cross-section E (Figure 70).

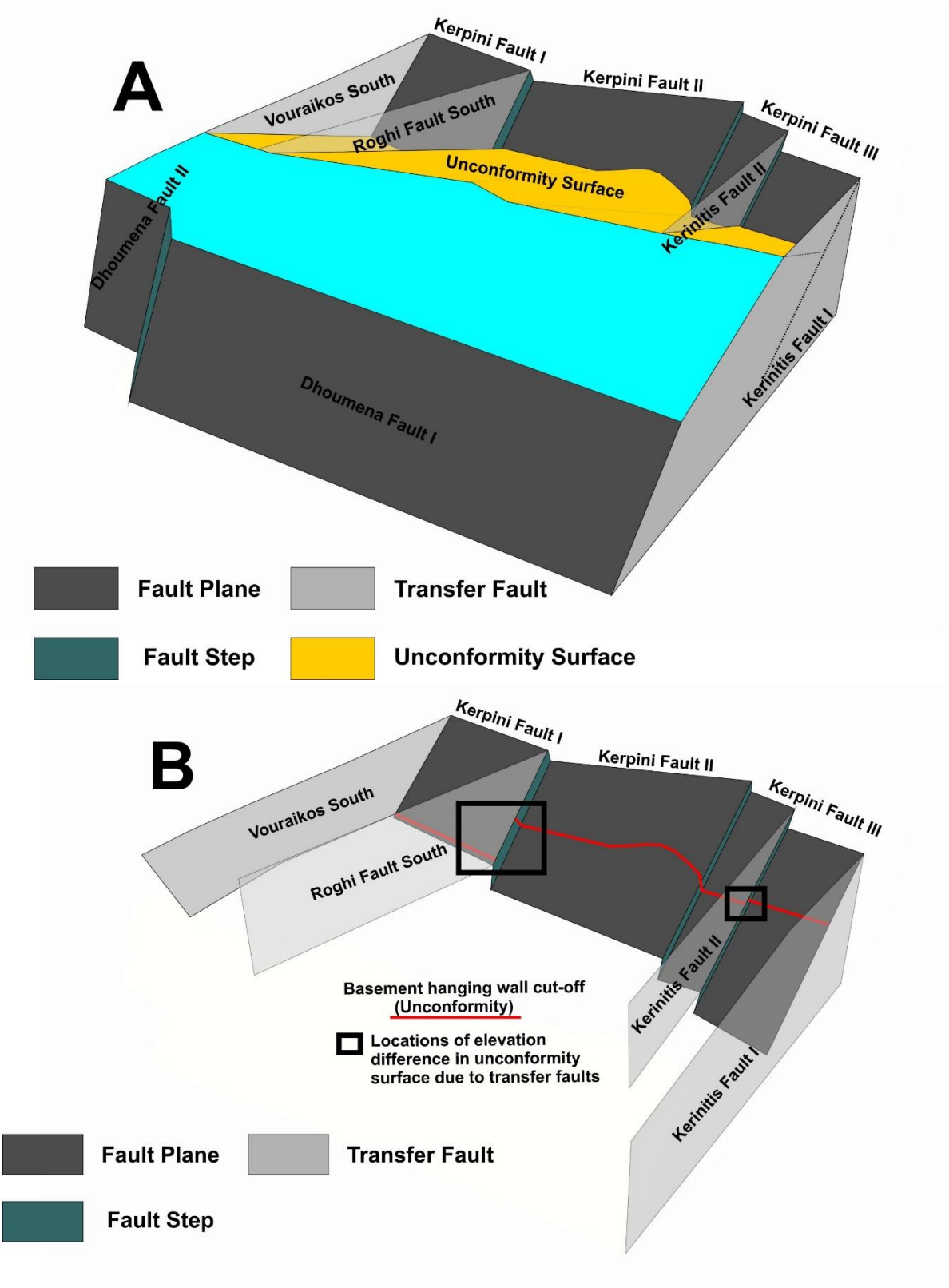

Figure 77: Block diagram of the Kerpini Fault Block. 77A shows the diagram where all the sediments have been stripped of while Figure 77B shows the Kerpini Fault, transfer faults and the hanging wall cut-off of the unconformity. The transfer faults coincide with steps in the Kerpini Fault, and the displacement of the unconformity changes across the transfer faults. On could say that the transfer fault segments the Kerpini Fault and its displacement.

Kerinitis Fault II has been interpreted as a transfer fault because Fault C has an approximate displacement of 300 m east of the transfer fault, while to the west of the transfer fault, Fault C is absent. This implies that Fault C terminates against Kerinitis Fault II with a significant displacement of approximately 300m. The unconformity is also offset in the immediate footwall of the Kerpini Fault. Therefore, based on the knowledge of other transfer faults in the region, Kerinitis Fault II is also interpreted as a transfer fault. The offset of the unconformity in the immediate footwall of the Kerpini Fault is less than observed between segment I and II of the Kerpini Fault.

Kerinitis Fault II coincides with the area where the Kerpini Fault splays into two smaller faults. This implies that the structural complexity of the step between segments II and III is higher than between segments I and II. In addition to the transfer fault, there are two small splay faults which terminate against the transfer fault. From there, the displacement is transferred to segment III of the Kerpini Fault. A full understanding of the step between segments II and III (including the splay faults) have not been resolved during this study.

Figure 78 displays two different interpretations of the throw profile along the Western Kerpini Fault. Figure 78A shows an interpretation where a continuous displacement has been drawn along the different segments. This implies that the transfer fault does not break the displacement of the Kerpini Fault into segments, but rather that the Kerpini Fault has a continuous throw profile across the transfer faults and towards the western tip of the fault. This throw profile (Figure 78A) contradicts the field observations, the best example is found within segment I of the Kerpini Fault where the unconformity surface is displaced by the Roghi Fault South. The unconformity has a steeper dip across the fault, and the thickness of the Roghi Conglomerates exceeds any other sediment thickness within the Kerpini Fault Block. In addition, the average (across all three segments) throw gradient along the Western Kerpini Fault is extremely high (0,39). Displacement gradient for segment III is even higher; 410m of throw goes to zero over a distance of 500m. This results in a throw gradient of 0,83 across segment III, meaning that there has to be a transfer fault present in the Kerinitis Valley that accommodates the displacement. Ferrill and Morris (2001) defined a throw gradient of 0,25 and 0,27 for the Northern Windy Wash and Fatigue Wash Faults, Yucca Mountain, Nevada. They characterized these throw gradients to be extremely steep, which means that the throw gradient observed for the Western

Kerpini Fault cannot be explained without including transfer faults that accommodates the displacement. A more likely interpretation of the throw profile is seen in Figure 78B where the transfer faults break the displacement into segments. This implies that the displacement of the Kerpini Fault is somewhat controlled by the transfer fault and changes across the different segments. It is unlikely that the displacement is constant within segments I and III, but due to lack of data points it has been presented so in Figure 78.

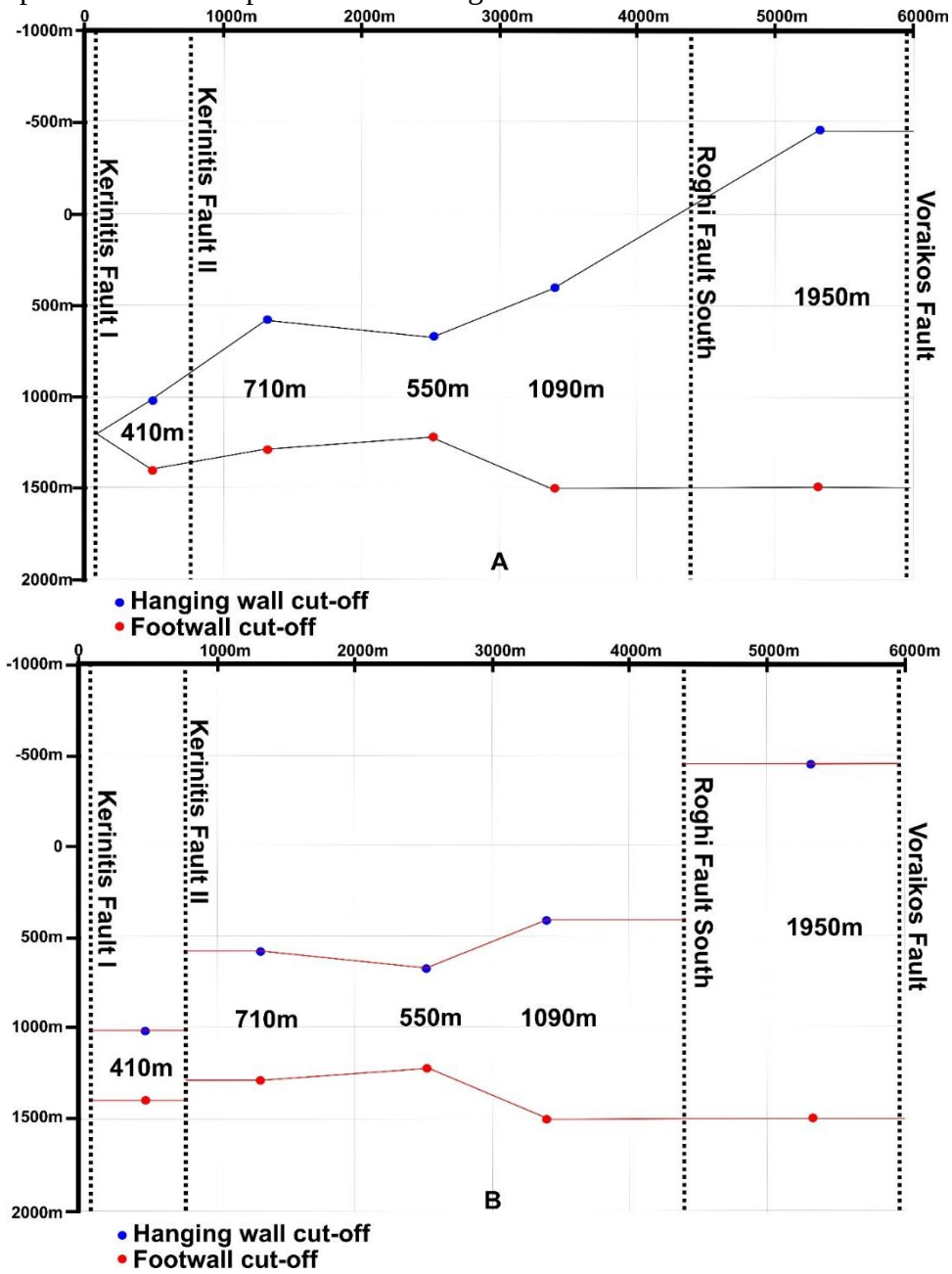

Figure 78: Two interpretations of the throw profile of the Western Kerpini Fault. Figure A shows the interpretation where a continuous throw has been interpreted across the transfer faults. Figure B shows an interpretation where the throw of the Western Kerpini Fault has been segmented by the transfer faults.

7.4 Evolutionary Models

7.4.1 Active Kalavryta Fault – Deposition of Kalavryta Fan

The first stage of the evolutionary models shows the active Kalavryta Fault and the widespread alluvial fan (Kalavryta Fan) deposits originating from south of the fault. The alluvial fan covers most of the Kalavryta and Kerpini Fault Blocks. The dashed black line on the surface of the model shows the location of the future Kerpini and Dhoumena Faults, this implies that the Kalavryta Fan was deposited over a large area. It is not known whether the alluvial fan were sourced from a single point (as shown in figure) or from multiple points. The origin of the Kalavryta Fan is difficult to determine from the available data, but maybe a future study could investigate the Kalavryta Conglomerates and determine their source. The channelization of the fan surface is based upon the observations of channel like features in the Kalavryta Conglomerates and Lower Conglomerates.

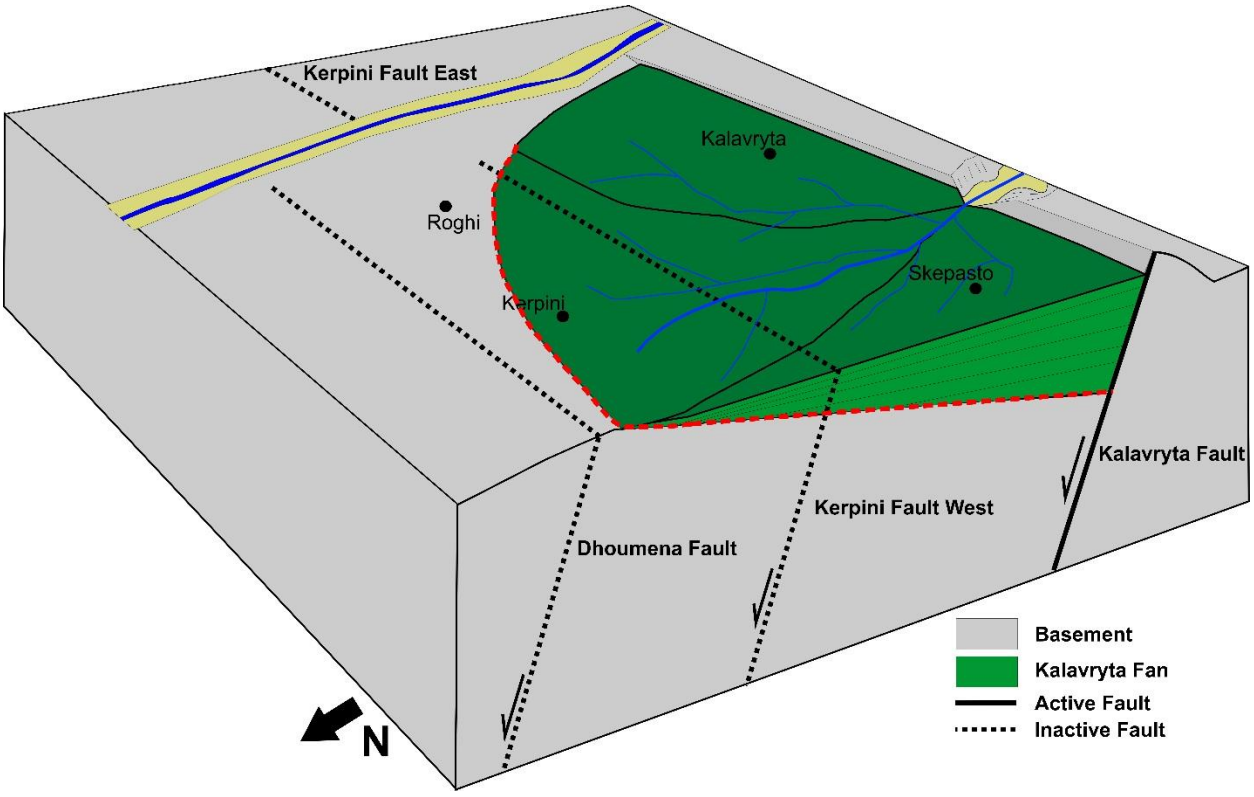

Figure 79: First stage. A large alluvial fan is deposited, the Kalavryta Fan. This conglomeratic deposit is widespread and covers all of the Kalavryta Fault Block and most of the future Kerpini Fault Block. Sandstone lenses observed in outcrops originates from channelization of the fan surface.

7.4.2 Active Kerpini Fault – Initial Stage

During the second stage of the evolutionary model, the Kerpini Fault displaces the Kalavryta Conglomerates and explains their presence in the immediate hanging wall to the Kerpini Fault. This implies that the lower sedimentary unit within the Kerpini Fault Block was deposited prior to the Kerpini Fault. It is also believed that the Roghi Conglomerates were deposited during the early stages of the Kerpini Fault, which implies that the step between segments I and II of the Kerpini Fault was present at an early stage. This has not been studied in detail during this project, hence the step is not marked in Figure 80. The step between segments II and III is shown in Figure 80, it is possible that the Kerpini Fault West grew as two individual faults (segments II and III) before eventually connecting trough the step observed in Figure 80. Upper Conglomerates (sourced from the step) lie immediately on top of the Kalavryta Conglomerates, which is further evidence for the step being present at early stages of the Kerpini Fault Block development. The implication of the steps being an integrated part of the early Kerpini Fault geometry is that the transfer faults are possibly reactivated basement faults, as suggested by Ghisetti and Vezzani (2005)

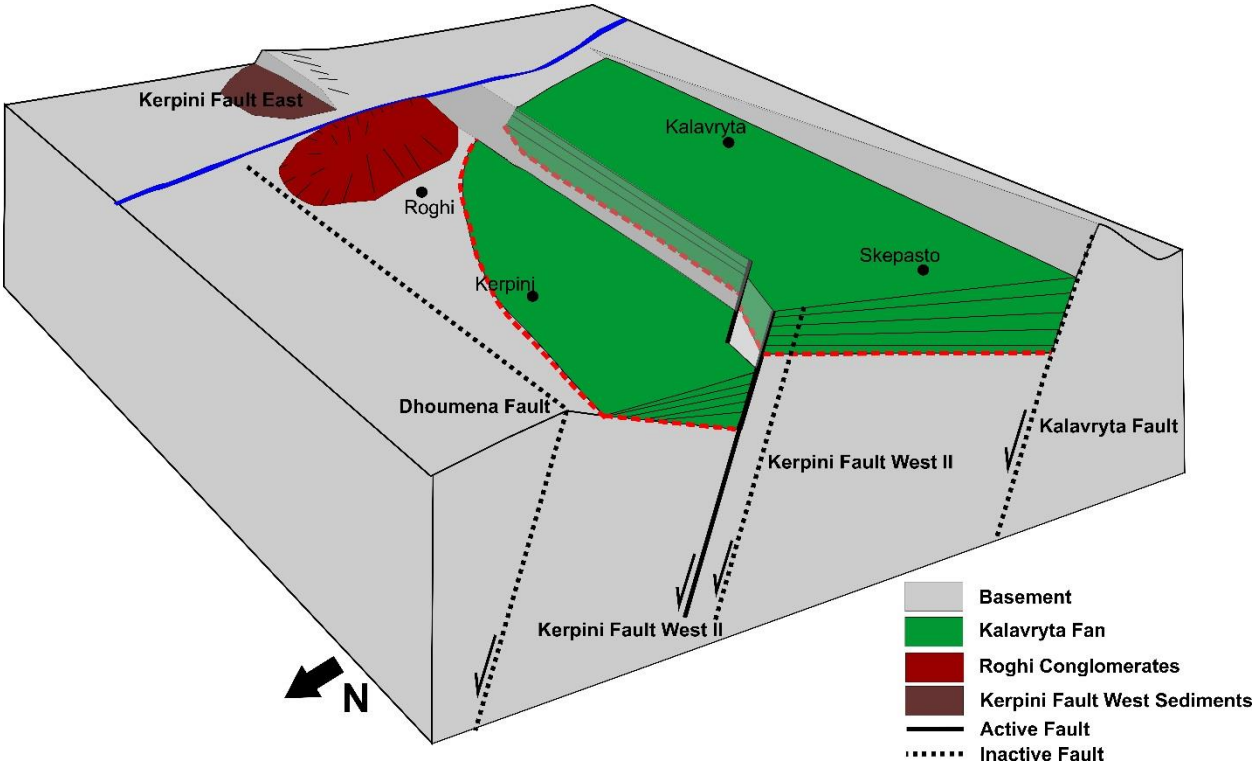

Figure 80: Second stage. The displacement of the Kalavryta Fault ceases and the displacement shifts northwards to the Kerpini Fault. Sediments from the Kalavryta Fan are displaced by the Kerpini Fault, and can be found in the immediate footwall and hanging wall of the Kerpini Fault (pre-Kerpini Fault strata). Deposition of the Roghi Conglomerates happened early in the evolution of the Kerpini Fault Block.

7.4.3 Active Kerpini Fault – Deposition of Southern Lobe

The deposition of the Southern Lobe occurred early in the development of the Kerpini Fault. The Kalandzi Fan filled the accommodation space in the immediate hanging wall to the Kerpini Fault. Early Southern Lobe deposits are characterized by debris-flows while sheetfloods and streamflow deposits characterize later deposits of the Southern Lobe. The sediments are sourced from the step between segments II and III of the Kerpini Fault, small streams transporting sediments possibly originate from a fluvial system in the Kalavryta Fault Block. The alluvial fan sediments flow eastwards after entering the Kerpini Fault Block, due to an early depocenter formed in the eastern end of the fault block interlinked with increased displacement on segment II at its eastern limit. The intersection point of the fan is therefore located very close to the apex of the fan.

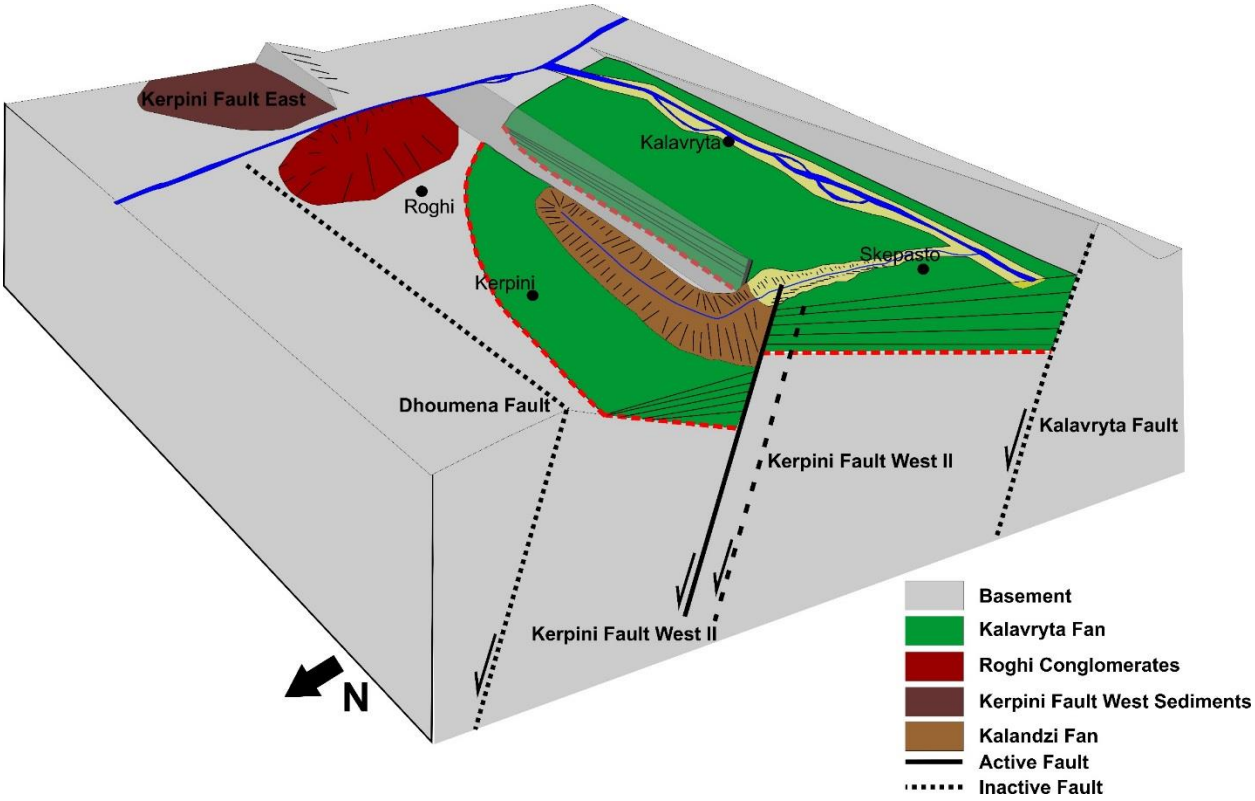

Figure 81: Third stage. The displacement of the Kerpini Fault continues, creating accommodation space in the hanging wall. It is in this accommodation space the alluvial fan sediments from the Southern Lobe are deposited. The sediments originate from a step in the Kerpini Fault. A possible stream/fluvial system in the Kalavryta Fault Block acts as the fluid/sediment supply.

7.4.4 Active Kerpini Fault –Deposition of Northern Lobe

At this stage of the evolution of the Kerpini Fault Block, the displacement of the Kerpini Fault has shifted to the hanging wall faults. Faults A and B develop and created accommodation space for the Kalandzi Fan. This implies that the deposition of the Kalandzi Fan shifted northwards into the accommodation space created by Fault A and B. These two fault are dipping in opposite direction (north and south), meaning a small graben formed within the Kerpini Fault Block. It is evident that the sediments of the Northern Lobe were deposited syn-Fault B due to the shallowing upwards of the dip angles. The depositional pattern of the Northern Lobe appears to follow the same pattern as for the Southern Lobe, debris-flows in the basal proximal parts, and sheetfloods in the central parts and streamflow in the distal parts. Deposition of debris-flows are often linked with high angled slopes, this could imply that rapid fault growth occurred in the early stages of the fault displacement. Rapid fault growth would create accommodation space rapidly and create large topographic relief between footwall and hanging wall.

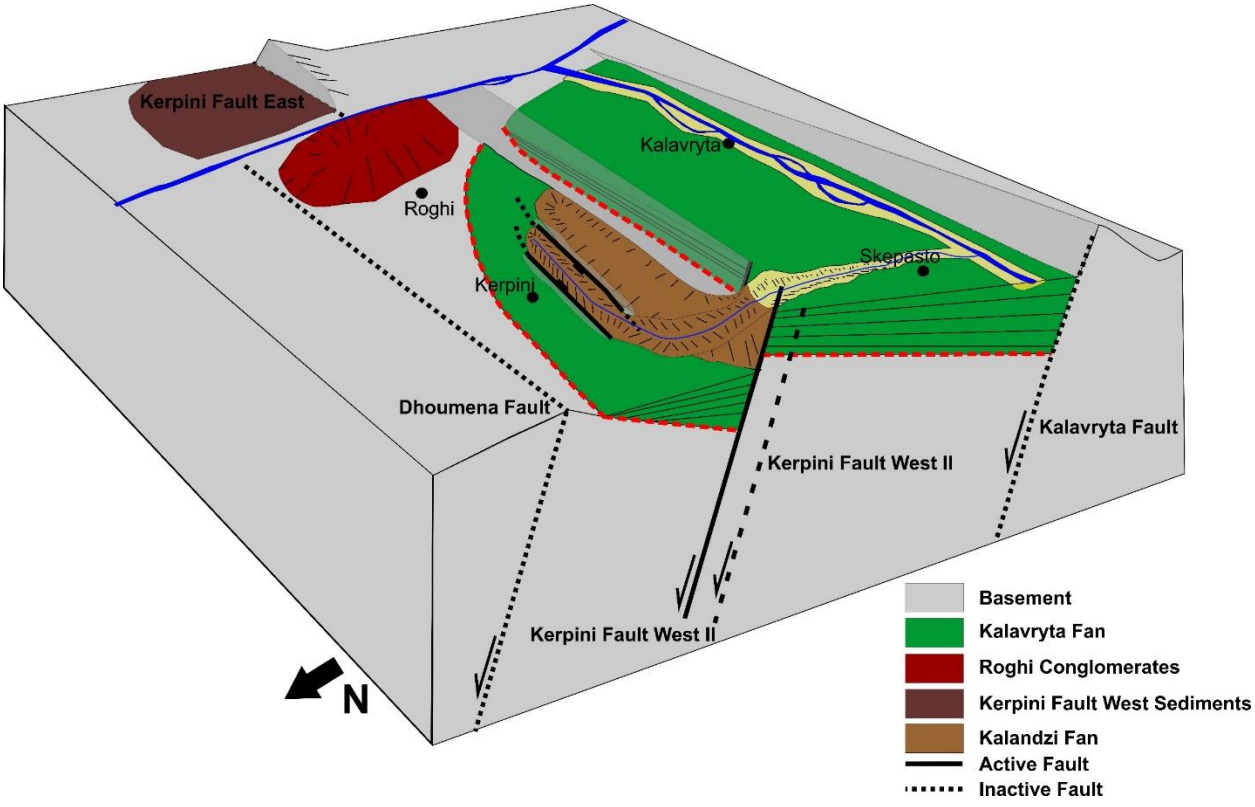

Figure 82: Fourth stage. The displacement of the Kerpini Fault shifts to the hanging wall faults, Fault A and B. These two faults pick up the displacement and create accommodation space for the sediments of the Northern Lobe. Fault A and B dips in opposite directions creating a graben for the sediments to be deposited.

7.4.5 Active Kerpini Fault – Deposition of Western Conglomerates

This stage of the evolution shows the time where the accommodation space in the hanging walls of the Kerpini Fault, Fault A and Fault B are filled. There was still a sediment supply originating from the drainage basin, most likely located in the Kalavryta Fault Block. These deposits are forced to be deposited in a chaotic matter westwards due to the limited accommodation space available. An alternative could be that Fault C was active and uplifted previous deposits of the Kalandzi Fan (Kalavryta Fan). This could mean that the sediment transportation route towards the accommodation space in the hanging walls of Fault A and B was blocked. The blockage of the transportation route led to deposition in a chaotic manner towards the west.

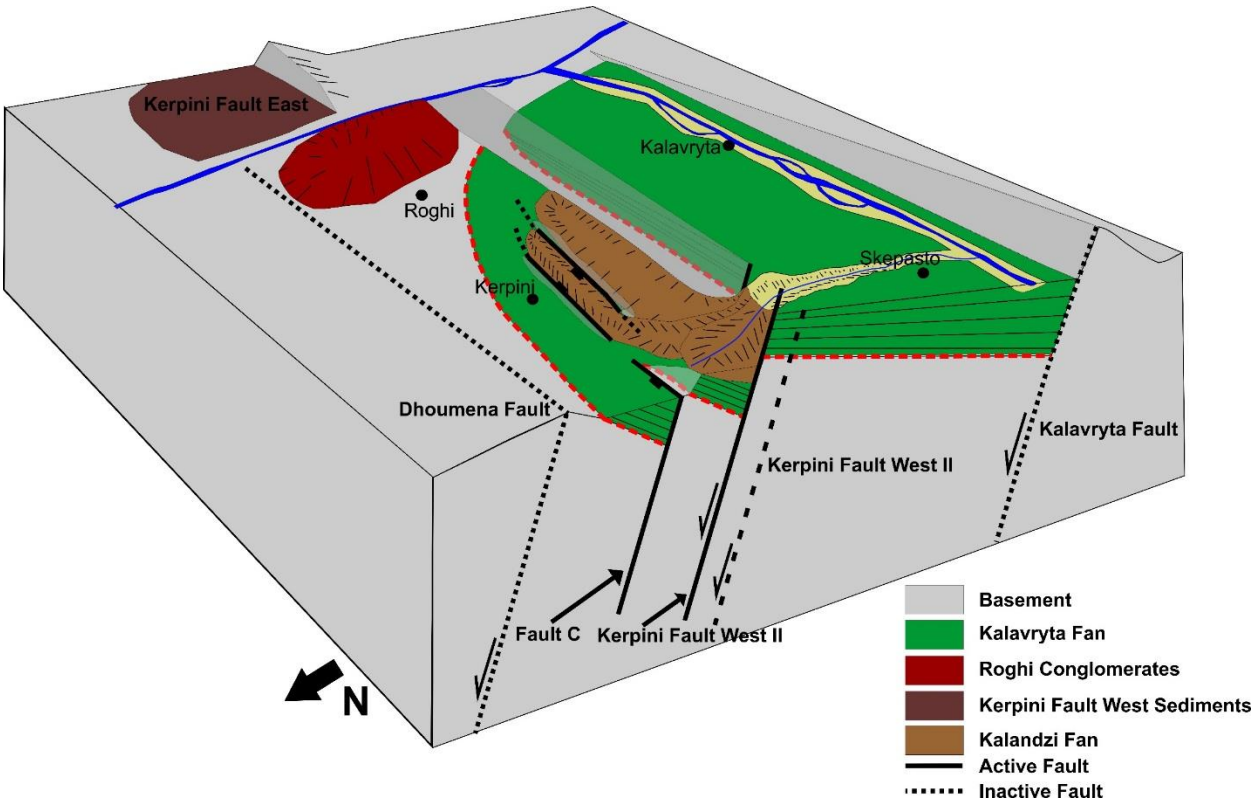

Figure 83: Fifth stage. The Kerpini Fault is still active, and Faults A and B are possibly still active. At this stage, Fault C becomes active and uplifts previous deposits of the Kalandzi Fan. There is not observed any sediments deposited in the hanging wall to Fault C. The Western Conglomerates are deposited towards the west as a possible response to the uplifted footwall of Fault C.

7.4.6 Active Dhoumena Fault - Deposition of Footwall Derived Fans

The relative timing of the Footwall Derived Fans is not well constrained as no field observations were made that clearly identified an age relationship with the Kalandzi Fan. It is assumed that they were deposited late in the Kerpini Fault Block evolution if the displacement propagated northwards from the Kerpini Fault to the Dhoumena Fault, but they could also be earlier if the regional displacement is distributed across several faults. As the displacement shifted northwards to the Dhoumena Fault, the Kerpini Fault Block is further rotated, and the Footwall Derived Fans were deposited. The slope at which they were deposited was created by rotation of the Kerpini Fault Block and the uplift of the Dhoumena footwall. There is large uncertainty linked with the sediment and fluid supply to the Footwall Derived Fans. Outcrop studies reveals that channeled flows are more pronounced in the Footwall Derived Fans than in other alluvial deposits within the fault block. The channels are not likely to develop in areas with high elevation, and it is therefore believed that the Footwall Derived Fans were developed in early stages of the uplift of the Dhoumena footwall before the large topographic relief developed. The present day steep dips of the fans are largely structural rather than depositional.

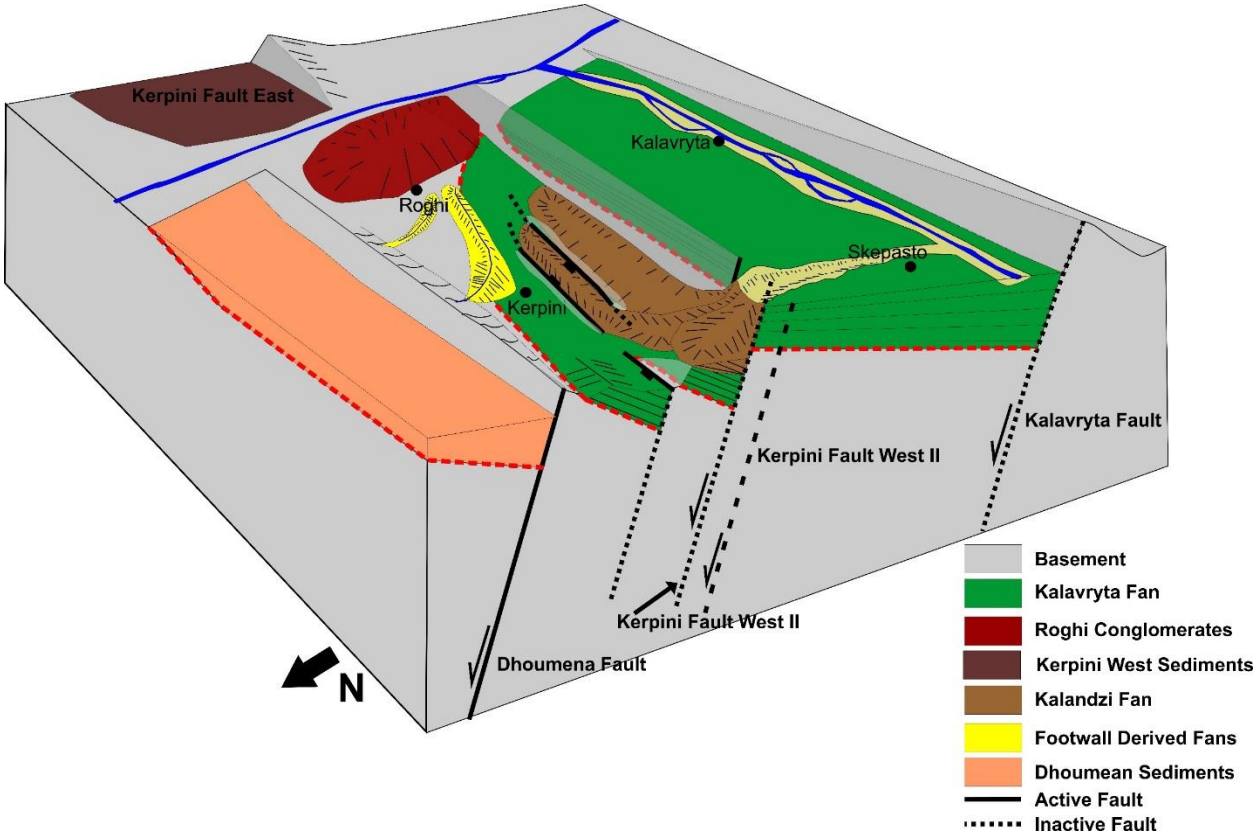

Figure 84: Sixth stage. Displacement of the Kerpini Fault has stopped and the displacement has shifted northwards to the Dhoumena Fault. Footwall Derived Fans are deposited in the slope created by the final rotation of the Kerpini Fault Block and the uplifted footwall of the Dhoumena Fault.

Chapter 8: Conclusion

The knowledge about the Kerpini Fault Block has increased significantly during the last years, as several master thesis projects from the University of Stavanger has worked within the Kerpini Fault Block and surrounding areas (Dahman, 2015; Rognmo, 2015; Stuvland, 2015; Syahrul, 2014). This thesis project has contributed further to the understanding of this fault block.

The Kerpini Fault Block consists of several different stratigraphic units, which contradicts some of the previous work (Ford et al., 2013) were a more general (simplified) stratigraphic framework has been applied. The presence of several different stratigraphic units also suggests that a general stratigraphic framework for the whole rift system (Gulf of Corinth rift system) cannot be applied to fit within individual fault blocks. Detailed outcrop analysis is needed in order to fully understand the processes of the sedimentary infill history of individual fault blocks.

The first and most important conclusion that can be drawn is the confirmation that the Kalandzi Fan is an internal alluvial fan within the Kerpini Fault Block as suggested by Syahrul (2014). The deposition of this fan has clearly been controlled by the step in the Kerpini Fault between segments II and III. This step forms as a response to the Kerinitis Fault II, which has been interpreted to be a transfer fault.

The Kerpini Fault Block consists of both pre and syn-fault strata. The pre-fault strata consist of the Lower Conglomerates, which can be correlated with the Kalavryta Conglomerates in the Kalavryta Fault Block. The syn-fault strata consists of the Upper Conglomerates (Kalandzi Fan) and the Footwall Derived Fans.

The Upper Conglomerates can be classified as an internal sheetflood dominated alluvial fan (Kalandzi Fan), which displays both vertical and lateral facies changes. Alluvial fan deposits within the Kerpini Fault Block have for the first time been characterized from a sedimentological/facies point of view. The characterization of the deposits can be classified into debris-flow, sheetflood and streamflow facies based on bedding, clast size, matrix content, grading and clast sorting.

The Kerpini Fault can be subdivided into three different segments, with a northwards (right) step separating the different segments. Transfer faults segment the displacement of the Kerpini Fault, which is evident by a difference in unconformity elevation across these north-south trending transfer faults.

There are still unanswered questions and features that need further investigations. This thesis projects has reached some conclusions that has contributed further to the understanding of the Kerpini Fault Block, but the following subjects need further explanation to get an even better understanding of the southern part of the Gulf of Corinth rift system:

- Detailed structural/sedimentological analysis of the Footwall Derived Fans and their bounding faults (Fault D, E and F). This project would emphasize on establishing the relative timing of the Footwall Derived Fans and the other stratigraphic units of the Kerpini Fault Block. This study could also potentially contribute to a better understanding of the relative timing between the Kerpini and Dhoumena Faults.
- Correlation of stratigraphic units across fault blocks. In order to fully understand the relative timing of the southern faults (Kalavryta, Kerpini and Dhoumena), a project emphasizing on the correlation of stratigraphic units across different fault blocks could potentially solve this issue. An example would be to investigate if the deposition of the Kalavryta Fan were spread across the three fault blocks.
- Detailed investigation of the presence and contribution of the transfer faults within the Kerpini Fault Block.

References

Armijo, R., B. Meyer, G. C. P. King, A. Rigo, and D. Papanastassiou, 1996, Quaternary evolution of the Corinth Rift and its implications for the Late Cenozoic evolution of the Aegean: Geophysical Journal International, v. 126, p. 11-53.

Barnett, J. A. M., J. Mortimer, J. H. Rippon, J. J. Walsh, and J. Watterson, 1987, Displacement Geometry in the Volume Containing a Single Normal Fault: The American Association of Petroleum Geologists Bulletin, v. 71, p. 925-937.

Blair, T. C., 1987, Sedimentary processes, vertical startification sequences, and geomorphology of the Roaring River alluvial fan, Rocky Mountain National Park, Colorado.: Journal of Sedimentary Petrology, v. 57, p. 1-18.

Blair, T. C., and J. G. McPherson, 1994a, Alluvial fans and their natural distinction from rivers based on morphology, hydraulic processes, sedimentary processes, and facies assemblages: Journal of Sedimentary Research, v. 65, p. 581-586.

Blair, T. C., and J. G. McPherson, 1994b, Processes and Forms of Alluvial Fans, *in* A. J. Parsons, and A. D. Abrahams, eds., Geomorphology of Desert Environments, Springer Science p. 55.

Blikra, L. H., and W. Nemec, 1998, Postglacial colluvium in western Norway: depositional processes, facies and paleoclimate record.: Sedimentology, v. 45, p. 909-959.

Collier, R., and G. Jones, 2004, Rift Sequences of the Southern Margin of the Gulf of Corinth (Greece) as Exploration / Production Analogues*: Search and Discovery v. 50007.

Contreras, J., C. P. Scholz, and G. C. P. King, 1997, A model of rift basin evolution constrained by first-order stratigraphic observations: Journal of geophysical Research v. 102, p. 7673-7690.

Cowie, P. A., 1998, Normal fault growth in three-dimensions in continental and oceanic crust Faulting and Magmatism at Mid-Ocean Ridges: Geophysical Monograph Series, v. 106, p. 325-348.

Dahman, A., 2015, The Vouraikos Valley: an example of rift segmentation in the Corinth Graben, Greece, University of Stavanger, 80 p.

Degnan, P. J., and A. H. F. Robertson, 1998, Mesozoic-early Tertiary passive margin evolution of the Pindos ocean (NW Peloponnese, Greece): Sedimentary Geology, v. 117, p. 33-70.

Ferrill, D. A., and A. P. Morris, 2001, Displacement gradient and deformation in normal fault systems: Journal of Structural Geology, v. 23, p. 619-638.

Ford, M., S. Rohais, E. A. Williams, S. Bourlange, D. Jousselin, N. Backert, and F. Malartre, 2013, Tectono-sedimentary evolution of the western Corinth rift (Central Greece): Basin Research, v. 25, p. 3-25.

Galloway, W. E., and D. K. Hobday, 1996, Terregenous Clastic Depositional Systems, Applications to Fossil Fuel and Groundwater Resources: Berlin, Heidelberg Springer - Verlag.

Gautier, P., J. P. Brun, R. Moriceau, D. Sokoutis, J. Martinod, and L. Jolivet, 1999, Timing, kinematics and causes of Aegean extension: a scenario based on a comparison with simple analogue experiments: Tectonophysics, v. 315, p. 31-72.

Gawthorpe, R. L., and M. R. Leeder, 2000, Tectono-sedimentary evolution of active extensional basins: Basin Research, v. 12, p. 195-218.

Ghisetti, F., and L. Vezzani, 2005, Inherited structural controls on normal fault architecture in the Gulf of Corinth (Greece): Tectonics, v. 24, p. 1-17.

Gibson, J. R., Walsh, J. J., Watterson, J., 1989, Modelling of bed contours and cross-sections adjacent to planar normal faults: Journal of Structural Geology, v. 11, p. 317-328.

Hampton, M. A., 1975, Competance of fine-grained debris flows: Journal of Sedimentary Petrology, v. 45, p. 834-844.

Hooke, R. L., 1967, Proscesses on arid-region alluvial fans: Journal of Geology, v. 75, p. 438-460.

Jackson, J., 1994, Active tectonics of the Aefean region: Annual Review of Earth and Planetary Sciences, v. 22, p. 239-271.

Jolivet, L., J. P. Brun, P. Gautier, S. Lallemant, and M. Patriat, 1994, 3D-kinematics of extension in the Aegean region from the early Miocene to the Present, insight from the ductile crust: Bulletin de la Societe Geologique de France, v. 165, p. 195-209.

Leeder, M. R., and R. L. Gawthorpe, 1987, Sedimentary models for extensional tilt-block/half-graben basins. : Geological Society of London, v. Special Publication 28, p. 139-152.

Moretti, I., D. Sakellariou, V. Lykousis, and L. Micarelli, 2003, The Gulf of Corinth: An active half graben?: Journal of Geodynamics, v. 36, p. 323-340.

Nichols, G., 2009, Sedimentology and stratigraphy v. 2: Chichester, Wiley-Blackwell.

Ori, G. G., 1989, Geological history of the extensional basin of the Gulf of Corinth (?Miocene-Pleistocene), Greece: Geology, v. 17, p. 918-921.

Papazachos, C. B., 1999, Seismological and GPS evidence for the Aegean-Anatolia interaction: Geophysical Research Letters, v. 26, p. 2653-2656.

Prothero, D. R., and F. Schwab, 2013, Sedimentary Geology, v. 3: New York, Freeman, W.H,.

Reading, H. G., 1986, Sedimentary environments and facies: Oxford, Blackwell.

Reilinger, R., S. McClusky, P. Vernant, S. Lawrence, S. Ergintav, R. Cakmak, H. Ozener, F. Kadirov, I. Guliev, R. Stepanyan, M. Nadariya, G. Hahubia, S. Mahmoud, K. Sakr, A. ArRajehi, D. Paradissis, A. Al-Aydrus, M. Prilepin, T. Guseva, E. Evren, A. Dmitrotsa, S. V. Filikov, F. Gomez, R. Al-Ghazzi, and G. Karam, 2006, GPS constraints on continental deformation in the

Africa-Arabia-Eurasia continental collision zone and implications for the dynamics of plate interactions: Journal of geophysical Research, v. 111.

Rognmo, T., 2015, Sedimentary infill in the Kalavrita faulted block, south-central Gulf of Corinth, Greece, University of Stavanger, 68 p.

Rust, B. R., 1978, Depositional models for braided alluvium., *in* A. D. Miall, ed., Fluvial sedimentology, Canadian Society of Petroluem Geologists, p. 605-625.

Schlische, R. W., 1991, Half-graben basin filling models: New constraints on continental extensional basin development: Basin Research, v. 3, p. 123-141.

Schlische, R. W., 1994, Rifting in eastern North America: Virginia Explorer, v. 10, p. 20-23.

Schlische, R. W., and M. H. Anders, 1996, Stratigraphic effects and tectonic implications of the growth of normal faults and extensional basins: Geological Society of America Special Publication, p. 183-203.

Scott, B., 1981, The Eurasian-Arabian and African continental margin from Iran to Greece Journal of the Geological Society of London, v. 138, p. 719-733.

Skourlis, K., and T. Doutsos, 2003, The Pindos Fold-and-thrust belt (Greece): Inversion kinematics of a passive continental margin: International Journal of Earth Sciences, v. 92, p. 891-903.

Sorel, D., 2000, A Pleistocene and still-active detachment fault and the origin of the Corinth-Patras rift, Greece: Geology, v. 28, p. 83-86.

Stuvland, M. E., 2015, Kalavryta and Kerpini Fault Block: Investigation into correlation and nature of sub-horizontal layers; Corinth Graben, Greece.: Master Thesis thesis, University of Stavanger, 132 p.

Syahrul, R. A., 2014, Fault Controlled Sedimentation: A case study of the Kerpini Fault, Greece.: Master Thesis thesis, Universiy of Stavanger, 142 p.

Taymaz, T., Y. Yilmaz, and Y. Dilek, 2007, The geodynamics of the Aegean and Anatolia: Introduction: The Geological Society of London, v. 291, p. 1-16.

Tucker, M. E., 2011, Sedimentary Rocks in the Field: A Practical Guide: Geological Field Guide, v. 4: Chicester, John Wiley & Sons.

Twiss, R. J., and E. M. Moores, 2007, Structural Geology, v. 2: New York, W.H. Freeman CO.

Wood, A. M., 2013, The influence of fault geometric uncertainty on hydrocarbon reservoir and simulation models: Doctoral thesis thesis, University of Leeds.